Volume 6 No. 3, June 2019

Transactions on Networks and Communications

ISSN: 2054-7420

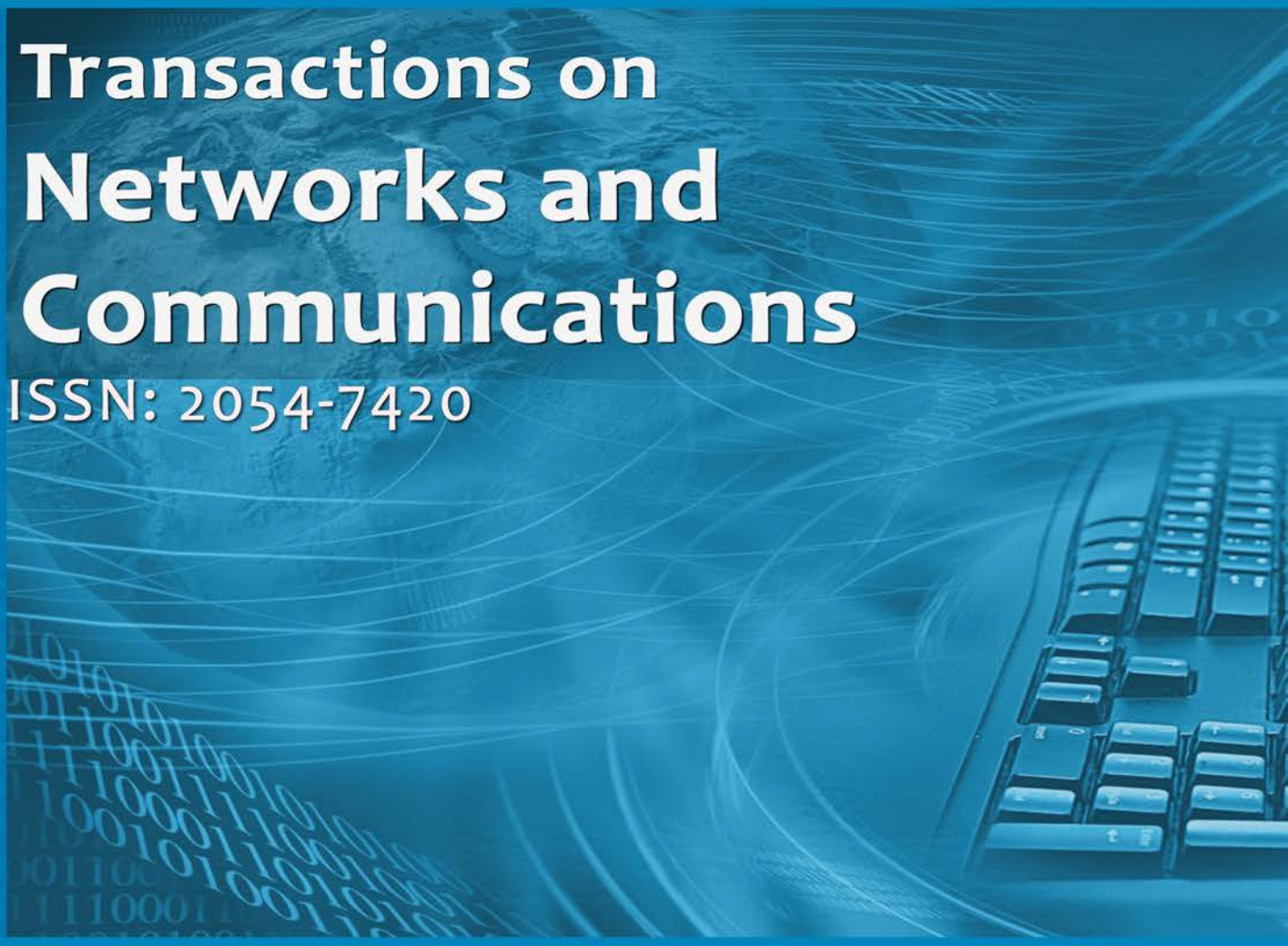

Society for Sciences and Education - United Kingdom

TABLE OF CONTENTS

DISCLAIMER

All the contributions are published in good faith and intentions to promote and encourage research activities around the globe. The contributions are property of their respective authors/owners and the journal is not responsible for any content that hurts someone's views or feelings etc.

SOCIETY FOR SCIENCE AND EDUCATION
UNITED KINGDOM

TNC TRANSACTIONS ON NETWORKS AND COMMUNICATIONS

VOLUME 7, NO. 3
ISSN: 2054 -7420

Prediction of Travel Time Using Fuzzy Logic Paradigm

[1]Ajasa, A. A., [2]Ajayi, I. I., [3]Akinwande, K. D., [4]Ajayi, T.O.,
[1]Lecturer, Department of Electronic and Computer Engineering, Lagos State University, Nigeria,
[2]Research Student, Institut Supérieur d'Electronique de Paris,
[3]Research Student, Interswitch Limited,
[4]Research Student, Montego Holdings,
ajasaaf@yahoo.com; ajasaaf@yahoo.com; idowu-iseoluwa.ajayi@isep.fr;
kolawole.akinwande@interswitchgroup.com; t.ajayi@montego-holdings.com

ABSTRACT

Predicting travel time is an important aspect of human life. It helps to effectively manage and successfully make the most of time. So much time is usually spent on the road when travelling from one place to another, particularly in developing countries and in a mega city like Lagos for example, a little time wasted is a lot of money lost, hence the need to envisage the likely time to reach destinations.

This research work explores the robustness of fuzzy logic to predict travel time on all major routes out of the town where the Engineering faculty of Lagos State University is situated. This paper takes into consideration important factors that can lead to delay in travel time; period of day, weather, car density, and construction, as the fuzzy inputs and based on experience, fuzzy rules are generated to give an estimated time of arrival.

To prove the validity of this work, data were collected from frequent road users and co-efficient of determination was calculated for all three routes. The co-efficient of determination ranked above 90% for all three routes, two of which are discussed.

Keywords: travel time, fuzzy logic, fuzzification, inference, defuzzication, car density, weather, construction, time of day.

1 Introduction

Free flow travel speed is one of the factors that affect travel time. However, the journey speed along an arterial road depends not only on the arterial road geometry but also on the traffic flow characteristics and traffic signal coordination **[1].** Other main factors related to travel time prediction that have also been cited in previous studies include holiday and special incidents, signal delay, weather conditions, traffic operation (disturbed level) and congestion level (traffic flow) **[2,3,4]**.

Direct travel time measurement has only been carried out under regional travel time research projects, mainly in USA and Western Europe in a limited selection of corridors. With few exceptions, the availability of valid travel time databases is very limited. This lack of ground truth data has been a recurrent problem for practitioners in developing and validating their road management schemes **[5]**.

DOI: 10.14738/tnc.73.6449
Publication Date: 16th May 2019
URL: http://dx.doi.org/10.14738/tnc.73.6449

In the past decades, researchers have been actively investigating how to estimate and predict travel time using numerous technologies and algorithms. Many algorithms performed with good accuracy in estimating travel time on freeways under incident and non-incident situations. However, the research of travel time estimation on main roads with signal intersections needs further work. Since vehicles may experience delays caused by intersection control, queue build up problems at intersection, lane drop at intersection, and bottleneck on the downstream link, it is more complicated to estimate the real time travel time on arterial streets than on freeway.

A travel time estimation procedure was developed which can be used for both peak, off-peak, and transition period traffic flow conditions. The methodology proposed is based on using fuzzy logic for the estimation of travel time from flow data obtained from history and experience. The model estimates speed and travel time as a function of time directly from flow measurements. This research incorporated several modifications to this theoretical model such that the model can be used for long analysis intervals and for varying traffic flow conditions. The proposed model is based on the effects of car density, weather, construction and time and day of the week. An estimated time of arrival for all the vehicles that travel during a particular time interval between two selected locations was calculated as output.

There are several methods available for the prediction of travel time, and they can be broadly classified into historic profile approaches, regression analysis, time series analysis, and Artificial Neural Network (ANN) and fuzzy logic models. This study involves the prediction of travel time using fuzzy logic.

Fuzzy Logic is a simple yet very powerful problem-solving technique with extensive applicability. It is currently used in the fields of business, systems control, electronics and traffic engineering. The technique can be used to generate solutions to problems based on "vague, ambiguous, qualitative, incomplete or imprecise information" **[6].** This concept was developed by Lotfi Zadeh in 1965. Fuzzy Logic helps to solve the problem generated by binary logic which classifies statements as either ‘true’ or ‘false’. Fuzzy logic allows a statement to be partially true or partially false removing the crisp boundary that traditional binary logic creates. For example, for a statement ‘I like my food hot’, the question may arise as how hot is hot. Fuzzy logic defines a food temperature of 50^{o}c as partially hot and at the same time partially cold. In fuzzy logic, everything is a matter of degree. Fuzzy logic mimics human control logic and is based on natural language.

Fuzzy logic finds application in many areas e.g. predicting genetic traits, bus time-tables, antilock braking system, medical diagnoses, economics, agriculture, meteorology, aerospace, geology, computer software etc. One of the most popular applications of fuzzy logic is that of the Sendai Subway system in Sendai, Japan. Hence fuzzy logic is used to predict travel time on routes that leads to Epe, a town in Lagos State.

Predicting travel time has been exploited in time past using several methods. Traffic data can be obtained historically, from loop detectors, registration plate matching technique, which recognizes plate number between check points and then measure the time taken; Automatic vehicle identification (AVI) transponders are located inside a vehicle and are used in electronic toll collection applications. A practical case of signpost-based system in Sydney is ANTTS (Automatic Network Travel Time System) **[7].** Other method includes: inductance loops, weigh-in-motion stations, or aerial video to estimate or calculate travel time. However, this research is not as considered about method of accumulating traffic data than the technique of predicting the travel time. Many research studies have used ANN techniques to estimate and predict travel-time that includes Advanced Neural Network and Mix-structure Neural Network **[8, 9]**.

In Anderson and Bell's study, they used traffic data from registration plate survey, traffic detectors and simulation software, VISSIM, to develop Neural Network estimation techniques and a queuing model for travel-time prediction in urban road networks. However, this research used fuzzy logic to estimate historical traffic data and to predict travel time on the roads specified.

2 Methodology

Fuzzy logic inference system was used in this project for predicting travel time. Fuzzy logic, the ultimate subject of this text, was developed to accommodate sentences containing vague predicates (as well as other vague parts of speech). One of the defining characteristics of fuzzy logic is that it admits truth-values other than true and false; in fact it admits infinitely many truth-values. Fuzzy logic does not assume the Principle of Bivalence **[10].**

Fuzzy logic interference systems are of two types namely: Mamdani and Sugeno. Mamdani inference style is used in this paper as it is more intuitive, has widespread acceptance and better suited to human input. Fuzzy inference system is divided into: Fuzzification, inference which includes aggregation and implication and then defuzzification.

Fuzzification is the process of determining the degree to which each input belongs to each of the appropriate fuzzy sets through membership functions. It converts a crisp numerical value from the universe of discourse of the input variable into a linguistic variable and corresponding level of belief. Inference implies the generation of rules and assigning weight to each rule using fuzzy operators.

Aggregation serves as the input to the defuzzication process. It involves making into fuzzy set, the output of each rule. The input of the aggregation process is the list of truncated output functions returned by the implication process for each rule. The output of the aggregation process is one fuzzy set for each output variable. The input of the aggregation process is the list of truncated output functions returned by the implication process for each rule. The output of the aggregation process is one fuzzy set for each output variable. Each rule gives an output which is aggregated; the output of the aggregation process is one fuzzy set for each output variable.

The process of converting these fuzzy sets back to a crisp value is known as defuzzification. Matlab fuzzy logic toolbox is used to design the prediction mechanism.

2.1 Input Space

The input variables to be considered are the factors that affect travel time which are time of the day, weather, car density and construction, while time of arrival is the output variable. The variables are then categorized into domains known as fuzzy sets. Table 1 shows the fuzzy sets defined in this system.

Table 1. Fuzzy sets used in predicting time travel.

Time	Weather	Car Density	Construction
Off peak	Clear	Low	None
Semi peak	Light rain	Medium	Minor
Peak	Heavy rain	High	Major

Input membership functions are then selected to accurately define the fuzzy sets. Membership functions are curves that determine the degree to which each i0nput belongs to a fuzzy set. Various membership functions were used in this research as provided by fuzzy logic Toolbox. E.g. triangular membership function (trimf), z-membership function (zmf) and s-membership function (smf). Others include guassmf, guass2mf, trapmf, dsigmf, sigmf, psigmf, gbellmf, pimf. The synopsis of the input membership functions used is shown below.

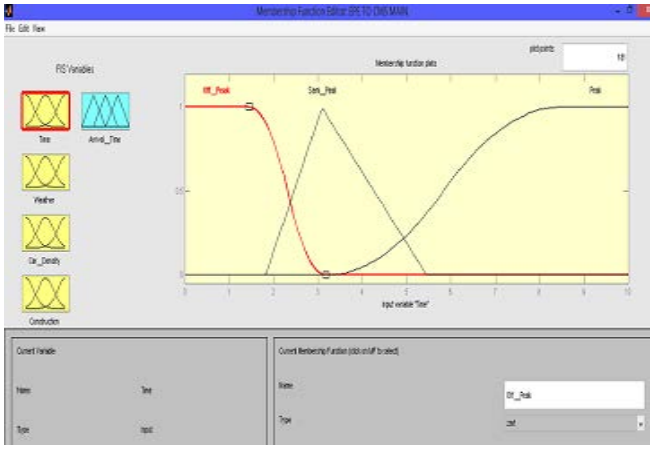

Figure 1. Input membership function

2.2 Output Space

The membership function description of the output space i.e.arrival time is considered in this section. All linguistic terms are described using the triangular membership function curves. A total of 81 rules were exhaustively used for this road. These rules combined all possible condtions that could ever happen using all the input variables.

2.3 Rule Construction

The rules are described using the "If (precedent), then (antecedent)" format. Examples of situations that could result are TIME: off peak, WEATHER: clear weather, CAR DENSITY: low car density and CONSTRUCTION: no construction, TIME: semi peak, WEATHER: heavy rain, CAR DENSITY: high car density, CONSTRUCTION: minor construction, to mention a few.

3 Result Analysis

As earlier mentioned, the three roads considered were CMS-Epe road, Ketu- Epe road and Ijebu-Ode-Epe road. A collection of data was carried out before the commencement of simulation. These data were collected through examination of the roads, interview of drivers that regularly ply these roads, visits to Lagos State Drivers Institute (Epe Branch) and also the internet. To predict the time of arrival, the rule view is used and three different situations are considered for each road.

3.1 Siuation Comparism for the three roads

Situation 1:this situation occurs when the rules says it is peak period, clear weather, low car density and no construction on the road. This situation is entered as [0 0 0 0] in the rule view of matlab fuzzy logic toolbox and the output which is the estimated time of arrival is 99.5 minutes.

Situation 2: It happens when the rule says it is peak period, there is heavy rain, high car density and a major construction. This situation represents worst conditions and is entered as [10 10 10 10] in the rule view. The output shows 203 minutes or 3 hours 23 minutes.

Situation 3: when the rule says the it is off-peak, there is heavy rain, low car density and a major construction. The output shows that it will take 127 minutes or 2hours 7 minutes.this is inputted as [0 10 0 10]. The figure below shows the result of the rule view.0

The estimated time of arrival for the other two roads are shown in Table 2.

Table 2. Arrival Time for the 3 situations

Situation	Epe-CMS (mins)	Epe-Ketu (mins)	Epe-Ijebu-Ode (mins)
[0 0 0 0]	99.5	99.5	46.4
[0 10 0 10]	127	142	92.3
[10 10 10 10]	203	203	100

3.2 Relationship Between the Input Variables

The relationship between the inputs variables such as the 'Time_and_Day', 'Weather', 'Car Density' ,and 'Construction' and 'Arrival_time' can be shown using the surface viewer of the matlab® fuzzy logic toolbox.

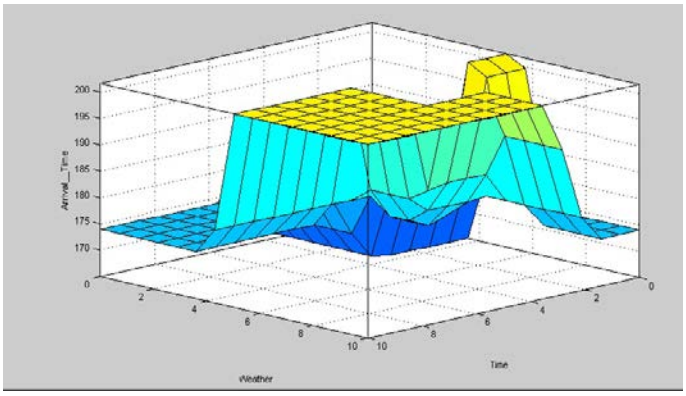

Figure 2. Weather against Time

Figure 2. shows the relationship between weather and time and how it affects the arrival time for the CMS_EPE route. Weather takes into consideration that although there may be a forecast of rainfall, the effect of light rain on the time of arrival, clearly differs from when the rainfall is heavy. Variations also occur during transitions from off-peak periods through semi-peak to peak periods. Analysing the individual effects of the inputs on the time of arrival would be considered simple to do but in a real life scenario that doesn't apply, but from the three-dimensional graph above, it is evident that at the peak of the day and at worst weather conditions the time of arrival is greatly affected i.e time of arrival is very late. There is a gradual and then steep rise in the curve of the weather as the weather grows worse but the effect is dependent on the period of the day. For example, the arrival time will be slightly affected when the rainfall is heavy in an off-peak period.

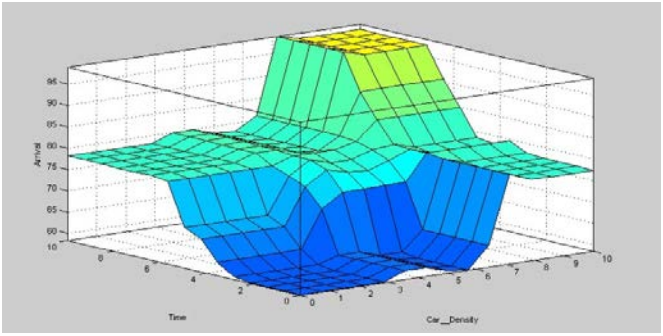

Figure 3. Weather against Time

Figure 3. shows the effects of 'time' and 'Car-density' on the EPE-IJEBU route. Obviously, when observing the action of time on arrival, it is seen that the time of arrival increases, and the same goes with the effect of car_density alone. Bank holidays and festive periods were taken into consideration in the determination of the effect of car density on the time of arrival. The fuzzified effect of both inputs can also be observed from the three-dimensional graph above. The time of arrival increses as both inputs increases.

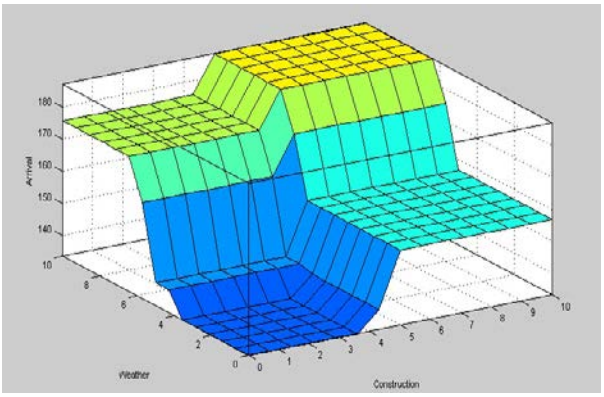

Figure 4. Weather against Construction

Weather against construction is considered for EPE-KETU route. Construction and weather are major impediments on lagos routes and a sharp increase is seen on the time of arrival as light rain graduates into heavy rain and as construction moves from minor to major. The effect of major construction is definite as that speaks of the flat bed observed from the point of 5-10 on the y-axis. The arrival time is very late as both inputs reach their peak conditions. With the absolute absence of construction and on a clear weather day, the arrival time is observed to be reasonably early.

3.3 Confirmation of Result Obtained using the Discussed Approach

The results of the prediction is compared with data collected from frequent road user via questionnaires. Questionnaires were issued to commercial cab/bus driver to know their time of arrival on specific situations.

Table 3. Predicted Time of Arrival vs. Collected Time of Arrival for Epe- Ketu

Time	Weather	Car Density	Construction	Predicted Time of arrival (mins)	Collected time of Arrival (mins)
off peak	clear weather	low car density	no construction.	99	100
off peak	heavy rain	low car density	no construction	142	148
semi-peak	clear weather	medium car density	no construction	133	142
semi peak	light rain	medium car density	major construction	157	143
Peak	heavy rain	low car density	major construction	174	178
semi-peak	heavy rain	medium car density	major construction	187	190
Peak	light rain	low car density	major construction	165	164
off-peak	light rain	low car density	minor construction	127	125
Peak	Clear	low car density	major construction	156	159
Peak	heavy rain	high car density	major construction	203	208

The co-efficient of determination calculated for the data for Ketu-Epe road is 0.9812. This demonstrates that the linear equation $1.0592x - 7.2950$ predicts 98% of the variance in the collected time of arrival.

Coefficient of determination, or R^2 (pronounced r-square) was calculated for this data. This statistic indicates how closely values we obtained from fitting a model match the dependent variable the model is intended to predict. Statisticians often define R^2 using the residual variance from a fitted model:

$$R^2 = 1 - \frac{\text{SSresid}}{\text{SStotal}}$$

SSresid is the sum of the squared residuals from the regression.

SStotal is the sum of the squared differences from the mean of the dependent variable (*total sum of squares*).

The co-efficient of determination for the data for Epe-Cms reads 0.9467. This demonstrates that the linear equation $1.0133x - 0.6445$ predicts 96% of the variance in the collected time of arrival.

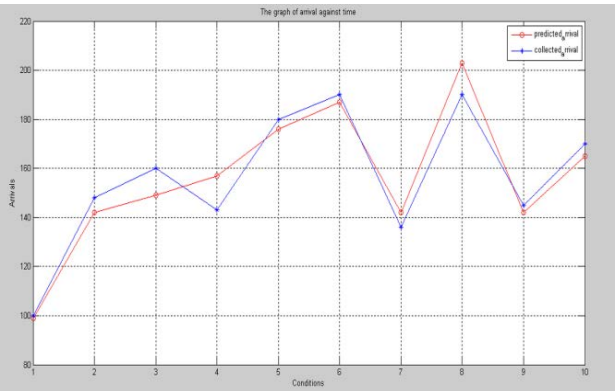

Figure 5. Graph showing relationship between predicted arrival and collected arrival for Epe-Ketu

Table 4. Predicted Time of Arrival vs. Collected Time of Arrival for Epe- Ijebu-Ode

Time	Weather	Car Density	Construction	Predicted Time of arrival (mins)	Collected tie of Arrival (mins)
off peak	clear weather	low car density	no construction	99	96
off peak	heavy rain	medium car density	no construction	127	130
semi-peak	clear weather	medium car density	no construction	165	167
semi-peak	light rain	medium car density	major construction	182	190
Peak	heavy rain	low car density	major construction	202	205
semi-peak	heavy rain	medium car density	major construction	202	200
Peak	light rain	low car density	major construction	165	170
off-peak	light rain	low car density	minor construction	152	145
Peak	Clear	low car density	major construction	174	185
Peak	heavy rain	high car density	major construction	203	209

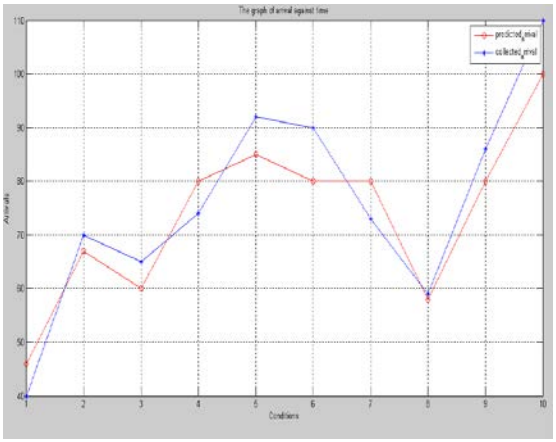

Figure 6. Graph showing relationship between predicted arrival and collected arrival for Epe-Ijebu-Ode

The co-efficient of determination for the data collected for Epe-Ijebu-Ode road reads 0.9114. This demonstrates that the linear equation $1.1912x - 11.7688$ predicts 91% of the variance in the collected time of arrival.

4 Conclusion

It can be concluded that the fuzzy logic paradigm approach to travel time prediction is very robust and even with not very precise input variables, we are still able to obtain near accurate output as seen from the coefficient of determination of the results obtained. Further work can be done to extend this model to other major roads and include more input variables for greater accuracy and resilience in computation.

REFERENCES

[1] Lum, K.M., Fan, H. S.L., Lam, S.H. and Olszewski, P. (1998) Speed-Flow Modeling of Arterial Roads in Singapore, Journal of Transportation Engineering, Vol. 124, no. 6, Proceedings of the Eastern Asia Society for Transportation Studies, Vol. 5, pp. 1433 - 1448, 2005 213-222.

[2] Karl, C.A., Charles, S. and Trayford, R. (1999) Delivery of Real-Time and Predictive Travel Time Information: Experiences from a Melbourne Trial. Proceedings of 6th World Congress on Intelligent Transport Systems, Toronto, Canada.

[3] Wu, C.-F. (2001) The Study of Vehicle Travel Time Estimation using GPS, Department of Transportation Technology & Management, (Master Thesis), National Chiao Tung University, Taipei.

[4] Chien, S.I-J. And Kuchipudi, C. M. (2003) Dynamic travel time prediction with real-time and historic data, Journal of Transportation Engineering, Vol. 129, No. 6,608-616.

[5] Francesc Soriguera Marti, (2016) Springer Tracts on Transportation and Traffic Volume 11, Highway Travel Time Estimation With Data Fusion, Technical University of Catalonia, Barcelona, Spain

[6] Fuzzy Logic in C, Viot G., Dr. Dobb's Journal, February 1993.

[7] Hong-En LIN, Rocco ZITO, Michael A P TAYLOR. A REVIEW OF TRAVEL TIME PREDICTION IN TRANSPORT AND LOGISTICS.

[8] Wei, C.-H., Lin, S.-C. And Li, Y. (2003) Empirical Validation of Freeway Bus Travel Time Forecasting, Transportation Planning Journal, Vol. 32, 651-679.

[9] Jiang, G. and Zhang, R. (2001) Travel Time Prediction for Urban Arterial Road: A Case on China. Proceedings of Intelligent Transport System, IEEE, 255-260.

[10] Merrrie Bergmann, (2008) An Introduction to Many-Valued and Fuzzy Logic: Semantics, Algebra, and Derivation Systems. Cambridge University Press/9780521881289

[11] Falola, T., & Olanrewaju, S.A. (Eds.). (1986). *Transport systems in Nigeria.* Syracuse, NY: Maxwell School of Citizenship and Public Affairs, Syracuse University.

[12] Kenworthy, J. R., & Newman, P. (1999). *Sustainability and cities*. Washington, DC: Island Press. ISBN: 1559636602.9781559636605.

[13] Van Grol, H.J.M., Danech-pajouh, M., Manfredi, S. and Whittaker, J. (1999) DACCORD: Proceedings of the Eastern Asia Society for Transportation Studies, Vol. 5, pp. 1433 - 1448, 2005 1447 on-line travel time prediction, World Conference on Transport Research Society (WCTRS), Vol. 2, 455-467.

SOCIETY FOR SCIENCE AND EDUCATION
UNITED KINGDOM

TNC TRANSACTIONS ON NETWORKS AND COMMUNICATIONS

VOLUME 7, NO. 3
ISSN: 2054 -7420

Decision Matrix Equation and Block Diagram of Multilayer Electromagnetoelastic Actuator Micro and Nanodisplacement for Communications Systems

Sergey Mikhailovich Afonin
National Research University of Electronic Technology (MIET), Moscow, Russia;
eduems@mail.ru

ABSTRACT

For the communications systems the parametric block diagram of the multilayer electromagnetoelastic actuator micro and nanodisplacement or the multilayer piezoactuator is determined in contrast to Cady and Mason's electrical equivalent circuits for the calculation of the piezoelectric transmitter and receiver, the vibration piezomotor. The decision matrix equation of the multilayer electromagnetoelastic actuator is used. The parametric block diagram of multilayer electromagnetoelastic actuator is obtained with the mechanical parameters the displacement and the force. The transfer functions of the multilayer electroelastic actuator are determined. The the generalized parametric block diagram, the generalized matrix equation for the multilayer electromagnetoelastic actuator micro and nanodisplacement are obtained. The deformations of the multilayer electroelastic actuator for the nanotechnology are described by the matrix equation. Block diagram and structural-parametric model of multilayer electromagnetoelastic actuator micro and nanodisplacement of the communications systems are obtained, its transfer functions are bult. Effects of geometric and physical parameters of multilayer electromagnetoelastic actuators and external load on its dynamic characteristics are determined. For calculations the communications systems with the multilayer piezoactuator for micro and nanodisplacement the parametric block diagram and the transfer functions of the multilayer piezoactuator are obtained.

Keywords: Multilayer electromagnetoelastic actuator; Parametric block diagram; Matrix transfer function; Multilayer piezoactuator.

1 Introduction

The multilayer electromagnetoelastic actuator is used for precise alignment in the range of movement from nanometers to tens of micrometers in nanotechnology, adaptive optics, communications systems. In the work the block diagram of multilayer electromagnetoelastic actuator for micro and nanodisplacement on the piezoelectric, piezomagnetic, electrostriction, magnetostriction effects, for example, the block diagram of the multilayer piezoactuator is determined in contrast to Cady and Mason's electrical equivalent circuits for the calculation of the piezotransmitter and piezoreceiver, the vibration piezomotor [1 – 11]. The block diagram of multilayer electromagnetoelastic actuator is obtained with the mechanical parameters the displacement and the force. Piezoactuator is piezomechanical device intended

DOI: 10.14738/tnc.73.6564
Publication Date: 9th June 2019
URL: http://dx.doi.org/10.14738/tnc.73.6564

for actuation of mechanisms, systems or management based on the piezoeffect, converts the electrical signals into the mechanical movement or the force [11 − 15].

The investigation of the static and dynamic characteristics of the multilayer piezoactuator is necessary for the calculation mechatronics systems of the micro and nanometric movements for the communications systems. The multilayer piezoactuators are used in the micro and nanomanipulators for scanning tunneling microscopes and atomic force microscopes [7 - 23].

By decision matrix equation of the multilayer electromagnetoelastic actuator with allowance for the corresponding equation of the electromagnetoelasticity, the boundary conditions on loaded working surfaces of the multilayer electromagnetoelastic actuators, and the strains along the coordinate axes, it is possible to construct a structural parametric model of the multilayer electromagnetoelastic actuator [8, 9, 16]. The transfer functions and the parametric block diagrams of the multilayer electromagnetoelastic actuators are obtained from the set of equations describing the corresponding structural parametric model of the multilayer actuator for the communications systems. The solution of the matrix equation of the multilayer electromagnetoelastic actuator with the Laplace transform are used for the construction the parametric block diagram of the electromagnetoelastic actuator. As the result of the joint solution of the matrix equation of the multilayer actuator with the Laplace transform, the equation of the electromagnetoelasticity, the boundary conditions on the two loaded working surfaces of the multilayer actuator, we obtain the corresponding structural-parametric model and the parametric block diagram of the multilayer electromagnetoelastic actuator.

2 Block diagram of multilayer electromagnetoelastic actuator

For the communications systems the parametric block diagram and the matrix transfer functions of the multilayer electromagnetoelastic actuator are obtained from the structural-parametric model of the multilayer actuator with the mechanical parameters the displacement and the force. The parametric block diagrams of the voltage or current-controlled multilayer piezoactuator are determined using the equation of the inverse piezoeffect in the form [8, 11]:

for the voltage control

$$S_i = d_{mi}E_m + s_{ij}^E T_j \tag{1}$$

for the current control

$$S_i = g_{mi}D_m + s_{ij}^D T_j \tag{2}$$

where the indexes $i = 1, 2, \ldots, 6$, $j = 1, 2, \ldots, 6$, $m = 1, 2, 3$, with 1, 2, 3 are mutually perpendicular coordinate axes, S_i is relative deformation with index *I*, d_{mi} is the piezoelectric module, E_m is electric field strength and D_m is the electric induction along the axis *m*, g_{mi} is the piezoelectric constant; s_{ij}^E, s_{ij}^D are the elastic compliances with $E = \text{const}$ and $D = \text{const}$, T_j is the mechanical stress with index *j*, therefore we obtain $\Psi = E, D$ generalized control parameter in the form of the electric field strength or the electric induction for the voltage or current-controlled of the multilayer piezoactuator.

The equation of the direct piezoeffect has the form [8, 11]

$$D_m = d_{mi} T_i + \varepsilon^T_{mk} E_k \tag{3}$$

where the indexes m = 1, 2, 3, k = 1, 2, 3, ε^T_{mk} is the dielectric constants for $T = \text{const}$.

Accordingly in general the equation of the electromagnetoelasticity of the multilayer electromagnetoelastic actuator [11, 14, 16, 20] has the form

$$S_i = \nu_{mi} \Psi_m(t) + s^{\Psi}_{ij} T_j(x,t) \tag{4}$$

where $S_i = \partial\xi(x,t)/\partial x$ is the relative displacement along axis i of the cross section of the actuator, therefore we obtain $\Psi = E, D, H$ generalized control parameter in the form E_m for the voltage control, D_m for the current control, H_m for magnetic field strength control along axis m, T_j is the mechanical stress along axis j, ν_{mi} is the coefficient of electromagnetoelasticity, for example, piezoelectric module or magnetostriction coefficient, s^{Ψ}_{ij} is the elastic compliance with $\Psi = \text{const}$. The multilayer piezoactuator on Figure 1 consist from the piezolayers or the piezoplates connected electrically in parallel and mechanically in series.

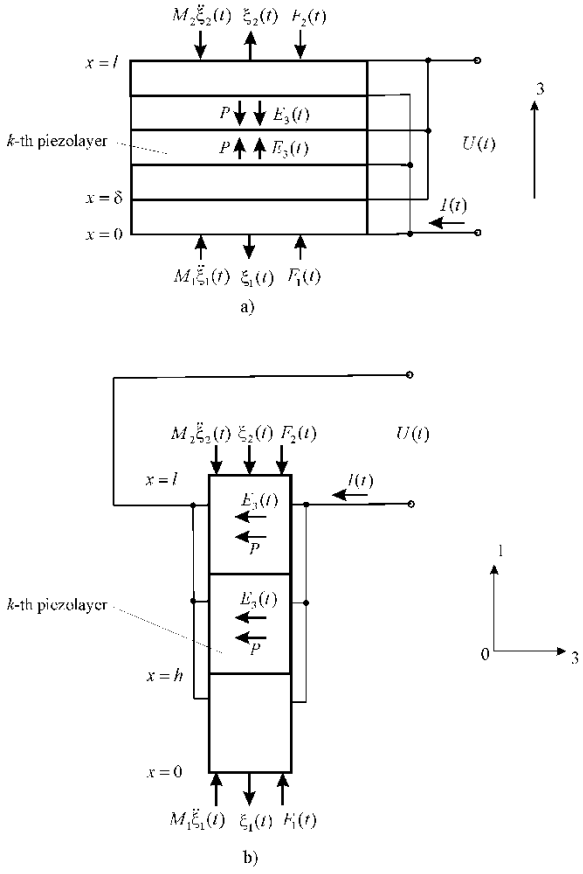

Figure 1. The multilayer piezoactuator a) for the longitudinal piezoeffect, b) for the transverse piezoeffect

For example, we consider the matrix equation for the Laplace transforms of the forces and of the displacements [7] at the input and output ends of the k-th piezolayer of the multilayer piezoactuator from n the layers. The equivalent T-shaped quadripole of the k-th piezolayer is shown on Figure 2.

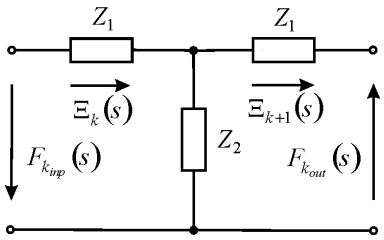

Figure 2. The quadripole for *k*-th piezolayer

The circuit of the multilayer piezoactuator on Fugure 3 is compiled from the equivalent *T*-shaped quadripole for the *k*-th piezolayer and the forces equations, acting on the faces the piezolayer. Therefore on Fugure 2 and Fugure 3 we have the Laplace transforms of the corresponding forces on the input and output faces of the *k*-th piezolayer of the multilayer piezoactuator in the form of the system of the equations for the equivalent *T*-shaped quadripole

$$F_{k_{inp}}(s) = -(Z_1 + Z_2)\Xi_k(s) + Z_2\Xi_{k+1}(s)$$

$$-F_{k_{out}}(s) = -Z_2\Xi_k(s) + (Z_1 + Z_2)\Xi_{k+1}(s) \tag{5}$$

where $Z_1 = \frac{S_0\gamma\,\mathrm{th}(\delta\gamma)}{s_{ij}^{\Psi}}$, $Z_2 = \frac{S_0\gamma}{s_{ij}^{\Psi}\,\mathrm{sh}(\delta\gamma)}$ are the resistance of the equivalent quadripole of the *k*-th piezolayer, δ is the thickness on Figure 1a, $\gamma = \frac{s}{c^{\Psi}} + \alpha$ is the coefficient of wave propagation, $F_{k_{inp}}(s)$, $F_{k_{out}}(s)$ are the Laplace transform of the forces at the input and output ends of the *k*-th piezolayer, $\Xi_k(s)$, $\Xi_{k+1}(s)$ are the Laplace transforms of the displacements at input and output ends of the *k*-th piezolayer, *s* is the Laplace operator, c^{Ψ} is the speed of sound in the piezoceramics with $\Psi = \mathrm{const}$, α is the attenuation coefficient, s_{ij}^{Ψ} is the elastic compliance with $\Psi = \mathrm{const}$.

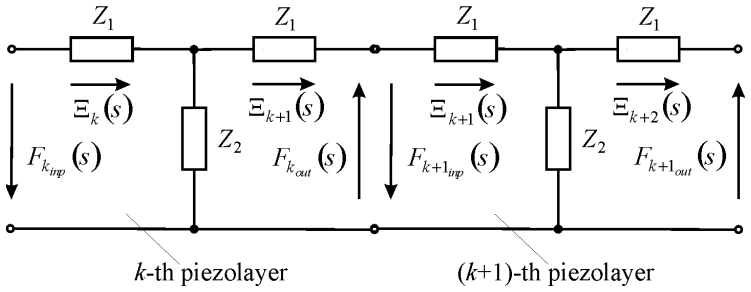

Figure 3. The circuit of the multilayer piezoactuator with the quadripoles for *k*-th and (*k*+1)-th piezolayers

Accordingly we have for Figure 2 the Laplace transforms the following system of the equations for the *k*-th piezolayer in the form

$$-F_{k_{inp}}(s)=\left(1+\frac{Z_1}{Z_2}\right)F_{k_{out}}(s)+Z_1\left(2+\frac{Z_1}{Z_2}\right)\Xi_{k+1}(s)$$

$$\Xi_k(s)=\frac{1}{Z_1}F_{k_{out}}(s)+\left(1+\frac{Z_1}{Z_2}\right)\Xi_{k+1}(s) \tag{6}$$

the matrix equation for the *k*-th piezolayer

$$\begin{bmatrix}-F_{k_{inp}}(s)\\ \Xi_k(s)\end{bmatrix}=[M]\begin{bmatrix}F_{k_{out}}(s)\\ \Xi_{k+1}(s)\end{bmatrix} \tag{7}$$

and the matrix $[M]$ in the form

$$[M]=\begin{bmatrix}m_{11} & m_{12}\\ m_{21} & m_{22}\end{bmatrix}=\begin{bmatrix}1+\frac{Z_1}{Z_2} & Z_1\left(2+\frac{Z_1}{Z_1}\right)\\ \frac{1}{Z_2} & 1+\frac{Z_1}{Z_2}\end{bmatrix} \tag{8}$$

where $m_{11}=m_{22}=1+\frac{Z_1}{Z_2}=\mathrm{ch}(\delta\gamma)$, $m_{12}=Z_1\left(2+\frac{Z_1}{Z_1}\right)=Z_0\mathrm{sh}(\delta\gamma)$, $m_{21}=\frac{1}{Z_2}=\frac{\mathrm{sh}(\delta\gamma)}{Z_0}$, $Z_0=\frac{S_0\gamma}{s_{ij}^{\Psi}}$.

For the multilayer piezoactuator of the Laplace transform the displacement $\Xi_{k+1}(s)$ and the force $F_{k_{out}}(s)$ acting on the output face of the *k*-th layer on Figure 3 are corresponded to Laplace transforms of displacement and force acting on the input face of the (*k* + 1)-th layer.

The force on the output face for the *k*-th piezolayer is equal in magnitude and opposite in direction to the force on the input face for the (*k* + 1)-th piezolayer, hence

$$F_{k_{out}}(s)=-F_{k+1_{inp}}(s)$$

From equation (7) the matrix equation for *n* piezolayers of the multilayer piezoactuator has the form

$$\begin{bmatrix}-F_{1_{inp}}(s)\\ \Xi_1(s)\end{bmatrix}=[M]^n\begin{bmatrix}F_{n_{out}}(s)\\ \Xi_{n+1}(s)\end{bmatrix} \tag{9}$$

with the matrix of the multilayer piezoactuator

$$[M]^n=\begin{bmatrix}\mathrm{ch}(n\delta\gamma) & Z_0\mathrm{sh}(n\delta\gamma)\\ \frac{\mathrm{sh}(n\delta\gamma)}{Z_0} & \mathrm{ch}(n\delta\gamma)\end{bmatrix}$$

Accordingly in general the matrix for the equivalent quadripole of the multilayer electromagnetoelastic actuator has the form

$$[M]^n=\begin{bmatrix}\mathrm{ch}(l\gamma) & Z_0\mathrm{sh}(l\gamma)\\ \frac{\mathrm{sh}(l\gamma)}{Z_0} & \mathrm{ch}(l\gamma)\end{bmatrix}$$

Therefore we have from the equation (9) the equivalent quadripole of the multilayer piezoactuator on Figure 1 for the longitudinal piezoeffect with length of the multilayer piezoactuator $l = n\delta$, for the transverse piezoeffect with length $l = nh$, for the shift piezoeffect with length $l = nb$, where δ, h, b are the thickness, the height, the width for the *k*-th piezolayer.

Equations of the forces acting on the faces of the multilayer piezoactuator:

$$\text{at } x = 0,\ T_j(0,s)S_0 = F_1(s) + M_1 p^2 \Xi_1(s)$$

$$\text{at } x = l,\ T_j(l,s)S_0 = -F_2(s) - M_2 p^2 \Xi_2(s) \tag{10}$$

where $T_j(0,s)$, $T_j(l,s)$ are the Laplace transforms of mechanical stresses at the two ends of the multilayer piezoactuator.

The Laplace transform of the displacement and the force for the first face of the multilayer piezoactuator has the form

$$\text{at } x = 0 \text{ and } \Xi_1(s),\ F_1(s)$$

the Laplace transforms of the displacement and the forces for the the second face of the piezoactuator has the following form

$$\text{at } x = l \text{ and } \Xi_2(s) = \Xi_{n+1}(s),\ F_2(s) = F_{n_{out}}(s)$$

Let us construct the structural-parametric model of the multilayer electromagnetoelastic actuator. From equation (4) the Laplace transform of the force, which causes the deformation, has the form

$$F(s) = \frac{\nu_{mi} S_0 \Psi_m(s)}{s_{ij}^{\Psi}} \tag{11}$$

Accordingly we have the equations for the structural-parametric model and the generalized block diagram of the multilayer electromagnetoelastic actuator on Figure 4. The structural-parametric model is obtained in result analysis of the equation of the force that causes deformation, of the system of the equations for the equivalent quadripole of the multilayer electromagnetoelastic actuator, the equation of the forces on its faces in the following form

$$\Xi_1(s) = \left[\frac{1}{M_1 s^2}\right]\left\{-F_1(s) + \left(\frac{1}{\chi_{ij}^{\Psi}}\right)\left[\begin{array}{l}\nu_{mi}\Psi_m(s) - \left[\dfrac{\gamma}{\mathrm{sh}(l\gamma)}\right]\times \\ \times\left[\mathrm{ch}(l\gamma)\Xi_1(s) - \Xi_2(s)\right]\end{array}\right]\right\}$$

$$\Xi_2(s) = \left[\frac{1}{M_2 s^2}\right]\left\{-F_2(s) + \left(\frac{1}{\chi_{ij}^{\Psi}}\right)\left[\begin{array}{l}\nu_{mi}\Psi_m(s) - \left[\dfrac{\gamma}{\mathrm{sh}(l\gamma)}\right]\times \\ \times\left[\mathrm{ch}(l\gamma)\Xi_2(s) - \Xi_1(s)\right]\end{array}\right]\right\} \tag{15}$$

where $\nu_{mi} = \begin{cases} d_{33}, d_{31}, d_{15} \\ g_{33}, g_{31}, g_{15} \\ d_{33}, d_{31}, d_{15} \end{cases}$, $\Psi_m = \begin{cases} E_3, E_1 \\ D_3, D_1 \\ H_3, H_1 \end{cases}$, $s_{ij}^{\Psi} = \begin{cases} s_{33}^{E}, s_{11}^{E}, s_{55}^{E} \\ s_{33}^{D}, s_{11}^{D}, s_{55}^{D} \\ s_{33}^{H}, s_{11}^{H}, s_{55}^{H} \end{cases}$, $c^{\Psi} = \begin{cases} c^{E} \\ c^{D} \\ c^{H} \end{cases}$, $\gamma = \begin{cases} \gamma^{E} \\ \gamma^{D} \\ \gamma^{H} \end{cases}$, $l = \begin{cases} \delta \\ h \\ b \end{cases}$, $\chi_{ij}^{\Psi} = s_{ij}^{\Psi} / S_0$.

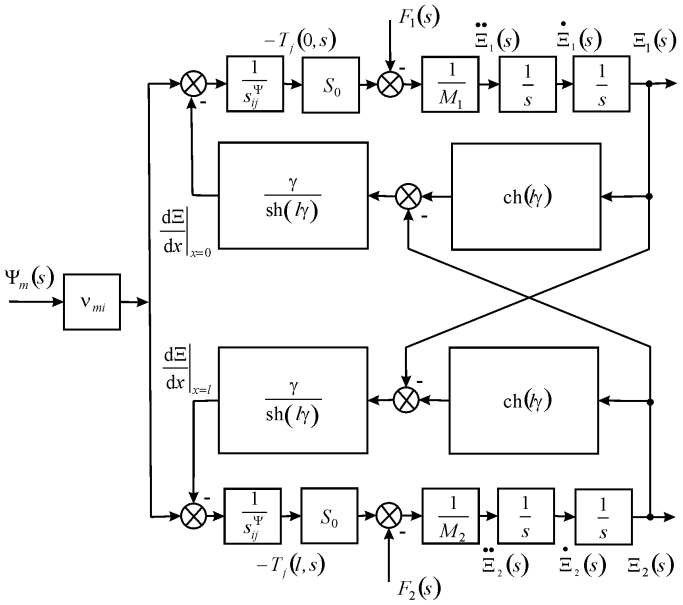

Figure 4. The generalized block diagram of the electromagnetoelastic actuator

The generalized block diagram of the electromagnetoelastic actuator is constructed using the generalized structural-parametric model of the multilayer electromagnetoelastic actuator micro and nanodisplacement for the communications systems.

3 Matrix transfer function of multilayer electromagnetoelastic actuator

The matrix transfer function of the multilayer electromagnetoelastic actuator determined from its structural-parametric model (15) has the form

$$\begin{bmatrix} \Xi_1(s) \\ \Xi_2(s) \end{bmatrix} = \begin{bmatrix} W_{11}(s) & W_{12}(s) & W_{13}(s) \\ W_{21}(s) & W_{22}(s) & W_{23}(s) \end{bmatrix} \begin{bmatrix} \Psi_m(s) \\ F_1(s) \\ F_2(s) \end{bmatrix} \tag{16}$$

Therefore in general the matrix transfer function of the multilayer electromagnetoelastic actuator is obtained in following form

$$[\Xi(s)] = [W(s)][P(s)] \tag{17}$$

$$[\Xi(s)] = \begin{bmatrix} \Xi_1(s) \\ \Xi_2(s) \end{bmatrix}, \quad [W(s)] = \begin{bmatrix} W_{11}(s) & W_{12}(s) & W_{13}(s) \\ W_{21}(s) & W_{22}(s) & W_{23}(s) \end{bmatrix}, \quad [P(s)] = \begin{bmatrix} \Psi_m(s) \\ F_1(s) \\ F_2(s) \end{bmatrix}$$

where $[\Xi(s)]$ is the column-matrix of the Laplace transforms of the displacements, $[W(s)]$ is the matrix transfer function, $[P(s)]$ the column-matrix of the Laplace transforms of the control parameter and the forces.

The generalized transfer functions of the electromagnetoelastic actuator are the ratio of the Laplace transform of the displacement of the face and the Laplace transform of the corresponding control parameter or the force at zero initial conditions

$$W_{11}(s)=\Xi_1(s)/\Psi_m(s)=\nu_{mi}\left[M_2\chi_{ij}^{\Psi}s^2+\gamma\mathrm{th}(l\gamma/2)\right]\Big/A_{ij}$$

$$\chi_{ij}^{\Psi}=s_{ij}^{\Psi}/S_0$$

$$A_{ij}=M_1M_2\left(\chi_{ij}^{\Psi}\right)^2s^4+\left\{(M_1+M_2)\chi_{ij}^{\Psi}/\left[c^{\Psi}\mathrm{th}(l\gamma)\right]\right\}s^3+$$
$$+\left[(M_1+M_2)\chi_{ij}^{\Psi}\alpha/\mathrm{th}(l\gamma)+1/\left(c^{\Psi}\right)^2\right]s^2+2\alpha s/c^{\Psi}+\alpha^2$$

$$W_{21}(s)=\Xi_2(s)/\Psi_m(s)=\nu_{ij}\left[M_1\chi_{ij}^{\Psi}s^2+\gamma\mathrm{th}(l\gamma/2)\right]\Big/A_{ij}$$

$$W_{12}(s)=\Xi_1(s)/F_1(s)=-\chi_{ij}^{\Psi}\left[M_2\chi_{ij}^{\Psi}s^2+\gamma/\mathrm{th}(l\gamma)\right]\Big/A_{ij}$$

$$W_{13}(s)=\Xi_1(s)/F_2(s)=$$
$$=W_{22}(s)=\Xi_2(s)/F_1(s)=\left[\chi_{ij}^{\Psi}\gamma/\mathrm{sh}(l\gamma)\right]/A_{ij}$$

$$W_{23}(s)=\Xi_2(s)/F_2(s)=-\chi_{ij}^{\Psi}\left[M_1\chi_{ij}^{\Psi}s^2+\gamma/\mathrm{th}(l\gamma)\right]\Big/A_{ij}$$

From generalized structural-parametric model of the multilayer electromagnetoelastic actuator its generalized block diagram and generalized matrix transfer function are determined to calculate the characteristics of the multilayer electromagnetoelastic actuator micro and nanodisplacement for the communications system.

For the approximation of the hyperbolic cotangent by two terms of the power series in the transfer function of the multilayer piezoactuator (16) for the elastic-inertial load with one fixed face at $M_1\to\infty$, $m<<M_2$ and for the longitudinal piezoeffect with the voltage control of the multilayer piezoactuator its block diagram on Figure 5 and expression of the transfer function are obtained in following form

$$W(s)=\frac{\Xi_2(s)}{U(s)}=\frac{d_{33}n}{\left(1+C_e/C_{33}^E\right)\left(T_t^2s^2+2T_t\xi_ts+1\right)} \tag{18}$$

$$T_t=\sqrt{M_2/\left(C_e+C_{33}^E\right)},\quad \xi_t=\alpha l^2C_{33}^E\Big/\left[3c^E\sqrt{M_2\left(C_e+C_{33}^E\right)}\right]$$

where $\Xi_2(s)$, $U(s)$ are the Laplace transforms the displacement face of the multilayer piezoactuator and the voltage, T_t is the time constant and ξ_t is the damping coefficient of the multilayer piezoactuator, $C_{33}^E = S_0 / \left(s_{33}^E l\right)$ is the is rigidity of the multilayer piezoactuator for the longitudinal piezoeffect for $E = \text{const}$.

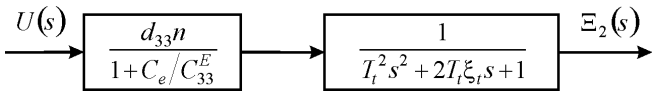

Figure 5. The block diagram of the voltage-controlled multilayer piezoactuator for the longitudinal piezoeffect and elastic-inertial load

Let us construct from (18) the transient response of the multilayer piezoactuator for the longitudinal piezoelectric effect with the voltage control. The expression for the transient response of the voltage-controlled the multilayer piezoactuator for the longitudinal piezoeffect and elastic-inertial load is determined in the form

$$\xi(t) = \xi_m \left[1 - \frac{e^{-\frac{\xi_t t}{T_t}}}{\sqrt{1-\xi_t^2}} \sin\left(\omega_t t + \varphi_t\right) \right]$$

$$\xi_m = \frac{d_{33} n U_m}{1 + C_e / C_{33}^E}, \quad \omega_t = \sqrt{1-\xi_t^2} / T_t, \quad \varphi_t = \operatorname{arctg}\left(\sqrt{1-\xi_t^2} / \xi_t \right)$$

where ξ_m is the steady-state value of displacement of the multilayer piezoactuator and U_m is the amplitude of the voltage.

For the voltage-controlled multilayer piezoactuator from the piezoceramics type of the lead zirconate titanate PZT under the longitudinal piezoelectric effect for the elastic-inertial load with one fixed face at $M_1 \to \infty$, $m << M_2$, the amplitude of the voltage U_m = 50 V, d_{33} = 4·10^{-10} m/V, n = 10, M = 1 kg, C_{33}^E = 6·10^7 N/m, C_e = 0.4·10^7 N/m, values the steady-state value of displacement ξ_m = 200 nm and the time constant T_t = 0.125·10^{-3} s are obtained.

4 Conclusion

The generalized parametric block diagram and the generalized structural-parametric model of the multilayer electromagnetoelastic actuator micro and nanodisplacement are constructed with the mechanical parameters the displacement and the force.

The parametric block diagrams of the multilayer piezoactuator for the transverse, longitudinal, shift piezoelectric effects are determined. The matrix transfer function of the multilayer electromagnetoelastic actuator is determined for the communications systems.

From the equation of the electromagnetoelasticity, the equation of the force that causes the deformation, the system of the equations for the equivalent quadripole of the multilayer actuator, the equations of the

forces on its faces we obtain the structural-parametric model of the multilayer electromagnetoelastic actuator micro and nanodisplacement.

The parametric structural schematic diagram and the transfer functions of the multilayer piezoactuator are considered using the structural-parametric model of the piezoactuator for the communications systems.

REFERENCES

[1]. Schultz, J., Ueda, J., Asada, H., *Cellular actuators*. Oxford: Butterworth-Heinemann Publisher, 2017. 382 p.

[2]. Afonin, S.M., *Absolute stability conditions for a system controlling the deformation of an elecromagnetoelastic transduser*. Doklady mathematics, 2006. 74(3): p. 943-948, doi:10.1134/S1064562406060391.

[3]. Zhou, S., Yao, Z., *Design and optimization of a modal-independent linear ultrasonic motor.* IEEE transaction on ultrasonics, ferroelectrics, and frequency control, 2014. 61(3): p. 535-546, doi:10.1109/TUFFC.2014.2937.

[4]. Przybylski, J., *Static and dynamic analysis of a flextensional transducer with an axial piezoelectric actuation*. Engineering structures, 2015. 84: p. 140-151, doi:10.1016/j.engstruct.2014.11.025.

[5]. Ueda, J., Secord, T., Asada, H.H., *Large effective-strain piezoelectric actuators using nested cellular architecture with exponential strain amplification mechanisms*. IEEE/ASME transactions on mechatronics, 2010. 15(5): p. 770-782, doi:10.1109/TMECH.2009.2034973.

[6]. Karpelson, M., Wei, G.-Y., Wood, R.J., *Driving high voltage piezoelectric actuators in microrobotic applications. Sensors and actuators* A: Physical, 2012. 176: p. 78-89, doi:10.1016/j.sna.2011.11.035.

[7]. Afonin, S.M., *Block diagrams of a multilayer piezoelectric motor for nano- and microdisplacements based on the transverse piezoeffect*. Journal of computer and systems sciences international, 2015. 54(3): p. 424-439, doi:10.1134/S1064230715020021.

[8]. Afonin, S.M., *Structural parametric model of a piezoelectric nanodisplacement transduse*r. Doklady physics, 2008. 53(3) p. 137-143, doi:10.1134/S1028335808030063.

[9]. Afonin, S.M., *Solution of the wave equation for the control of an elecromagnetoelastic transduser*. Doklady mathematics, 2006. 73(2), p. 307-313, doi:10.1134/S1064562406020402.

[10]. Cady W.G., *Piezoelectricity: An introduction to the theory and applications of electromechancial phenomena in crystals*. New York, London: McGraw-Hill Book Company, 1946. 806 p.

[11]. *Physical acoustics*: *Principles and methods. Vol.1. Part A. Methods and devices*. Mason, W., Editor, New York: Academic Press, 1964. 515 p.

[12]. Zwillinger, D., *Handbook of differential equations.* Boston: Academic Press, 1989. 673 p.

[13]. Afonin, S.M., *Structural-parametric model and transfer functions of electroelastic actuator for nano- and microdisplacement*. Chapter 9 in *Piezoelectrics and nanomaterials: Fundamentals, developments and applications*. Parinov, I.A., Editor, New York: Nova Science, 2015. p. 225-242.

[14]. Afonin, S.M., *A structural-parametric model of electroelastic actuator for nano- and microdisplacement of mechatronic system*. Chapter 8 in *Advances in nanotechnology. Volume 19*. Bartul, Z., Trenor, J., Editors, New York: Nova Science, 2017. p. 259-284.

[15]. Afonin, S.M., Nano- and micro-scale piezomotors. Russian engineering research, 2012. 32(7-8): p. 519-522, doi:10.3103/S1068798X12060032.

[16]. Afonin, S.M., *Generalized parametric structural model of a compound electromagnetoelastic transducer*. Doklady physics, 2005. 50(2) p. 77-82, doi: 10.1134/1.1881716.

[17]. Afonin, S.M., *Elastic compliances and mechanical and adjusting characteristics of composite piezoelectric transducers*. Mechanics of solids, 2007. 42(1): p. 43-49, doi:10.3103/S0025654407010062.

[18]. Afonin, S.M., *Stability of strain control systems of nano-and microdisplacement piezotransducers*. Mechanics of solids, 2014. 49(2): p. 196-207, doi:10.3103/S0025654414020095.

[19]. Afonin, S.M., *Structural-parametric model electromagnetoelastic actuator nanodisplacement for mechatronics*. International journal of physics, 2017. 5(1): p. 9-15, doi:10.12691/ijp-5-1-2.

[20]. Afonin, S.M., *A block diagram of electromagnetoelastic actuator nanodisplacement for communications Systems*. Transactions on Networks and Communications, 2018. 6(3): p. 1-9, doi:10.14738/tnc.63.4641.

[21]. Afonin, S.M., *Electromagnetoelastic nano- and microactuators for mechatronic systems*. Russian Engineering Research, 2018. 38(12): p. 938-944, doi:10.3103/S1068798X18120328.

[22]. *Springer handbook of nanotechnology*. Bhushan, B., Editor, Springer, Berlin, New York, 2004. 1222 p.

[23]. *Encyclopedia of nanoscience and nanotechnology*. 10-Volume set. Nalwa, H.S., Editor. American Scientific Publishers, Los Angeles, 2004.

SOCIETY FOR SCIENCE AND EDUCATION
UNITED KINGDOM

TNC TRANSACTIONS ON NETWORKS AND COMMUNICATIONS

VOLUME 7, NO. 3
ISSN: 2054 -7420

Scalable Multicast Using MPLS in Software Defined Network

Lie Qian

Dept. of Chemistry, Computer & Physical Science, Southeastern Oklahoma State University, Durant, OK, USA
lqian@se.edu

ABSTRACT

Multicast helps to deliver data to multiple receivers efficiently. One scalability challenge faced by multicast is the per-channel forwarding states being maintained in the network layer, which increases linearly with the number of established multicast channels. MPLS helps to alleviate this problem by removing forwarding states from non-branch routers on the multicast tree and label switch packets in non-branch routers. To reduce the number of forwarding states in branch routers, many solutions were proposed to merge multicast trees/subtrees from different channels. Software Defined Network (SDN) decouples the control plane from the data plane, which enables low cost commodity design in routers and flexible network feature deployments through software implementation in centralized controllers. Equipped with SDN's flexible policy and packet processing action installation, multicast tree/subtree merging becomes more convenient in SDN. This paper proposes a new scalable multicast solution in SDN to further reduce the number of forwarding states in routers. In the new solution, first a 2 level MPLS label switching scheme is used to reduce the extra point to point LSPs needed when multicast trees are merged. Secondly, a new multicast tree construction algorithm is designed to pursue more aggressive subtree matching between channels by taking advantage of per channel packet dropping actions in SDN. Simulation results show that the new solution can achieve 10-20 percent reduction in the number of forwarding entries needed for multicast traffic's forwarding.

Keywords: Software Defined Network, OpenFlow, Multicast, MPLS, Scalability

1 Introduction

Multicast was proposed to deliver data from one or multiple sources to a set of destinations in a network efficiently. A set of destinations and the source(s) that receive/send the same data are identified by a multicast channel (group) [1]. A multicast channel is defined as a collection of packets identified by the same channel ID [2]. In case multiple sources exist, the multicast channel ID is a multicast IP address. For a single source multicast channel, a (S, G) address pair [3,4] is used as channel ID, where S is the source's address and G is a multicast group address. A logical multicast tree is created by the multicast protocol for each channel to connect the source(s) to destinations. Data packets are forwarded along the tree and duplicated in the routers at the branch of the tree. For single source channel, the source is the root and all destinations are leaves on the tree, which is called a source specific multicast tree. For multiple source channels, a Rendezvous Point router is chosen as the root, which collects data from all sources [3,5].

DOI: 10.14738/tnc.73.6561
Publication Date: 21st June 2019
URL: http://dx.doi.org/10.14738/tnc.73.6561

To forward packets of a channel properly along the multicast tree, routers on the multicast tree need to maintain a forwarding states for this channel. Forwarding state is composed of the channel ID and a list of the child routers on the multicast tree. The number of forwarding states increases linearly with the number of passing multicast channels, which causes scalability problems in routers. Multi-protocol label switching (MPLS) [6] is a network technology that promises to offer high speed packet forwarding, QoS, traffic engineering and many other new features to the current best-effort, IP-based Internet. MPLS can coexist with many existing network layer and data link layer protocols to provide scalability in today's networks. Scalable multicast in MPLS network has been proposed to reduce forwarding states in routers. MMT [7] removes forwarding states from non-branch routers. In [8], we proposed to replace forwarding states in branch routers with point to multipoint MPLS label switching when a tree or subtree could be used by multiple channels to reach the same set of destinations and a tree matching algorithm, TMST, was proposed in [8] to detect such multicast tree sharing. In [2], we proposed a multicast tree construction algorithm to further reduce forwarding states in branch routers by performing Partial Matching between SubTrees (PMST), which achieves higher matching rate between channels.

Software Defined Network (SDN) is proposed to decouple the control plane from the data plane [9]. In SDN, data plane is still implemented by the device vendor in hardware while the control plane is realized by software in one or multiple centralized controllers. Software such as network management applications, network operating systems and OpenFlow protocols work together to control how packets are handled in each devices' data plane. Deploying new internet architecture, network management, services or protocols is simplified to software update in the controllers and no change is needed in the large number of traffic forwarding devices. Network services such as QoS, virtualization, security, traffic engineering, Information centered networking, forensic analysis, transferrable network applications, deep packet inspection, cloud data center, dynamic middle box deployment, virtual collaborative working environment, VLAN, etc. are becoming more realistic in SDN [10][11].

With SDN's support, per-channel policies could be easily installed into any router in the network, which allows better, finer control over router's per channel packet processing. First, SDN can help to reduce the number of point to point (P2P) LSPs between branch routers. In previous solutions [2][8], to share point to multipoint (P2MP) MPLS LSPs between channels, extra P2P LSPs need to be setup in non-branch routers so that the proper ingress MPLS label used by branch routers could be pushed into the packets by these new P2P LSPs. Such extra P2P LSPs hurt the scalability in non-branch routers. In this paper, a new 2 level MPLS label switching design is proposed to remove the need for extra P2P LSPs in non-branch routers. Secondly, in both TMST and PMST algorithms [2][8], exact destination set match is required in the tree or subtree to avoid any channel's data being forwarded beyond the destination set G. In SDN, per channel packet dropping policies could be easily installed in any router using existing OpenFlow protocol [12]. In this paper, a new algorithm is proposed to merge subtrees between channels when they share enough common destinations. Such more aggressive sharing criteria enables more subtree sharing between channels and further reduces the number of forwarding states in branch routers. Simulations show that the new solution needs less branch router forwarding entries than both MMT and TMST/PMST solutions. The new solution needs a little bit more non-branch router forwarding entries than MMT but 21.8% less than that of TMST/PMST. Counting all forwarding entries, in both branch router and non-branch routers, the new solution has 16.38% less entries than MMT and 10.51% less than TMST/PMST.

The remainder of this paper is organized as follows. Section 2 presents the background review including network model, MPLS, SDN and existing scalable multicast solutions. In section 3 the new multicast solution, including a new 2 level MPLS label switching scheme and a new tree construction algorithm, is presented. Simulation results are shown and discussed in Section 4 and conclusion is drawn in Section 5.

2 Related Works

In this section, a brief review is given for the network model, MPLS networks, Software Defined Network and related works in scalable multicast.

This paper focuses on the single source multicast model. A multicast tree is constructed for a channel with source as root and destinations as leaves. There are 3 types of routers on the tree 1) Branch Routers - root router and routers having more than one child on the tree, 2) Non-Branch Routers - routers having only one child, and 3) Destination Routers - leaf routers that deliver data to end hosts. Data packets are duplicated in Branch Routers. Given a branch router BR1, its next hop Branch Routers are the branch routers reachable on the tree from BR1 via non-branch routers only.

2.4 MPLS Network

MPLS [6] is a versatile data transport solution that addresses network problems such as scalability, QoS management, and traffic engineering. Ingress routers in MPLS networks compute and insert a 32-bit long MPLS shim header that includes a 20-bit long MPLS label, to each incoming packet. A MPLS enabled router, called Label Switching Router (LSR), maintains a MPLS label switching table, with each entry specifying an ingress MPLS label L_{in}, one or multiple egress MPLS labels L_{out} and egress interface ID(s) I_{out}. When packet P carrying MPLS label L_{in} arrives at LSR R, R searches for an entry with ingress label L_{in} in the MPLS label switching table. For each pair (L_{out}, I_{out}) in the matched entry, R swaps L_{in} in P with L_{out} and forwards packet P to neighbor router through egress interface I_{out}. Such process is called "label switching" of the packet. The specific path through the MPLS network that a packet follows based on its MPLS labels is called Label Switched Path (LSP). Label distribution protocol, such as LDP (Label Distribution Protocol) [13], or RSVP (Resource ReServation Protocol) [14] are used to setup LSPs. In this paper, all the routers in a MPLS network are LSRs.

2.5 Scalable Multicast

Various solutions have been proposed to improve the scalability of multicast through reducing the number of forwarding states in the network layer. Network layer aggregation solutions [15-17] reduce the storage and routing complexity in routers through replacing multiple forwarding states in a router with one forwarding state. Due to the non-hierarchical allocation of multicast IP addresses, existing network layer aggregation solutions yield either insignificant reduction in the number of forwarding states or leaky bandwidth, in which multicast packets are transmitted to links not on the multicast tree.

Smart packet solutions are proposed in [18], in which the information of packet forwarding is stored in packet headers to eliminate multicast forwarding states in routers. Routers forward packets based on information extracted from the packet headers. Smart packet solutions require changes in the format of packet headers, limit the number of branch routers, and cause problems due to excessive packet fragmentation. IP encapsulation solutions [19][20] transport packets from one branch router to its next hop BR through unicast IP encapsulation, in which the original packet is encapsulated in a new packet that has the next hop BR's address as destination address. Forwarding states are removed from non-branch

routers. IP encapsulation solutions involve resource intensive extra IP packet en/decapsulation at branch routers.

A framework that explains IP multicast deployment in MPLS environment was proposed by Ooms et al [21], which is a pure MPLS layer multicast routing solution. In this framework, a point to multipoint (P2MP) LSP is used for a multicast tree. One P2MP LSP could be shared by multiple trees only if they have the same tree structure. Therefore, large number of multicast channels with various tree structures consumes too many MPLS labels to establish large number of P2MP LSPs and introduce scalability problem in MPLS layer.

MPLS Multicast Tree (MMT) solution was proposed in [7] for scalable multicast in MPLS networks, in which packets are transported from one branch router to its next hop BRs by point to point (P2P) MPLS label switching. Forwarding states are only stored in branch routers. However, MMT made no effort to reduce the forwarding states in branch routers. We proposed tunnel sharing scheme in [8] to reduce the number of forwarding states and MPLS label consumption by using the same P2MP LSP for multiple channels' forward. Such sharing is possible when the tree structures of different channels are similar enough. TMST solution was also proposed in [8] to merge Total Matched SubTree (TMST)'s LSPs to reduce the forwarding states and MPLS label consumption. In TMST solution, a centralized Network Information Management System (CNIMS) keeps records of all established multicast trees, branch routers and LSPs. When a new channel's request comes in, CNIMS tries to find an existing multicast subtree, whose downstream destination list exactly matches to the new channel's destination list. If such subtree exists, no new tree will be created. Instead, new channel's data will be sent to the matched subtree's root router through a newly established P2P LSP, and further delivered to destinations through the existing subtree's existing LSPs. If no such subtree exists, a new tree will be built. The performance gain in tunnel sharing and TMST is based on the match rate between multicast trees, which is not always realistic in real network. Partially Matched SubTree (PMST) solution was proposed in [2] to improve the performance of TMST. PMST tries to match subset of new channel's destinations to any existing subtree in the network. By doing this, the number of destinations remained in the new channel that need a new tree to deliver data to them could be further reduced.

2.6 Software Defined Network and OpenFlow Protocol

Traditional network devices like switches or routers bound data plane (packet forwarding, dropping and modification) and control plane (QoS, routing, network monitoring, per-flow control) in the same equipment. When any new network service, protocol or architecture need to be deployed, the control plane usually requires significant modifications. Even when the change could be accommodated by reconfiguration, still all devices need to be reconfigured by the network administrator. More often, the change needed is too significant and go beyond what is allowed in reconfiguration. In such cases new devices that support the new control plane need to be purchased and deployed if you are lucky to find them on the market while most vendors are reluctant to implement new service into their products before the service become widely accepted on the market, which is not always the case for newly proposed services, protocols or architectures.

Software Defined Network (SDN) was proposed to decouple the control plane and data plane [9]. In SDN, the data plane remains in network devices like switches/routers and the control plane is moved to one or multiple centralized controllers. The controllers install policies in the network devices to control how

network traffic are processed in each switch. Network device vendors can focus on improving the data plane performance and lowering the cost of the devices and don't need worry about the constantly changing control plane [22]. Whenever the control plane needs to be changed, controllers could be reprogrammed (install a new software) to be capable of installing different policies in switches to realize the new services or protocols. With SDN, the network service that can be provided in a network is not limited by what the vendor implemented inside the devices anymore, which encourages and enables new network technology, services, protocols and architecture's design.[23]

In a SDN, one or multiple controllers are deployed to make network management decisions. Network management applications, network operating systems and protocol interfacing the controller and switches are installed in the controllers. Network management applications are responsible for making network control decision. Network operating systems provide API to allow quick and easy network management applications programming and shield the network management application from the heterogeneous network technology. Openflow [12] protocol is installed in both switches and controllers. Openflow defines how the rules from the controller could be installed, updated, and removed in the switches and how these rules can be used in the switches for packet processing.

In an OpenFlow switch [12], there are one or multiple flow tables and one group table. Using OpenFlow protocol, the controller can add, modify and remove entries in the tables inside each switch. Each entry in any table consists of match fields, counters, and a set of instructions to apply to matching packets. Packets may need to be processed by multiple flow tables one by one when they come to a switch. When a packet is processed in a table, if a match is found, the associated instruction of that matched entry will be executed. If no match is found, a special miss entry in that table will determine the fate of the packet. The packet could be forwarded to the controller using Packet-in message, dropped or forwarded to the next flow table in the same switch depending on the policy installed in the miss entry. Controller can use Modify-State message to add flow entries in any table.

For a matched packet, instructions associated with the matched flow entry are executed. Some of the instructions edit the action set associated with the packet. All actions in the action set will be executed after the packet finishes its processing in the last flow table in the same switch. In addition to the actions in the action set, "Apply-Action" instruction could execute action of choice during the table's processing. Instruction "Goto" specify which table is the next to process the packet. Instructions also can send metadata to the next table to assist the packet processing there. Actions are defined in OpenFlow to describe the forwarding, modification of the packet, applying meters to the packet, sending the packet to specific queue for QoS purpose, etc.

3 New Scalable Multicast Solution in Software Defined Network

Software Defined Network (SDN) uses controllers to centralize network management. Controllers have complete picture of the whole network and can install forwarding policy in all routers in real time. In this section, a new scalable multicast solution in SDN is presented. The new solution uses a 2 level MPLS label scheme to share point to point LSPs on non-branch routers between channels and share point to multiple point LSPs on branch routers between channels without extra point to point LSP. The new solution also uses a newly proposed multicast tree construction algorithm to increase LSP sharing between channels to improve scalability.

2.7 Multicast in SDN with 2 Level MPLS Label Switching

SDN has one or multiple controllers responsible for control plane decisions, including multicast channel establishment, multicast membership management, MPLS policy setup, multicast tree construction, and forward states installation. After collecting membership information, the controller computes the multicast tree for that channel in the network. Using the TMST/PMST based multicast tree construction algorithm together with the new algorithm proposed in the next section to discover all branch and non-branch routers.

After identifying all routers on the tree, controller sends messages to all on tree routers to install policies to forward data along the multicast tree. In SDN using OpenFlow protocol [12], each incoming packet will be matched to one or multiple flow tables in a router. Table entries stored in these tables are used to specify traffic processing policy such as where to forward the packet, if the packet should be modified, if the packet should be dropped, etc. MPLS labels, IP addresses, TCP ports, etc. could be used to match flow entry in these tables.

In this new solution, there are 3 kinds of forwarding table entries for multicast traffic, 1) Point to Point MPLS switch entry (P2P Entry), 2) network layer IP entry (IP Entry), and 3) Point to Multiple Point MPLS switch entry (P2MP Entry). P2P entry is used in non-branch routers to deliver traffic from one branch router to another. Such P2P LSPs could be statically or dynamically established between branch routers and can be shared by all channels trying to send between the same pair of branch routers. In SDN, each P2P entry applies following actions: pop ingress MPLS label, push egress MPLS label and forward the packets to the port toward the next hop router.

IP entries are used in branch routers to forward single channel's traffic. Routers match the packet's channel ID against the IP entry. The table entry first duplicates the packet for each next hop branch router. For each next hop branch router BR_{next}, the table entry pushes MPLS label so that the packet could be label switched in a P2P LSP toward BR_{next} (pushes the chosen P2P LSP's first ingress MPLS label). Then the packet is forwarded to the interface toward BR_{next}.

In a branch router where multiple channels try to reach the same set of downstream destinations, IP entries for these channels are merged into one P2MP entry. A special MPLS label is used to identify packets from these channels in this branch router and all downstream branch routers. Let's call such special MPLS label Aggregation Label (AG Label). In a branch router where a channel C_1 starts to share another channel C_2's sub multicast tree, the Aggregation Label used on the C_2's shared subtree will be pushed into the C_1's packets. C_1's packets then will use P2MP entries for branch router routing in the rest of the shared subtree. In a branch router on the subtree, the table entry that matches Aggregation MPLS label specifies following actions: duplicate the packet for each next hop branch, push P2P LPS ingress label in each duplicate, forward all duplicates to corresponding egress interface.

This 2 level MPLS label switching design, Aggregation Label and P2P Label, helps to reduce the number of P2P entries in non-branch routers. [2][8] use 1 level P2MP label switch in branch routers where the P2MP ingress labels need to be pushed into packets by the router at the end of each P2P LSP so that the label could be identified in the branch routers. Because each P2P LSP can only specify one last hop egress MPLS label therefore it can only be used to forward traffic for one tree/subtree. Such extra P2P LSPs cause scalability problem in non-branch routers. In the new 2 level MPLS label switching design, the last router on any P2P LSP doesn't need to push any MPLS label into a packet, because the packets will be routed

based on 2nd level aggregation label or IP channel ID in branch routers. Such design totally relieves routers in P2P LSPs from being aware of their downstream subtree structure. Only one P2P LSP is needed between any pair of branch routers and it can be used by all channels that need deliver traffic between this pair branch routers.

To establish a P2P LSP in a router, say the packet from ingress interface I_{in} with label L_{in} will be switched to egress interface I_{out} with label L_{out}. One entry is installed in the first flow table of the router using OpenFlow. The entry's matching field uses I_{in} and L_{in} to identify packets with L_{in} coming from interface I_{in} while set value ANY to any other parts of the matching field. A "Write Action" instruction is in the Instructions part of the flow entry. The "Write Action" instruction writes following actions into this packet's action set 1) pop MPLS label, 2) push MPLS label L_{out}, 3) output on interface I_{out}. After the flow table processing, the packet will leave the table processing and has all actions in the action set executed, where the MPLS label L_{in} will be replaced by L_{out} and then the packet will be forwarded to interface I_{out}.

To establish a P2MP entry (IP or aggregation label based) in a router, say the packet from ingress interface I_{in} with aggregation label L_{ag} will be switched to egress interface I_{in_1} with label L_{out_1}, to I_{in_2} with L_{out_2}… to I_{in_n} with L_{out_n}. One entry is installed in the first flow table of the router. The entry's matching field use I_{in} and L_{ag} to identify packets with L_{ag} label coming from interface I_{in} while set value ANY to any other parts of the matching field (or use channel ID instead of L_{ag} if it is an IP entry). An "Apply-Actions" instruction is in the Instructions part of the flow entry. The "Apply-Actions" instruction specifies a list of 3n actions, 3 actions for each branch. For I_{out_i} and L_{out_i}, the 3 actions are 1) pop MPLS label, 2) push MPLS label L_{out_i}, 3) output on interface I_{out_i}. Each output action in the apply-action instruction makes a clone of the packet (with new MPLS label just pushed in) and forwarded to the corresponding output port. After all actions being executed, the packet will leave the flow table processing. Because there is no output action in its action set, the packet will be dropped.

2.8 OLST (Overlap SubTree) Algorithm

Base on the discussion in subsection 3.1, it is obvious that the multicast scalability performance in SDN depends on the extent of MPLS LSP sharing between multicast channels. Such sharing could be achieved when trees or subtrees from different channels are identical. Both TMST and PMST algorithms [2][8] try to construct new multicast trees by reusing existing subtrees.

However, TMST and PMST only reuse the existing subtrees whose destination set is a subset of the new channel's destination set. Existing subtrees that reach any destination beyond the new channel's designation list cannot be used on the new channel's tree construction. This design makes sense on traditional network. Because when an existing subtree is used to forward data of a new channel, all destinations reachable from that subtree will receive data from this new channel. If any destination is not in the destination list of the new channel, the resource such as bandwidth and forwarding state used to forward the data to these undesired destinations are wasted.

In SDN network, per channel packet processing (such as dropping) policy could be easily installed. Such flexibility allows the tree construction algorithm to reuse the existing subtree even if the tree reaches some non-destination routers. The resource waste could be limited to minimum by installing dropping policies in routers to drop the packets of this new channel to prevent them from being forwarded toward undesired destinations. To implement such drop policy in a router, a new table entry is created in the flow

table to match the multicast channel's id (source address and port number). The entry has its priority field set to be greater than the P2MP entry or P2P entry. The priority field setting is necessary to guarantee that the packets from this channel be matched to this new entry but not the MPLS label switch entry. Action "Drop" is specified in this new entry to drop packets from this channel. Now the packets carrying the same ingress MPLS label could be matched to one of the two flow entries. If the packets belong to the new channel, they will match the channel ID entry with high priority and be dropped. If the packets belong to any other channel, they will match the MPLS label entry and be label switched to next hop router(s).

Equipped with the capability of dropping specific channel's packets on a shared subtree, I am proposing a new **OverLap SubTree** (**OLST**) algorithm in Software Defined Network to improve the multicast tree sharing between channels. OLST reuses existing subtrees whose downstream destination set overlaps significantly with new channels destination set. First let's define **overlap factor** (**OF**) for an existing subtree and a new channel as the ratio between the number of destinations on the subtree that are not in the new channel's destination set and the number of new channel's destinations that reachable from the subtree. In PTMST, only the existing subtrees with OF = 0 can be used to build the tree for a new channel. Now, in SDN, the acceptable OF value could be set by the SDN controller based on historical multicast tree statistics. In next section, simulation results are used to demonstrate how the optimal OF value could be estimated.

SDN controller maintains a list of existing subtrees in the network for existing multicast channels. Only subtrees rooted at branch routers are included in the list. A subtree rooted at branch router $BR1$ for channel D is denoted as $T\_sub(D, BR1)$. It records the reachable destinations on this subtree, denoted as $Dest(D, BR1)$. The list of subtrees is sorted based on the number of reachable destinations in descending order.

Assume C is a new arriving channel with source S. OLST algorithm builds a multicast tree using following steps:

Step 1. Compute a temporary multicast tree $T_{temp}(C, S)$ rooted at source S using any existing multicast tree algorithm to connect all destinations of channel C (e.g. shortest path tree, Steiner tree)

Step 2. For each branch router *BR* in $T_{temp}(C, S)$:

a. Compare set $Dest(C, BR)$ using every existing subtree record maintained by the controller. An existing subtree $T\_sub(a, B)$ with $Dest(a, B)$ is deemed as a match when 1) $Dest(C, BR) \subseteq Dest(a, B)$ and 2) $\frac{|Dest(a,B) - Dest(c,BR)|}{|Dest(a,B) \cap Dest(c,BR)|} \leq OF$.

b. For a matched $T\_sub(a, B)$, remove $Dest(C, BR)$ from L_C, add B into L_C if B was not there. Install drop policies for channel C to prevent packets reach any destination in set $Dest(a, B) - Dest(C, BR)$.

Step 3. If L_C is not empty, for every existing subtree $T\_sub(a, B)$ from controller's subtree list

a. Compare $Dest(a, B)$ against L_C, $T\_sub(a, B)$ is deemed as a match when $\frac{|Dest(a,B) - L_c|}{|Dest(a,B) \cap L_c|} \leq OF$

b. If $T\_sub(a, B)$ is a match, remove $Dest(a, B) \cap L_c$ from L_C and add B into L_C if B was not there. Install drop policies for channel C to prevent packets reach any destination in set $Dest(a, B) - Dest(c, BR)$.

Step 4. Build a final tree T_{final} to connect all members in L_C with source S. Install a new IP entry in every branch router on T_{final}. On any leaf node on T_{final}, if it is not the destination of channel C, add push action in the upstream branch router's IP entry to push Aggregation Label into channel C's packets as discussed in section 3.1.

Packets of channel C are first label switched on the new tree T_{final}using the IP entries in branch routers. When the packets reach the leaf routers on T_{final}, either they reach the destinations, or they will be switched on existing subtrees with an Aggregation MPLS Label, which is pushed into the packets in the last branch router before the leaf router. Drop policies for channel C are installed in existing subtrees to prevent them from reaching destinations not in channel c. The cost added to the network from new channel C includes the new IP entries on $T_{final}$and all the IP entries with drop actions. If the OF is set too large, the cost from the drop policy entries will surpass the save from sharing P2MP entries. In simulation section, such tradeoff will be further studied.

Figure 1 depicts an example of this new solution. There are 2 channels. $C1$ has source $S1$ and $C2$ has source $S2$. Channel $C1$'s destination set is $\{d1, d2, d3, d4, d5, d6\}$. Before $C2$'s existence, $C1$'s traffic is identified in branch routers $BR1$, $BR2$, $BR3$ and $BR4$ using IP entry as Figure 2 shows. 10 P2P LSPs are used to deliver packets between branch routers. Branch routers need duplicate the packets, push P2P LSP's labels and forward the packets toward each branch.

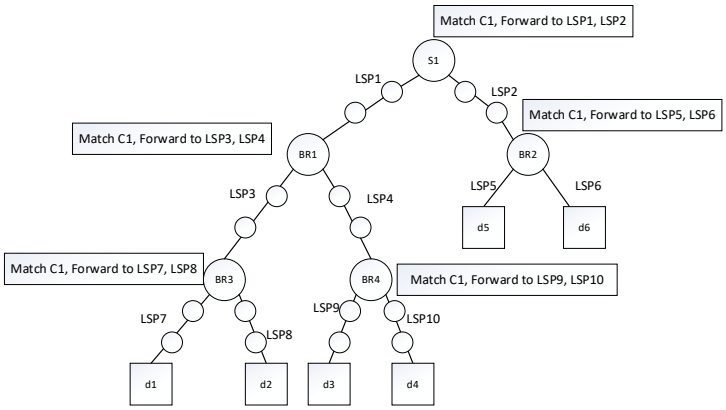

Figure 1: Single Channel without Tree Sharing

When channel $C2$ with destination set $\{d2, d3, d4\}$ needs to be established, through running OLST algorithm, SDN controller decides to reuse the subtree including $BR1$, $BR3$ and $BR4$. As shown in Figure 2, the IP entries in $BR1$, $BR2$ and $BR4$ are changed to P2MP entries with Aggregation Label L_{ag}. In $BR1$'s previous hop branch routers ($S2$ for $C2$, $S1$ for $C1$), L_{ag} label is pushed into the packets of $C1$ and $C2$ toward $BR1$ so that they can be matched with L_{ag} on the subtree. Therefore, no new entry is added into branch routers for $C2$ in the subtree rooted at $BR1$. Because $d1$ is not a destination of $C2$, an extra drop entry that match $C2$'s channel ID needs to be installed in the first router after $BR3$ toward $d1$ to drop the traffic of $C2$ but let $C1$'s traffic pass.

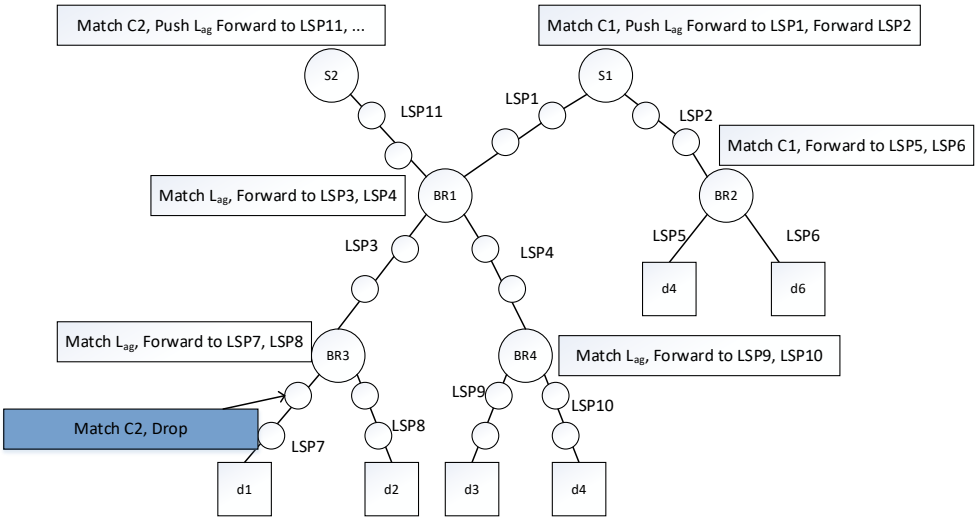

Figure 2: Two Channels with Overlapped Subtree Sharing and 2 Level Label Switching

4 Simulation Results

Simulations are used to evaluate the new multicast solution with OLST algorithm. In the simulations, topology is randomly generated with 4000 routers and 2000 multicast channels, each of which has one source and a maximum of 1200 destinations (the actual number of destinations for each channel is randomly selected between 500 and 1000). Shortest path multicast tree algorithm is used for tree construction. For the sake of controller's processing burden, SDN controller only keeps records of any subtree whose destination size is greater than 10. The number of flow entries in router's tables is measured to evaluate the scalability.

Three solutions' are simulated and measured, 1) MMT solution [7] (label switch between branch routers, channel id forward state in branch routers without subtree reuse), 2) 1 level MPLS label solution with TMST/PMST tree construction algorithms [2] (shared P2MP LSPs with TMST/PMST algorithm), and 3) 2 level MPLS label solution with OLST tree construction algorithm using different overlap factors.

The results are plotted in Figure 3. MMT solution needs 588782 flow table entries in all routers to support all 2000 multicast channels, including 535226 point to multipole point IP entries in branch routers and 53556 P2P MPLS label entries in non-branch routers. TMST/PMST solution installs 550187 table entries in all routers. Among these entries, there are 458245 point to multipoint entries in branch routers, which is fewer than MMT because of multicast tree sharing. However, as described in section 3.1, extra P2P LSPs are needed in 1 level label switching solutions to enable multicast tree sharing. In the TMST/PMST simulation, 91942 P2P entries are installed in non-branch routers, which is about 71% more than that of MMT. When the overlap factor is set to about 0.1-0.125, the newly proposed solution with 2 level MPLS label switching and OLST algorithm only installs 400798-403361 point to multiple points entries in branch routers (including both IP and Aggregation Label matched entries), 71591-71899 P2P entries in non-branch routers and 17576-19669 dropping entries. The new solution reaches the best performance compared to MMT and TMST/PMST solutions. The overall table entry number is 16.38% less than that of MMT solution and is 10.51% less than that of the solution using 1 level label switching and TMST/PMST algorithm.

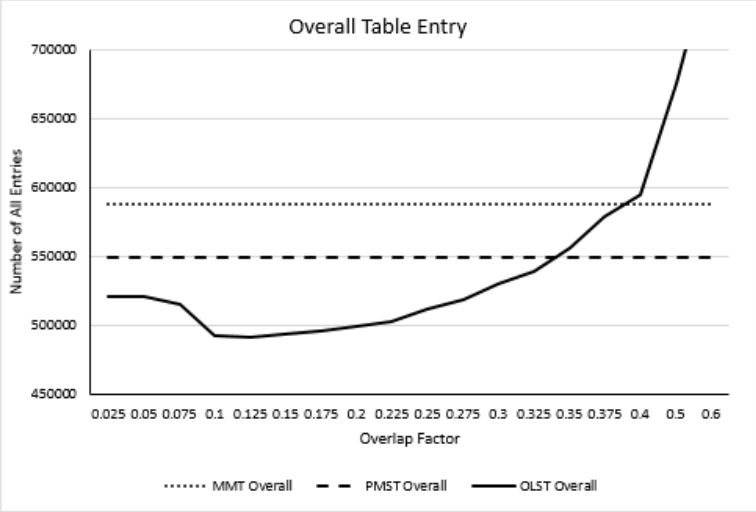

Figure 3: Overall Table Entry Number Comparison

If the P2P LSPs between branch routers are statically setup and therefore have no effect on the scalability, the scalability is only affected by the number of dynamically created table entries (P2MP entries and IP entries for both forwarding and dropping). Figure 4 shows that the new solution's dynamic table entry number is 21.44% less than that of MMT and 8.24% less than that of TMST/PMST algorithm.

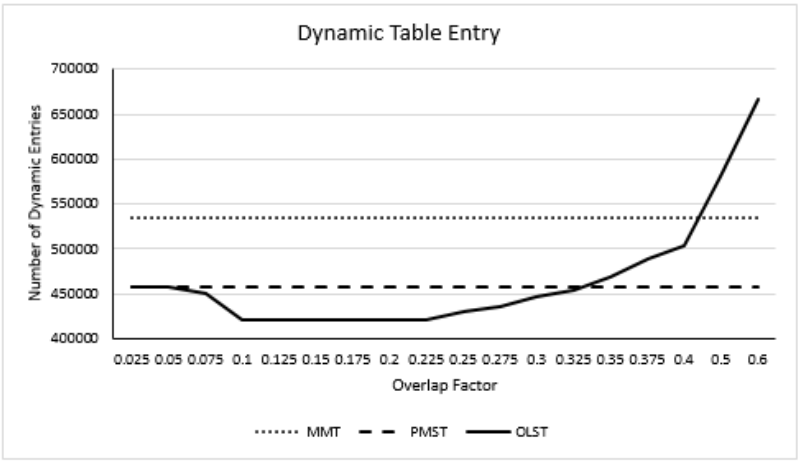

Figure 3: Dynamic Table Entry Number Comparison

The overlap factor plays an important role in the performance of the new solution. When the overlap factor becomes larger, new subtrees will be matched to existing subtrees with more unnecessary destinations, which requires more per channel drop policies to be installed on routers. The results in Figure 3 and 4 show that after overlap factor reaches 0.1, the new solution's performance starts getting worse. Overall number of entries needed become worse than PMST solution after overlap value >0.35, and worse than MMT after overlap value >0.4.

5 Conclusion

Reducing the number of forwarding entries in branch routers and non-branch routers help to improve the scalability of multicasting. MPLS network allows traffic from different channel share the same point to

point or point to multipoint label switching entries in a network. Software Defined Network enables flexible per flow policy installation and MPLS label action in routers. In this paper, a 2 level MPLS label switching design and a new multicast tree construction algorithm are proposed to encourage more forwarding entry sharing in SDN MPLS network to improve multicast scalability. Simulations show that the new solution can reduce 10-20 percent table entries in the SDN network for multicast traffic forwarding.

REFERENCES

[1]. S. Deering, "Host extensions for IP multicasting," *RFC 1112,* August 1989.

[2]. Qian, L., Liu, X., & Wang, Y. (2010). A New Tree Construction Algorithm for Scalable Multicast in MPLS Networks. Accepted in Proceedings of International Symposium on Computer Network and Multimedia Technology, 2010, CNMT.

[3]. S. Bhattacharyya, "An overview of source-specific multicast (SSM)," RFC 3569, July 2003.

[4]. H. Holbrook, and B. Cain, "Source-specific multicast for IP," Internet draft, draft-ietf-ssm-arch-04.txt, Oct. 2003.

[5]. D. Estrin, D. Farinacci, A. Helmy, D. Thaler, S. Deering, M. Handley, V. Jacobson, C. Liu, P. Sharma, and L. Wei, "Protocol independent multicast-sparse mode (PIN-SM): protocol specification," RFC 2362, June 1998.

[6]. E. Rosen et al., "Multipotocol label switching architecture," RFC 3031, January 2001.

[7]. A. Boudani, B. Cousin, and J. –M. Bonnin, "An effective solution for multicast scalability: the MPLS multicast tree (MMT)," Internet draft, draft-boudani-mpls-multicast-tree-06.txt, October 2004.

[8]. Lie Qian, Yiyan Tang, Yuke Wang, Bashar Bou-Diab, and Wladek Olesinski, "A New Scalable Multicast Solution in MPLS Networks," IEEE GLOBECOM 2006, San Francisco, November 2006.

[9]. H. Yin et al., SDNi: A Message Exchange Protocol for Software Defined Networks (SDNS) across Multiple Domains, Jun. 2012, Internet draft. [Online]. Available: http://www.cisco.com/en/US/solutions/collateral/ns341/ns525/ns537/ns705/ns827/white_paper_c11-481360.pdf

[10]. W. Xia, Y. Wen, C. Foh, D. Niyato and H. Xie, A Survey on Software-Defined Networking, IEEE Communication Surveys & Tutorials, Vol. 17, no. 1, pp. 27-51, 1st Quarter 2015

[11]. F. Hu, Q. Hao and K. Bao, A Survey on Software-Defined Network and OpenFlow: From Concept to Implementation, IEEE Communication Surveys & Tutorials, Vol. 16, no. 4, pp. 2181-2206, 4th Quarter 2014

[12]. OpenFlow Switch Specification, version 1.5.1, Open Networking Foundation, March 26, 2015, [Online]. Available: https://www.opennetworking.org/wp-content/uploads/2014/10/openflow-switch-v1.5.1.pdf

[13]. L. Andersson, P. Doolan, N. Feldman, A. Fredette, and B. Thomas, "Label Distribution Protocol Specification," RFC 3036, January 2001.

[14]. D. Awdeche, L. Berger, D. Gan, T. Li, V. Srinivasan, and G. Swallow, "RSVP-TE: Extensions to RSVP for LSP tunnels," RFC3209, December 2001.

[15]. Jun-Hong Cui, Li Lao, Dario Maggiorini, Mario Gerla, "BEAM: A distributed aggregated multicast protocol using bi-directional trees," IEEE ICC 2003, vol. 1, pp. 689 – 695, 11-15 May 2003.

[16]. A. Fei, J. H. Cui, M. Gerla, and M. Faloutsos, "Aggregated multicast: an approach to reduce multicast state," Proc. Of Sixth Global Internet Symposium (GI2001), November 2001.

[17]. Jun-Hong Cui, Jinkyu Kim, A. Fei, M. Faloutsos, and M. Gerla, "Scalable QoS multicast provisioning in Diff-Serv-supported MPLS networks," IEEE GLOBECOM 2002, vol. 2, pp. 1450 – 1454, 17-21 November 2002.

[18]. A. Striegel, and G. Manimaran, "A scalable approach for DiffServ multicasting," IEEE ICC 2001, vol. 8, pp. 2327-2331, 11-14 June 2001.

[19]. A. Boudani, and B. Cousin, "Simple explicit multicast (SEM)," Internet draft, draft-boudani-simple-xcast-04.txt, March 2004.

[20]. Jining Tian, and Gerald Neufeld, "Forwarding state reduction for sparse mode multicast Communication," IEEE INFOCOM 1998, March 1998.

[21]. D. Ooms et al., "Framework for IP multicast in MPLS", RFC 3353, August 2002.

[22]. S.H. Yeganeh, A. Tootoonchian, and Y. Ganjali. *On scalability of software-defined networking*. IEEE Commun. Mag., 51(2):136–141, February 2013.

[23]. E. Kissel, G. Fernandes, M. Jaffee, M. Swany, and M. Zhang, *Driving software defined networks with xsp*. In SDN12: Workshop on Software Defined Networks, 2012.

SOCIETY FOR SCIENCE AND EDUCATION
UNITED KINGDOM

TNC TRANSACTIONS ON NETWORKS AND COMMUNICATIONS

VOLUME 7, NO. 3
ISSN: 2054 -7420

Free Running VCO based on an Unstable Transistor Circuit System Stability Optimization under Delayed Electromagnetic Interferences and Parasitic Effects and Engineering Applications

Ofer Aluf
Netanya, Israel
oferaluf@bezeqint.net

ABSTRACT

In this article, Very Crucial subject discussed in free running VCO based on an unstable transistor circuit system stability optimization under delayed electromagnetic interferences and parasitic effects. Additionally we discuss Free running VCO integrated circuit applications (PLLs, DLL, clock generation, etc.). There are many techniques to generate a Wideband Frequency Modulation (WBFM) signal: analog based, digitally based and hybrid based techniques. The VCO is a very low cost method of generating WBFM signals, such as chirp signals. The VCO has some important properties that are common to all frequency sources. These properties are frequency range, settling time, post-tuning drift, sensitivity and Maximum Sensitivity Ratio (MSR), frequency total accuracy, frequency modulation span, and modulation frequency bandwidth. The VCO frequency of oscillation depends on the resonance frequency set by its equivalent capacitance and inductance. By applying variable bias voltage to a Varactor diode, the capacitance is changed and the oscillation frequency is changed accordingly. The first delay line in our circuit (τ_1) represents the electromagnetic interference in the Varactor diode (D_1). We neglect the voltage on the first delay line ($V_{\tau 1} \rightarrow \varepsilon$) and the delay is on the current which flows through Varactor diode. The second and third delay lines (τ_2 and τ_3) represent the circuit microstrip line's parasitic effects before and after the matching circuit. We neglect the voltages on the second and third delay lines ($V_{\tau k} \rightarrow \varepsilon$; k=2, 3) and the delays are only on the current which flow through the microstrip lines. The free running VCO circuit can represent as delayed differential equations which, depending on variable parameters and delays. There is a practical guideline which combines graphical information with analytical work to effectively study the local stability of models involving delay dependent parameters. The stability of a given steady state is determined by the graphs of some function of τ_1, τ_2, τ_3.

Index Terms – Free running VCO, PLL, WBFM, Delay Differential Equations (DDEs), Bifurcation, Stability, Integrated circuit, CMOS, Bi-CMOS, Clock generation, ASIC, FPGA.

1 Introduction

In this article, Very Critical and useful subject is discussed: free running VCO based on an unstable transistor circuit system stability optimization under delayed electromagnetic interferences and parasitic

DOI: 10.14738/tnc.73.6400
Publication Date: 30th June 2019
URL: http://dx.doi.org/10.14738/tnc.73.6400

effects (Fig. 1). Frequency Modulation (FM) is used extensively in audio communication and data transfer. When spectrum efficiency is important Narrowband FM (NBFM) is used but when better signal quality is required Wideband FM (WBFM) is used at the expense of greater spectrum usage. The term WBFM is used in applications where the modulation index is equal to or larger than 1. We discuss applications and techniques for WBFM with modulation indexes much larger than that, going up to 100 and beyond. In such applications spectral efficiency is less important and sometimes large spectral spread is actually desired. The purpose of this article is to present some major application's stability issues in the commercial and defense markets. The common techniques of generating WBFM are presented. There are many techniques to generate a WBFM signal: analog based techniques, digitally based techniques and hybrid techniques. A free running VCO is a device based on an unstable transistor circuit. The frequency of oscillation depends on the resonance frequency set by its equivalent capacitance and inductance. By applying variable bias voltage to a Varactor diode, the capacitance is changed and the oscillating frequency is changed accordingly. The VCO is a very low cost method of generating WBFM signals, such as chirp signals. The VCO has some important properties that are common to all frequency sources. These properties are frequency range, settling time, post-tuning drift, sensitivity and Maximum Sensitivity Ratio (MSR), frequency total accuracy, frequency modulation span, and modulation frequency bandwidth. The sensitivity parameter is defined as the "voltage to frequency" transfer function of the VCO and is measured in MHz/Volt. A perfect VCO will have a constant sensitivity throughout its range of operation. Unfortunately there are no ideal VCOs and therefore the sensitivity varies across the VCO frequency range. The Maximum Sensitivity divided by the Minimum Sensitivity is defined as MSR. Using a VCO with poor MSR (>>1) will yield a wide range of problems. The WBFM techniques is to use the PLL in order to jump to the new center frequency, then to keep the tuning voltage to the VCO at a constant value (e.g., by a S/H) and inject the modulating voltage directly to the tuning voltage. This technique is called "DTO Mode" since the loop is open during the modulation and the VCO is actually in free running mode. This technique suffers from all the drawbacks explained previously for the "DTO Mode" in DTOs and in FLOs. The below figure describe the free running VCO based on an unstable transistor circuit with delay elements due to electromagnetic interferences and parasitic effects [1][2].

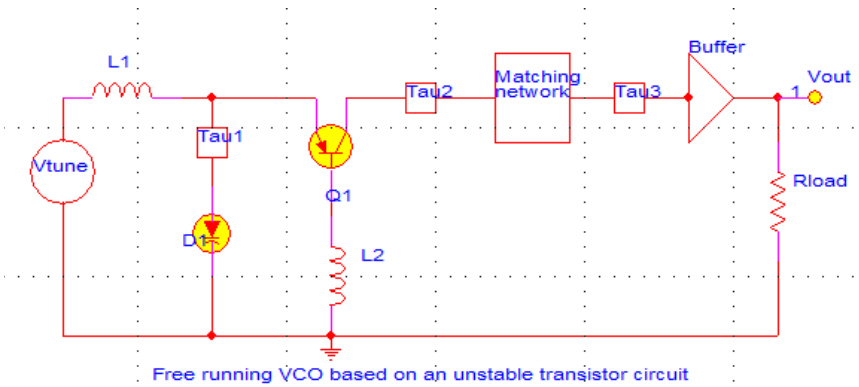

Figure 1. Free running VCO is based on an unstable transistor circuit.

The free running VCO circuit uses Varactor which is diode that has been designed specifically to exploit the variable capacitance of a reverse biased P-N junction (The Varactor diode is constantly reverse bias - V_b through inductor which is not appear in Fig 1 and V_{tune} tunes the diode reverse bias accordingly). The

capacitance versus voltage characteristic of a Varactor depends on the impurity density as a function of distance from the P-N interface.

Many engineering applications include Free running VCO circuit which fit to different purposes.

2 Free Running VCO Based on an Unstable Transistor Equivalent Circuit and represent Delay Differential Equations

A voltage-controlled oscillator (VCO) is an electronic oscillator whose oscillation frequency is controlled by the voltage input. The applied input voltage determines the instantaneous oscillation frequency. Our free running VCO is a device based on an unstable transistor circuit. The frequency of oscillation depends on the resonance frequency set by its equivalent capacitance and inductance. By applying variable bias voltage (reverse biased) to a Varactor diode, the capacitance is changed and the oscillating frequency is changed accordingly. The varactor diode working principles, if the reverse voltage of the diode is increased, then the size of the depletion region increases. Likewise, if the reverse voltage of the varactor diode is decreased, then the size of the depletion region decreases. Varactor diodes are widely used within the RF design arena. They provide a method of varying the capacitance within a circuit by the application of a control voltage. The advantage of Varactor diode is low noise. It generates less noise as compared to the other P-N junction diode. Thus, the power loss due to noise is low in Varactor diodes. The varactor diode is portable due to the small size and light weight. A Varactor diode modulator is the direct method of FM generation wherein the carrier frequency varied by the modulation signal (V_{tune}). A Varactor diode is a semiconductor diode whose junction capacitance varies linearly with applied voltage when the diode is reverse biased. The Varactor diode is arranged in reverse biased to offer Junction capacitance effect. The modulation voltage (V_{tune}) which is in series with the Varactor diode will vary the bias and hence the junction capacitance of the capacitance, resulting the oscillator frequency to change accordingly. The Varactor diode equivalent circuit (equivalent electrical model at high frequencies) for spice model includes the following elements: The package inductance L_p, is due to the lead inductance, wire bonds and other interconnect required to get to the diode device (Fig 2). The package capacitance, C_p, is due to the stray capacitance from the package and other features to the surrounding ground. In general, better quality diodes have minimal package effects and therefore C_p and L_p are small. The device resistance R(V) is the device resistance in the physical diode and will have some voltage dependence. If the tuning voltage range is limited, the voltage dependence of the resistance can be ignored. The resistance accounts of the finite Q of the diode and is due to the un-depleted region of the diode and contact resistance. The tuning capacitance, C(V), is the desired capacitance and it is strongly dependent upon the bias voltage. The equation which accurate predict C(V) over the expected range of V. The equation used to model the capacitance is $C(V) = \frac{C_0}{(1+\frac{V}{\phi})^{\gamma}}$, $C(V)$ - Varactor diode capacitance, C_0 - Zero bias capacitance, V - Reverse bias voltage, ϕ - Built in potential, γ - Slope of the Log C vs. Log V curve. The Varactor can be a critical component in VCO design for several reasons. Satisfying the required tuning range is only the first consideration. Varactor can also plays a role in the phase noise performance of the oscillator. The noise current source associated with all active devices there is a phase noise degradation resulting from finite Q. The component Q is reduced by the inverse of the value of parasitic resistance [3][4].

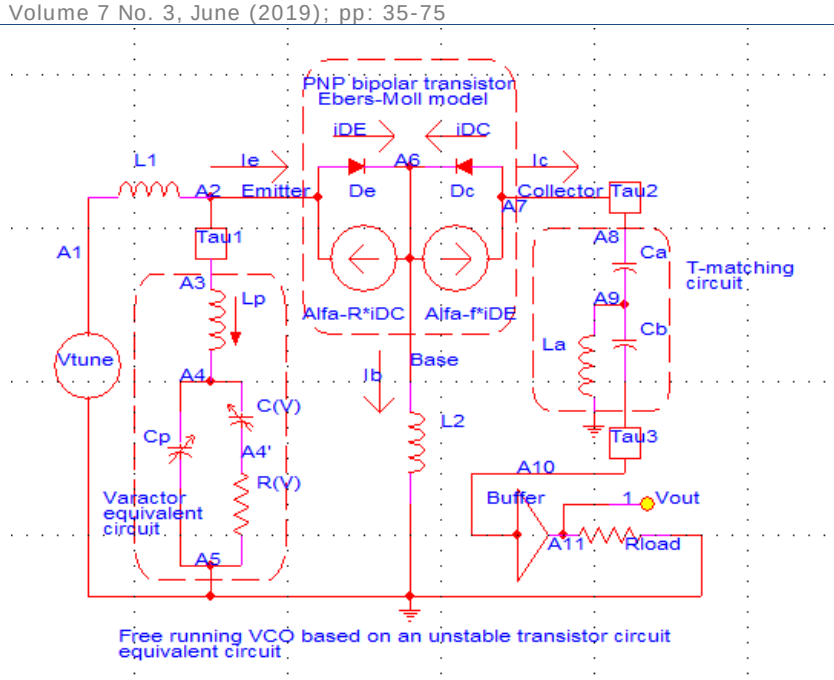

Figure 2. Free running VCO is based on an unstable transistor equivalent circuit.

We can write above free running VCO is based on an unstable transistor equivalent circuit's equations.

$$V_{tune}=V_{A_1}\ ;\ V_{A_2}=V_{A_3}\ ;\ V_{\tau_1}\to\varepsilon\ ;\ V_{A_7}=V_{A_8}\ ;\ V_{\tau_2}\to\varepsilon\ \ ;\ V_{A_{11}}=V_{A_{10}}\ ;\ V_{\tau_2}\to\varepsilon \text{ (Buffer Op-Amp)} \quad (1)$$

$$V_{A_2}=V_{A_3}\ ;\ (V_{\tau_1}\to\varepsilon)\ ;\ V_{A_7}=V_{A_8}\ ;\ (V_{\tau_2}\to\varepsilon)\ ;\ I_{L_p}=I_{L_1}(t-\tau_1)-I_e(t-\tau_1)\ ;\ I_c=\alpha_f\cdot i_{DE}-i_{DC} \quad (2)$$

$$V_{A_1}-V_{A_2}=L_1\cdot\frac{dI_{L_1}}{dt}\ ;\ V_{A_3}-V_{A_4}=L_p\cdot\frac{d}{dt}(I_{L_1}(t-\tau_1)-I_e(t-\tau_1))\ ;\ I_e=i_{DE}-\alpha_r\cdot i_{DC}\ ;\ I_c(t-\tau_2)=I_{C_a} \quad (3)$$

$$I_e(t-\tau_1)=i_{DE}(t-\tau_1)-\alpha_r\cdot i_{DC}(t-\tau_1)\ ;\ I_{L_p}=I_{C_p}+I_{C(V)}\ ;\ V_{A_5}=0 \text{ volt (ground)}\ ;\ V_{A_3}=V \quad (4)$$

$$I_{C_p}=C_p\cdot\frac{dV_{A_4}}{dt}\ ;\ I_{C(V)}=C(V)\cdot\frac{d}{dt}(V_{A_4}-V_{A_4'})\ ;\ I_{R(V)}=\frac{V_{A_4'}}{R(V)}\ ;\ I_{C(V)}=I_{R(V)} \quad (5)$$

$$I_{R(V)}=C(V)\cdot\frac{d}{dt}(V_{A_4}-V_{A_4'})\Rightarrow\frac{V_{A_4'}}{R(V)}=C(V)\cdot\frac{d}{dt}(V_{A_4}-V_{A_4'})\ ;\ V_{A_4'}=R(V)\cdot C(V)\cdot\frac{d}{dt}(V_{A_4}-V_{A_4'}) \quad (6)$$

Assumption: The tuning voltage range of the Varactor is very narrow then we ignored the voltage dependence of the resistance, $R(V)=R$.

$$\frac{V_{A_4'}}{R}=C(V)\cdot\frac{d}{dt}(V_{A_4}-V_{A_4'})\ ;\ V_{A_4'}=R\cdot C(V)\cdot\frac{d}{dt}(V_{A_4}-V_{A_4'}) \quad (7)$$

The reverse bias on the Varactor is V then $V=V_{A_3}$.

$$C(V=V_{A_3})=\frac{C_0}{(1+\frac{V_{A_3}}{\phi})^{\gamma}}\ ;\ \frac{V_{A_4'}}{R}=\frac{C_0}{(1+\frac{V_{A_3}}{\phi})^{\gamma}}\cdot\frac{d}{dt}(V_{A_4}-V_{A_4'})\ ;\ V_{A_4'}=\frac{C_0\cdot R}{(1+\frac{V_{A_3}}{\phi})^{\gamma}}\cdot\frac{d}{dt}(V_{A_4}-V_{A_4'}) \quad (8)$$

KCL @ A_6: $i_{DC}+i_{DE}-\alpha_f\cdot i_{DE}-\alpha_r\cdot i_{DC}-I_{L_2}=0\ ;\ V_{A_6}=L_2\cdot\frac{dI_{L_2}}{dt}\ ;\ I_b=I_{L_2}\ ;\ I_e=I_b+I_c$ (9)

KCL @ A_7: $i_{DC}+I_c=\alpha_f\cdot i_{DE}\ ;\ I_{C_a}=I_c(t-\tau_2)$ (10)

$$I_{C_a}=C_a\cdot\frac{d}{dt}(V_{A_8}-V_{A_9})\Rightarrow I_c(t-\tau_2)=C_a\cdot\frac{d}{dt}(V_{A_8}-V_{A_9}) \quad (11)$$

KCL @ A_9: $I_{L_a}+I_{C_b}-I_{C_a}=0\ ;\ I_{C_b}=I_{C_a}-I_{L_a}\ ;\ V_{A_9}=L_a\cdot\frac{dI_{L_a}}{dt}\ ;\ I_{C_b}=C_b\cdot\frac{d}{dt}(V_{A_9}-V_{A_{10}})\ ;\ (V_{\tau_3}\approx 0)$ (12)

$$V_{A_{11}}=I_{R_{load}}\cdot R_{load}\ ;\ V_{A_{11}}=V_{A_{10}}\Rightarrow I_{R_{load}}=\frac{V_{A_{11}}}{R_{load}}=\frac{V_{A_{10}}}{R_{load}} \quad (13)$$

$$V_{A_1}-V_{A_2}=L_1\cdot\frac{dI_{L_1}}{dt}\Rightarrow V_{tune}-V_{A_2}=L_1\cdot\frac{dI_{L_1}}{dt}\ ;\ V_{A_2}=V_{tune}-L_1\cdot\frac{dI_{L_1}}{dt}\ ;\ V_{A_2}=V_{A_3} \quad (14)$$

$$V_{A_2}=V_{A_3}\Rightarrow V_{A_2}=V_{A_4}+L_p\cdot\frac{d}{dt}(I_{L_1}(t-\tau_1)-I_e(t-\tau_1)) \quad (15)$$

$$V_{tune}-L_1\cdot\frac{dI_{L_1}}{dt}=V_{A_4}+L_p\cdot\frac{d}{dt}(I_{L_1}(t-\tau_1)-I_e(t-\tau_1)) \quad (16)$$

$$V_{A_4}=V_{tune}-L_1\cdot\frac{dI_{L_1}}{dt}-L_p\cdot\frac{d}{dt}(I_{L_1}(t-\tau_1)-I_e(t-\tau_1)) \quad (17)$$

$$\frac{dV_{A_4}}{dt}=\frac{dV_{tune}}{dt}-L_1\cdot\frac{d^2I_{L_1}}{dt^2}-L_p\cdot\frac{d^2}{dt^2}(I_{L_1}(t-\tau_1)-I_e(t-\tau_1)) \quad (18)$$

$$I_{C_p}=C_p\cdot\frac{dV_{A_4}}{dt}=C_p\cdot\frac{d}{dt}\{V_{tune}-L_1\cdot\frac{dI_{L_1}}{dt}-L_p\cdot\frac{d}{dt}(I_{L_1}(t-\tau_1)-I_e(t-\tau_1))\} \quad (19)$$

$$I_{C_p}=C_p\cdot\{\frac{dV_{tune}}{dt}-L_1\cdot\frac{d^2I_{L_1}}{dt^2}-L_p\cdot\frac{d^2}{dt^2}(I_{L_1}(t-\tau_1)-I_e(t-\tau_1))\} \quad (20)$$

$$I_{C_p}=C_p\cdot\{\frac{dV_{tune}}{dt}-L_1\cdot\frac{d^2I_{L_1}}{dt^2}-L_p\cdot\frac{d^2}{dt^2}I_{L_1}(t-\tau_1)+L_p\cdot\frac{d^2}{dt^2}I_e(t-\tau_1)\} \quad (21)$$

$$V_{A_4'}=\frac{C_0\cdot R}{(1+\frac{V_{A_3}}{\phi})^{\gamma}}\cdot\frac{d}{dt}(V_{A_4}-V_{A_4'})\Rightarrow V_{A_4'}=\frac{C_0\cdot R}{(1+\frac{1}{\phi}\cdot[V_{tune}-L_1\cdot\frac{dI_{L_1}}{dt}])^{\gamma}}\cdot\frac{d}{dt}(V_{A_4}-V_{A_4'}) \quad (22)$$

$$V_{A_4^{'}}=\frac{C_0\cdot R}{(1+\frac{1}{\phi}\cdot[V_{tune}-L_1\cdot\frac{dI_{L_1}}{dt}])^{\gamma}}\cdot(\frac{dV_{A_4}}{dt}-\frac{dV_{A_4^{'}}}{dt}) \tag{23}$$

$$V_{A_4^{'}}=\frac{C_0\cdot R}{(1+\frac{1}{\phi}\cdot[V_{tune}-L_1\cdot\frac{dI_{L_1}}{dt}])^{\gamma}}\cdot(\frac{dV_{tune}}{dt}-L_1\cdot\frac{d^2I_{L_1}}{dt^2}-L_p\cdot\frac{d^2}{dt^2}(I_{L_1}(t-\tau_1)-I_e(t-\tau_1))-\frac{dV_{A_4^{'}}}{dt}) \tag{24}$$

Hint 1: $V_{D_c}=V_{A_7}-V_{A_6}$; $V_{D_e}=V_{A_2}-V_{A_6}$; $i_{DC}=I_0\cdot(e^{\frac{1}{V_T}\cdot V_{D_C}}-1)=I_0\cdot(e^{\frac{1}{V_T}\cdot(V_{A_7}-V_{A_6})}-1)$ (25)

$$i_{DE}=I_0\cdot(e^{\frac{1}{V_T}\cdot V_{D_e}}-1)=I_0\cdot(e^{\frac{1}{V_T}\cdot(V_{A_2}-V_{A_6})}-1) \tag{26}$$

I_0 is the magnitude of the reverse saturation current, the assumption is that current is the same in two Ebers-Moll's diodes (D_c and D_e). V_T is the thermal voltage, $V_T=\frac{k\cdot T}{q}$; k is Boltzmann's constant which is constant, q is the charge of an electron, T is temperature and it is not constant but humans exist in a fairly narrow range of temperatures around 300^0K then 25mV to 26mV is a reasonable value for room temperature V_T. "T" in V_T stands for 'thermal' that is a function of (absolute) temperature.

$$\frac{i_{DC}}{I_0}+1=e^{\frac{1}{V_T}\cdot(V_{A_7}-V_{A_6})}\Rightarrow\frac{1}{V_T}\cdot(V_{A_7}-V_{A_6})=\ln(\frac{i_{DC}}{I_0}+1)\Rightarrow V_{A_7}-V_{A_6}=V_T\cdot\ln(\frac{i_{DC}}{I_0}+1) \tag{27}$$

$$\frac{i_{DE}}{I_0}+1=e^{\frac{1}{V_T}\cdot(V_{A_2}-V_{A_6})}\Rightarrow\frac{1}{V_T}\cdot(V_{A_2}-V_{A_6})=\ln(\frac{i_{DE}}{I_0}+1)\Rightarrow V_{A_2}-V_{A_6}=V_T\cdot\ln(\frac{i_{DE}}{I_0}+1) \tag{28}$$

Hint 2: We use for the PNP transistor equivalent circuit the Ebers-Moll model. The model involves two ideal diodes placed back to back with reverse saturation currents $-I_{EO}$ and $-I_{CO}$ and two dependent current-controlled current sources shunting the ideal diodes. For a PNP transistor, both I_{EO} and I_{CO} are negative, so that $-I_{EO}$ and $-I_{CO}$ are positive values, giving the magnitudes of the reverse saturation currents of the diodes. We consider $I_0\approx-I_{CO}$ and $I_0\approx-I_{EO}$. The Ebers-Moll model is valid for both forward and reverse static voltages applied across the transistor junctions. It is impossible to construct a transistor by simply connecting two separate (isolated) diodes in series opposing. A cascade of two p-n diodes exhibits transistor properties (capable of amplification) only if carriers injected across one junction diffuse across the second junction.

$$V_{A_2}=V_{tune}-L_1\cdot\frac{dI_{L_1}}{dt}\Rightarrow V_{tune}-L_1\cdot\frac{dI_{L_1}}{dt}-V_{A_6}=V_T\cdot\ln(\frac{i_{DE}}{I_0}+1)\Rightarrow V_{A_6}=V_{tune}-L_1\cdot\frac{dI_{L_1}}{dt}-V_T\cdot\ln(\frac{i_{DE}}{I_0}+1) \tag{29}$$

$$V_{A_7} = V_{A_6} + V_T \cdot \ln(\frac{i_{DC}}{I_0} + 1) \Rightarrow V_{A_7} = V_{tune} - L_1 \cdot \frac{dI_{L_1}}{dt} - V_T \cdot \ln(\frac{i_{DE}}{I_0} + 1) + V_T \cdot \ln(\frac{i_{DC}}{I_0} + 1) \quad (30)$$

$$V_{A_7} = V_{tune} - L_1 \cdot \frac{dI_{L_1}}{dt} + V_T \cdot \{\ln(\frac{i_{DC}}{I_0} + 1) - \ln(\frac{i_{DE}}{I_0} + 1)\} \; ; \; V_{A_7} = V_{tune} - L_1 \cdot \frac{dI_{L_1}}{dt} + V_T \cdot \ln\{\frac{(\frac{i_{DC}}{I_0} + 1)}{(\frac{i_{DE}}{I_0} + 1)}\} \quad (31)$$

$$V_{A_6} = L_2 \cdot \frac{dI_{L_2}}{dt} \Rightarrow V_{tune} - L_1 \cdot \frac{dI_{L_1}}{dt} - V_T \cdot \ln(\frac{i_{DE}}{I_0} + 1) = L_2 \cdot \frac{dI_{L_2}}{dt} \quad (32)$$

$$I_{C_a} = C_a \cdot \frac{d}{dt}(V_{A_8} - V_{A_9}) \overset{V_{A_7} = V_{A_8}}{=} C_a \cdot \frac{d}{dt}(V_{A_7} - V_{A_9}) \quad (33)$$

$$I_{C_a} = C_a \cdot \frac{d}{dt}(V_{tune} - L_1 \cdot \frac{dI_{L_1}}{dt} + V_T \cdot \ln\{\frac{(\frac{i_{DC}}{I_0} + 1)}{(\frac{i_{DE}}{I_0} + 1)}\} - V_{A_9}) \; ; \; V_{A_9} = L_a \cdot \frac{dI_{L_a}}{dt} \quad (34)$$

$$I_{C_a} = C_a \cdot \frac{d}{dt}(V_{tune} - L_1 \cdot \frac{dI_{L_1}}{dt} + V_T \cdot \ln\{\frac{(\frac{i_{DC}}{I_0} + 1)}{(\frac{i_{DE}}{I_0} + 1)}\} - L_a \cdot \frac{dI_{L_a}}{dt}) \quad (35)$$

$$I_{C_b} = C_b \cdot \frac{d}{dt}(V_{A_9} - V_{A_{10}}) \Rightarrow I_{C_b} = C_b \cdot \frac{d}{dt}(L_a \cdot \frac{dI_{L_a}}{dt} - V_{A_{10}}) \quad (36)$$

$$I_{R_{load}} = \frac{V_{A_{10}}}{R_{load}} \Rightarrow V_{A_{10}} = I_{R_{load}} \cdot R_{load} \Rightarrow I_{C_b} = C_b \cdot \frac{d}{dt}(L_a \cdot \frac{dI_{L_a}}{dt} - I_{R_{load}} \cdot R_{load}) \quad (37)$$

Assumption: $I_{R_{load}} = I_{C_b}(t - \tau_3) \; ; \; I_{R_{load}} = I_{R_{load}}(t) \Rightarrow I_{C_b} = C_b \cdot \frac{d}{dt}(L_a \cdot \frac{dI_{L_a}}{dt} - I_{C_b}(t - \tau_3) \cdot R_{load})$ (38)

$$V_{A_4} = V_{C_p} \; ; \; V_{A_4} = V_{C(V)} + V_{R(V)} \; ; \; V_{C(V)} = V_{A_4} - V_{A_4'} \; ; \; V_{C_p} = V_{C(V)} + V_{R(V)} \overset{I_{R(V)} = I_{C(V)}}{=} V_{C(V)} + I_{C(V)} \cdot R \; ; \; V_{A_3} = V \quad (39)$$

$$V_{C_p} = V_{A_4} = \frac{1}{C_p} \cdot \int I_{C_p} \cdot dt \; ; \; V_{C(V)} = \int \frac{I_{C(V)}}{C(V)} \cdot dt \quad (40)$$

$$V_{C_p} = V_{C(V)} + I_{C(V)} \cdot R \Rightarrow \frac{1}{C_p} \cdot \int I_{C_p} \cdot dt = \int \frac{I_{C(V)}}{C(V)} \cdot dt + I_{C(V)} \cdot R \quad (41)$$

We operate $\frac{d}{dt}$ on the two sides of the above integral equation and get the following equation:

$$\frac{1}{C_p}\cdot I_{C_p}=\frac{I_{C(V)}}{C(V)}+\frac{dI_{C(V)}}{dt}\cdot R\ ;\ C(V=V_{A_3})=\frac{C_0}{(1+\frac{[V_{tune}-L_1\cdot\frac{dI_{L_1}}{dt}]}{\phi})^{\gamma}} \tag{42}$$

$$\frac{1}{C_p}\cdot I_{C_p}=\frac{(1+\frac{[V_{tune}-L_1\cdot\frac{dI_{L_1}}{dt}]}{\phi})^{\gamma}}{C_0}\cdot I_{C(V)}+\frac{dI_{C(V)}}{dt}\cdot R \tag{43}$$

$$\frac{1}{C_p}\cdot I_{C_p}=(1+\frac{1}{\phi}\cdot[V_{tune}-L_1\cdot\frac{dI_{L_1}}{dt}])^{\gamma}\cdot\frac{1}{C_0}\cdot I_{C(V)}+\frac{dI_{C(V)}}{dt}\cdot R \tag{44}$$

We can summery our circuit Key differential equations (1):

$$(*)\ I_{C_p}=C_p\cdot\{\frac{dV_{tune}}{dt}-L_1\cdot\frac{d^2I_{L_1}}{dt^2}-L_p\cdot\frac{d^2}{dt^2}I_{L_1}(t-\tau_1)+L_p\cdot\frac{d^2}{dt^2}I_e(t-\tau_1)\} \tag{45}$$

$$(**)V_{tune}-L_1\cdot\frac{dI_{L_1}}{dt}-V_T\cdot\ln(\frac{i_{DE}}{I_0}+1)=L_2\cdot\frac{dI_{L_2}}{dt} \tag{46}$$

$$(***)\ I_{C_a}=C_a\cdot\frac{d}{dt}(V_{tune}-L_1\cdot\frac{dI_{L_1}}{dt}+V_T\cdot\ln\{\frac{(\frac{i_{DC}}{I_0}+1)}{(\frac{i_{DE}}{I_0}+1)}\}-L_a\cdot\frac{dI_{L_a}}{dt}) \tag{47}$$

$$(****)\ I_{C_b}=C_b\cdot\frac{d}{dt}(L_a\cdot\frac{dI_{L_a}}{dt}-I_{C_b}(t-\tau_3)\cdot R_{load}) \tag{48}$$

$$(*****)\ \frac{1}{C_p}\cdot I_{C_p}=(1+\frac{1}{\phi}\cdot[V_{tune}-L_1\cdot\frac{dI_{L_1}}{dt}])^{\gamma}\cdot\frac{1}{C_0}\cdot I_{C(V)}+\frac{dI_{C(V)}}{dt}\cdot R \tag{49}$$

###

$$V_{tune}=L_2\cdot\frac{dI_{L_2}}{dt}+L_1\cdot\frac{dI_{L_1}}{dt}+V_T\cdot\ln(\frac{i_{DE}}{I_0}+1)\Rightarrow\frac{dV_{tune}}{dt}=L_2\cdot\frac{d^2I_{L_2}}{dt^2}+L_1\cdot\frac{d^2I_{L_1}}{dt^2}+\frac{V_T}{(\frac{i_{DE}}{I_0}+1)}\cdot\frac{1}{I_0}\cdot\frac{di_{DE}}{dt} \tag{50}$$

$$\frac{dV_{tune}}{dt}=L_2\cdot\frac{d^2I_{L_2}}{dt^2}+L_1\cdot\frac{d^2I_{L_1}}{dt^2}+\frac{V_T}{(i_{DE}+I_0)}\cdot\frac{di_{DE}}{dt} \tag{51}$$

(**) → (*) :

$$I_{C_p} = C_p \cdot \{L_2 \cdot \frac{d^2 I_{L_2}}{dt^2} + L_1 \cdot \frac{d^2 I_{L_1}}{dt^2} + \frac{V_T}{(i_{DE} + I_0)} \cdot \frac{di_{DE}}{dt} - L_1 \cdot \frac{d^2 I_{L_1}}{dt^2} - L_p \cdot \frac{d^2}{dt^2} I_{L_1}(t-\tau_1) + L_p \cdot \frac{d^2}{dt^2} I_e(t-\tau_1)\} \quad (52)$$

(**) → (***) :

$$I_{C_a} = C_a \cdot \frac{d}{dt}(L_2 \cdot \frac{dI_{L_2}}{dt} + L_1 \cdot \frac{dI_{L_1}}{dt} + V_T \cdot \ln(\frac{i_{DE}}{I_0} + 1) - L_1 \cdot \frac{dI_{L_1}}{dt} + V_T \cdot \ln\{\frac{(\frac{i_{DC}}{I_0} + 1)}{(\frac{i_{DE}}{I_0} + 1)}\} - L_a \cdot \frac{dI_{L_a}}{dt}) \quad (53)$$

(**) → (*****) :

$$\frac{1}{C_p} \cdot I_{C_p} = (1 + \frac{1}{\phi} \cdot [L_2 \cdot \frac{dI_{L_2}}{dt} + L_1 \cdot \frac{dI_{L_1}}{dt} + V_T \cdot \ln(\frac{i_{DE}}{I_0} + 1) - L_1 \cdot \frac{dI_{L_1}}{dt}])^{\gamma} \cdot \frac{1}{C_0} \cdot I_{C(V)} + \frac{dI_{C(V)}}{dt} \cdot R \quad (54)$$

We can summery our circuit Key reduced differential equations (2):

$$I_{C_p} = C_p \cdot \{L_2 \cdot \frac{d^2 I_{L_2}}{dt^2} + L_1 \cdot \frac{d^2 I_{L_1}}{dt^2} + \frac{V_T}{(i_{DE} + I_0)} \cdot \frac{di_{DE}}{dt} - L_1 \cdot \frac{d^2 I_{L_1}}{dt^2} - L_p \cdot \frac{d^2}{dt^2} I_{L_1}(t-\tau_1) + L_p \cdot \frac{d^2}{dt^2} I_e(t-\tau_1)\} \quad (55)$$

$$I_{C_a} = C_a \cdot \frac{d}{dt}(L_2 \cdot \frac{dI_{L_2}}{dt} + L_1 \cdot \frac{dI_{L_1}}{dt} + V_T \cdot \ln(\frac{i_{DE}}{I_0} + 1) - L_1 \cdot \frac{dI_{L_1}}{dt} + V_T \cdot \ln\{\frac{(\frac{i_{DC}}{I_0} + 1)}{(\frac{i_{DE}}{I_0} + 1)}\} - L_a \cdot \frac{dI_{L_a}}{dt}) \quad (56)$$

$$I_{C_b} = C_b \cdot \frac{d}{dt}(L_a \cdot \frac{dI_{L_a}}{dt} - I_{C_b}(t-\tau_3) \cdot R_{load}) \quad (57)$$

$$\frac{1}{C_p} \cdot I_{C_p} = (1 + \frac{1}{\phi} \cdot [L_2 \cdot \frac{dI_{L_2}}{dt} + L_1 \cdot \frac{dI_{L_1}}{dt} + V_T \cdot \ln(\frac{i_{DE}}{I_0} + 1) - L_1 \cdot \frac{dI_{L_1}}{dt}])^{\gamma} \cdot \frac{1}{C_0} \cdot I_{C(V)} + \frac{dI_{C(V)}}{dt} \cdot R \quad (58)$$

We can summery our circuit Key reduced differential equations (3):

$$\frac{1}{C_p} \cdot I_{C_p} = L_2 \cdot \frac{d^2 I_{L_2}}{dt^2} + \frac{V_T}{(i_{DE} + I_0)} \cdot \frac{di_{DE}}{dt} - L_p \cdot \frac{d^2}{dt^2} I_{L_1}(t-\tau_1) + L_p \cdot \frac{d^2}{dt^2} I_e(t-\tau_1) \quad (59)$$

$$\frac{1}{C_a} \cdot I_{C_a} = L_2 \cdot \frac{d^2 I_{L_2}}{dt^2} - L_a \cdot \frac{d^2 I_{L_a}}{dt^2} + V_T \cdot \frac{1}{(i_{DC} + I_0)} \cdot \frac{di_{DC}}{dt} \quad (60)$$

$$\frac{1}{C_b} \cdot I_{C_b} = L_a \cdot \frac{d^2 I_{L_a}}{dt^2} - \frac{dI_{C_b}(t-\tau_3)}{dt} \cdot R_{load} \quad (61)$$

$$\frac{1}{C_p} \cdot I_{C_p} = (1 + \frac{1}{\phi} \cdot [L_2 \cdot \frac{dI_{L_2}}{dt} + V_T \cdot \ln(\frac{i_{DE}}{I_0} + 1)])^{\gamma} \cdot \frac{1}{C_0} \cdot I_{C(V)} + \frac{dI_{C(V)}}{dt} \cdot R \quad (62)$$

We have the following currents equations in our circuit (include delay elements τ_1, τ_2, τ_3):

$$I_{L_p} = I_{L_1}(t-\tau_1) - I_e(t-\tau_1)\ ;\ I_c = \alpha_f \cdot i_{DE} - i_{DC}\ ;\ I_e = i_{DE} - \alpha_r \cdot i_{DC}\ ;\ I_c(t-\tau_2) = I_{C_a} \tag{63}$$

$$I_e(t-\tau_1) = i_{DE}(t-\tau_1) - \alpha_r \cdot i_{DC}(t-\tau_1)\ ;\ I_{L_p} = I_{C_p} + I_{C(V)}\ ;\ I_{C(V)} = I_{R(V)} \tag{64}$$

$$i_{DC} + i_{DE} - \alpha_f \cdot i_{DE} - \alpha_r \cdot i_{DC} - I_{L_2} = 0\ ;\ I_b = I_{L_2}\ ;\ I_e = I_b + I_c\ ;\ I_{C_a} = I_c(t-\tau_2) \Rightarrow I_{C_a}(t+\tau_2) = I_c(t) \tag{65}$$

$$I_{L_a} + I_{C_b} - I_{C_a} = 0\ ;\ I_{R_{load}} = I_{C_b}(t-\tau_3) \text{ By assumption }\ ;\ I_{R_{load}} = I_{R_{load}}(t) \tag{66}$$

$$I_e(t) = I_b(t) + I_c(t)\ ;\ I_e(t) = I_{L_2}(t) + I_{C_a}(t+\tau_2)\ ;\ I_e(t-\tau_1) = I_{L_2}(t-\tau_1) + I_{C_a}(t+\tau_2-\tau_1) \tag{67}$$

We define $\Delta_\tau = \tau_2 - \tau_1$ then $I_{C_a}(t+\Delta_\tau) = I_c(t-\tau_1)\ ;\ I_e(t-\tau_1) = I_b(t-\tau_1) + I_{C_a}(t+\Delta_\tau)$ (68)

$$I_b(t) = I_{L_2}(t) \Rightarrow I_b(t-\tau_1) = I_{L_2}(t-\tau_1)\ ;\ I_e(t-\tau_1) = I_{L_2}(t-\tau_1) + I_{C_a}(t+\Delta_\tau) \tag{69}$$

We choose $\tau_2 = \tau_1 \Rightarrow \Delta_\tau = 0$ then $I_e(t-\tau_1) = I_{L_2}(t-\tau_1) + I_{C_a}(t)$ (70)

$$I_{L_a} + I_{C_b} - I_{C_a} = 0 \Rightarrow I_{C_b} = I_{C_a} - I_{L_a}\ ;\ (1-\alpha_r)\cdot i_{DC} + (1-\alpha_f)\cdot i_{DE} - I_{L_2} = 0 \tag{71}$$

$$i_{DC} = \frac{I_{L_2} - (1-\alpha_f)\cdot i_{DE}}{(1-\alpha_r)} = \frac{1}{(1-\alpha_r)}\cdot I_{L_2} - \frac{(1-\alpha_f)}{(1-\alpha_r)}\cdot i_{DE} = \frac{1}{(1-\alpha_r)}\cdot[I_{L_2} - (1-\alpha_f)\cdot i_{DE}] \tag{72}$$

$$\frac{di_{DC}}{dt} = \frac{1}{(1-\alpha_r)}\cdot\frac{dI_{L_2}}{dt} - \frac{(1-\alpha_f)}{(1-\alpha_r)}\cdot\frac{di_{DE}}{dt} = \frac{1}{(1-\alpha_r)}\cdot[\frac{dI_{L_2}}{dt} - (1-\alpha_f)\cdot\frac{di_{DE}}{dt}] \tag{73}$$

We can summery our circuit Key reduced differential equations (4):

$$\frac{1}{C_p}\cdot I_{C_p} = L_2\cdot\frac{d^2 I_{L_2}}{dt^2} + \frac{V_T}{(i_{DE}+I_0)}\cdot\frac{di_{DE}}{dt} - L_p\cdot\frac{d^2}{dt^2}I_{L_1}(t-\tau_1) + L_p\cdot\frac{d^2 I_{L_2}(t-\tau_1)}{dt^2} + L_p\cdot\frac{d^2 I_{C_a}(t)}{dt^2} \tag{74}$$

$$\frac{1}{C_a}\cdot I_{C_a} = L_2\cdot\frac{d^2 I_{L_2}}{dt^2} - L_a\cdot\frac{d^2 I_{L_a}}{dt^2} + V_T\cdot\frac{1}{([I_{L_2} - (1-\alpha_f)\cdot i_{DE}] + I_0\cdot(1-\alpha_r))}\cdot[\frac{dI_{L_2}}{dt} - (1-\alpha_f)\cdot\frac{di_{DE}}{dt}] \tag{75}$$

$$\frac{1}{C_b}\cdot[I_{C_a} - I_{L_a}] = L_a\cdot\frac{d^2 I_{L_a}}{dt^2} - \frac{dI_{C_b}(t-\tau_3)}{dt}\cdot R_{load} \tag{76}$$

$$\frac{1}{C_p}\cdot I_{C_p} = (1+\frac{1}{\phi}\cdot[L_2\cdot\frac{dI_{L_2}}{dt} + V_T\cdot\ln(\frac{i_{DE}}{I_0}+1)])^{\gamma}\cdot\frac{1}{C_0}\cdot I_{C(V)} + \frac{dI_{C(V)}}{dt}\cdot R \tag{77}$$

3 Free Running VCO Based on an Unstable Transistor Characteristic Equation and Stability Analysis $\tau_1=\tau\ ;\ \tau_1=\tau_2\ ;\ \tau_3=\tau$

At fixed points: $\frac{dI_{L_2}}{dt}=0\Rightarrow\frac{d^2I_{L_2}}{dt^2}=0\ ;\ \frac{dI_{L_1}}{dt}=0\Rightarrow\frac{d^2I_{L_1}}{dt^2}=0\ ;\ \lim_{t\to\infty}I_{L_1}(t-\tau_1)|_{t\square\ \tau_1}=I_{L_1}(t)$ (78)

$\lim_{t\to\infty}I_{L_2}(t-\tau_1)|_{t\square\ \tau_1}=I_{L_2}(t)\ ;\ \frac{dI_{C_a}(t)}{dt}=0\Rightarrow\frac{d^2I_{C_a}(t)}{dt^2}=0\ ;\ \frac{dI_{L_a}}{dt}=0\Rightarrow\frac{d^2I_{L_a}}{dt^2}=0$ (79)

$\frac{di_{DE}}{dt}=0\ ;\ \lim_{t\to\infty}I_{C_b}(t-\tau_3)|_{t\square\ \tau_3}=I_{C_b}(t)\ ;\ \frac{dI_{C_b}(t)}{dt}=0\ ;\ \frac{dI_{C(V)}}{dt}=0\ ;\ \frac{1}{C_b}\cdot I^*_{C_b}|_{C_b\neq0}=0$ (80)

$\frac{1}{C_p}\cdot I^*_{C_p}=0\Rightarrow I^*_{C_p}|_{C_p\neq0}=0\ ;\ \frac{1}{C_a}\cdot I^*_{C_a}=0\Rightarrow I^*_{C_a}|_{C_a\neq0}=0\ ;\ I^*_{C_a}-I^*_{L_a}=0\Rightarrow I^*_{C_a}=I^*_{L_a}\ ;\ I^*_{L_a}=0$ (81)

$\frac{1}{C_p}\cdot I^*_{C_p}=(1+\frac{1}{\phi}\cdot[V_T\cdot\ln(\frac{i^*_{DE}}{I_0}+1)])^{\gamma}\cdot\frac{1}{C_0}\cdot I^*_{C(V)}\ ;\ I^*_{L_p}=I^*_{C_p}+I^*_{C(V)}|_{I^*_{C_p}|_{C_p\neq0}=0}=I^*_{C(V)}\Rightarrow I^*_{L_p}=I^*_{C(V)}$ (82)

$I^*_{C_p}|_{C_p\neq0}=0\Rightarrow(1+\frac{1}{\phi}\cdot[V_T\cdot\ln(\frac{i^*_{DE}}{I_0}+1)])^{\gamma}\cdot\frac{1}{C_0}\cdot I^*_{C(V)}=0\ ;\ C_0\neq0$ (83)

Case I: $(1+\frac{1}{\phi}\cdot[V_T\cdot\ln(\frac{i^*_{DE}}{I_0}+1)])^{\gamma}=0\Rightarrow1+\frac{1}{\phi}\cdot[V_T\cdot\ln(\frac{i^*_{DE}}{I_0}+1)]=0\Rightarrow\ln(\frac{i^*_{DE}}{I_0}+1)=-\frac{\phi}{V_T}$ (84)

$e^{-\frac{\phi}{V_T}}=\frac{i^*_{DE}}{I_0}+1\Rightarrow\frac{i^*_{DE}}{I_0}=e^{-\frac{\phi}{V_T}}-1\Rightarrow i^*_{DE}=I_0\cdot(e^{-\frac{\phi}{V_T}}-1)$; Case II: $I^*_{C(V)}=0$. (85)

$i^*_{DC}=\frac{1}{(1-\alpha_r)}\cdot[I^*_{L_2}-(1-\alpha_f)\cdot i^*_{DE}]=\frac{1}{(1-\alpha_r)}\cdot[I^*_{L_2}-(1-\alpha_f)\cdot I_0\cdot(e^{-\frac{\phi}{V_T}}-1)]$ (86)

$i^*_{DC}=\frac{1}{(1-\alpha_r)}\cdot[I^*_{L_2}-(1-\alpha_f)\cdot I_0\cdot(e^{-\frac{\phi}{V_T}}-1)]$ (87)

We can summery our system fixed points:

First fixed point: $I^*_{C_p}=0\ ;\ I^*_{C_a}=0\ ;\ I^*_{L_a}=0\ ;\ I^*_{C_b}=0\ ;\ i^*_{DE}=I_0\cdot(e^{-\frac{\phi}{V_T}}-1)\ ;\ I^*_{C(V)}\ ;\ I^*_{L_p}=I^*_{C(V)}$

(88)

$i^*_{DC}=\frac{1}{(1-\alpha_r)}\cdot[I^*_{L_2}-(1-\alpha_f)\cdot I_0\cdot(e^{-\frac{\phi}{V_T}}-1)]\ ;\ I^*_{L_1}\ ;\ I^*_{L_2}$

(89)

Second fixed point: $I^*_{C_p}=0\ ;\ I^*_{C_a}=0\ ;\ I^*_{L_a}=0\ ;\ I^*_{C_b}=0\ ;\ I^*_{C(V)}=0\ ;\ I^*_{L_p}=0\ ;\ i^*_{DE}$ (90)

$$i_{DC}^{*}=\frac{1}{(1-\alpha_r)}\cdot[I_{L_2}^{*}-(1-\alpha_f)\cdot i_{DE}^{*}]\ ;I_{L_1}^{*}\ ;I_{L_2}^{*} \tag{91}$$

Stability analysis: The standard local stability analysis about any one of the equilibrium points of the Free running VCO is based on an unstable transistor circuit consists in adding to coordinate [$I_{C_p},I_{L_2},i_{DE},I_{L_1},I_{C_a},I_{L_a},I_{C_b},I_{C(V)},i_{DC}$] arbitrarily small increments of exponential form $[i_{C_p},i_{L_2},i_{DE},i_{L_1},i_{C_a},i_{L_a},i_{C_b},i_{C(V)},i_{DC}]\cdot e^{\lambda\cdot t}$ and retaining the first order terms in $I_{C_p},I_{L_2},i_{DE},I_{L_1},I_{C_a},I_{L_a},I_{C_b},I_{C(V)},i_{DC}$. The system of homogeneous equations leads to a polynomial characteristic equation in the eigenvalues. The polynomial characteristic equations accept by set the below variables ($I_{C_p},I_{L_2},i_{DE},I_{L_1},I_{C_a},I_{L_a},I_{C_b},I_{C(V)},i_{DC}$) and variables derivatives with respect to time into system equations. System fixed values with arbitrarily small increments of exponential form $[i_{C_p},i_{L_2},i_{DE},i_{L_1},i_{C_a},i_{L_a},i_{C_b},i_{C(V)},i_{DC}]\cdot e^{\lambda\cdot t}$ are: j=0 (first fixed point), j=1 (second fixed point), j=2 (third fixed point), etc. [10][11].

$$I_{C_p}(t)=I_{C_p}^{(j)}+i_{C_p}\cdot e^{\lambda\cdot t}\ ;I_{L_2}=I_{L_2}^{(j)}+i_{L_2}\cdot e^{\lambda\cdot t}\ ;i_{DE}=i_{DE}^{(j)}+i_{DE}\cdot e^{\lambda\cdot t}\ ;I_{L_1}=I_{L_1}^{(j)}+i_{L_1}\cdot e^{\lambda\cdot t}\ ;I_{C_a}=I_{C_a}^{(j)}+i_{C_a}\cdot e^{\lambda\cdot t} \tag{92}$$

$$I_{L_a}=I_{L_a}^{(j)}+i_{L_a}\cdot e^{\lambda\cdot t}\ ;I_{C_b}=I_{C_b}^{(j)}+i_{C_b}\cdot e^{\lambda\cdot t}\ ;I_{C(V)}=I_{C(V)}^{(j)}+i_{C(V)}\cdot e^{\lambda\cdot t}\ ;i_{DC}=i_{DC}^{(j)}+i_{DC}\cdot e^{\lambda\cdot t} \tag{93}$$

$$I_{L_1}(t-\tau_1)=I_{L_1}^{(j)}+i_{L_1}\cdot e^{\lambda\cdot(t-\tau_1)}\ ;I_{L_2}(t-\tau_1)=I_{L_2}^{(j)}+i_{L_2}\cdot e^{\lambda\cdot(t-\tau_1)}\ ;I_{C_b}(t-\tau_3)=I_{C_b}^{(j)}+i_{C_b}\cdot e^{\lambda\cdot(t-\tau_3)} \tag{94}$$

$$\frac{d^2I_{L_2}}{dt^2}=i_{L_2}\cdot\lambda^2\cdot e^{\lambda\cdot t}\ ;\ \frac{di_{DE}}{dt}=i_{DE}\cdot\lambda\cdot e^{\lambda\cdot t}\ ;\ \frac{d^2}{dt^2}I_{L_1}(t-\tau_1)=i_{L_1}\cdot\lambda^2\cdot e^{\lambda\cdot(t-\tau_1)}\ ;\ \frac{d^2I_{L_2}(t-\tau_1)}{dt^2}=i_{L_2}\cdot\lambda^2\cdot e^{\lambda\cdot(t-\tau_1)} \tag{95}$$

$$\frac{d^2I_{C_a}(t)}{dt^2}=i_{C_a}\cdot\lambda^2\cdot e^{\lambda\cdot t}\ ;\ \frac{d^2I_{L_a}}{dt^2}=i_{L_a}\cdot\lambda^2\cdot e^{\lambda\cdot t}\ ;\ \frac{dI_{C_b}(t-\tau_3)}{dt}=i_{C_b}\cdot\lambda\cdot e^{\lambda\cdot(t-\tau_3)}\ ;\ \frac{dI_{C(V)}}{dt}=i_{C(V)}\cdot\lambda\cdot e^{\lambda\cdot t} \tag{96}$$

We implement the above equations with arbitrarily small increments of exponential form in our system's differential equations (First fixed point).

First equation:

$$\frac{1}{C_p}\cdot I_{C_p}=L_2\cdot\frac{d^2I_{L_2}}{dt^2}+\frac{V_T}{(i_{DE}+I_0)}\cdot\frac{di_{DE}}{dt}-L_p\cdot\frac{d^2}{dt^2}I_{L_1}(t-\tau_1)+L_p\cdot\frac{d^2I_{L_2}(t-\tau_1)}{dt^2}+L_p\cdot\frac{d^2I_{C_a}(t)}{dt^2} \tag{97}$$

$$\frac{1}{C_p}\cdot(I_{C_p}^{(j)}+i_{C_p}\cdot e^{\lambda\cdot t})=L_2\cdot i_{L_2}\cdot\lambda^2\cdot e^{\lambda\cdot t}+\frac{V_T}{(i_{DE}^{(j)}+i_{DE}\cdot e^{\lambda\cdot t}+I_0)}\cdot i_{DE}\cdot\lambda\cdot e^{\lambda\cdot t}-L_p\cdot i_{L_1}\cdot\lambda^2\cdot e^{\lambda\cdot t}\cdot e^{-\lambda\cdot\tau_1}$$
$$+L_p\cdot i_{L_2}\cdot\lambda^2\cdot e^{\lambda\cdot t}\cdot e^{-\lambda\cdot\tau_1}+L_p\cdot i_{C_a}\cdot\lambda^2\cdot e^{\lambda\cdot t} \tag{98}$$

Since $I_{C_p}^{(j)}=0\ ;\ i_{DE}^{(j)}=I_0\cdot(e^{-\frac{\phi}{V_T}}-1)$ then

$$\frac{1}{C_p}\cdot i_{C_p}=L_2\cdot i_{L_2}\cdot\lambda^2+\frac{V_T}{(I_0\cdot(e^{-\frac{\phi}{V_T}}-1)+i_{DE}\cdot e^{\lambda\cdot t}+I_0)}\cdot i_{DE}\cdot\lambda-L_p\cdot i_{L_1}\cdot\lambda^2\cdot e^{-\lambda\cdot\tau_1}+L_p\cdot i_{L_2}\cdot\lambda^2\cdot e^{-\lambda\cdot\tau_1}+L_p\cdot i_{C_a}\cdot\lambda^2 \quad (99)$$

$$\frac{1}{C_p}\cdot i_{C_p}=L_2\cdot i_{L_2}\cdot\lambda^2+\frac{V_T}{(I_0\cdot e^{-\frac{\phi}{V_T}}+i_{DE}\cdot e^{\lambda\cdot t})}\cdot i_{DE}\cdot\lambda-L_p\cdot i_{L_1}\cdot\lambda^2\cdot e^{-\lambda\cdot\tau_1}+L_p\cdot i_{L_2}\cdot\lambda^2\cdot e^{-\lambda\cdot\tau_1}+L_p\cdot i_{C_a}\cdot\lambda^2 \quad (100)$$

$$\frac{1}{C_p}\cdot i_{C_p}=L_2\cdot i_{L_2}\cdot\lambda^2+\frac{V_T}{(I_0\cdot e^{-\frac{\phi}{V_T}}+i_{DE}\cdot e^{\lambda\cdot t})}\cdot\frac{(I_0\cdot e^{-\frac{\phi}{V_T}}-i_{DE}\cdot e^{\lambda\cdot t})}{(I_0\cdot e^{-\frac{\phi}{V_T}}-i_{DE}\cdot e^{\lambda\cdot t})}\cdot i_{DE}\cdot\lambda-L_p\cdot i_{L_1}\cdot\lambda^2\cdot e^{-\lambda\cdot\tau_1} \quad (101)$$
$$+L_p\cdot i_{L_2}\cdot\lambda^2\cdot e^{-\lambda\cdot\tau_1}+L_p\cdot i_{C_a}\cdot\lambda^2$$

$$\frac{1}{C_p}\cdot i_{C_p}=L_2\cdot i_{L_2}\cdot\lambda^2+\frac{V_T}{(I_0^2\cdot e^{-\frac{\phi}{V_T}}-i_{DE}^2\cdot e^{2\cdot\lambda\cdot t})}\cdot(I_0\cdot e^{-\frac{\phi}{V_T}}\cdot i_{DE}-i_{DE}^2\cdot e^{\lambda\cdot t})\cdot\lambda-L_p\cdot i_{L_1}\cdot\lambda^2\cdot e^{-\lambda\cdot\tau_1} \quad (102)$$
$$+L_p\cdot i_{L_2}\cdot\lambda^2\cdot e^{-\lambda\cdot\tau_1}+L_p\cdot i_{C_a}\cdot\lambda^2$$

Since $i_{DE}^2\approx 0$

$$\frac{1}{C_p}\cdot i_{C_p}=L_2\cdot i_{L_2}\cdot\lambda^2+\frac{V_T}{I_0^2\cdot e^{-\frac{\phi}{V_T}}}\cdot I_0\cdot e^{-\frac{\phi}{V_T}}\cdot i_{DE}\cdot\lambda-L_p\cdot i_{L_1}\cdot\lambda^2\cdot e^{-\lambda\cdot\tau_1}+L_p\cdot i_{L_2}\cdot\lambda^2\cdot e^{-\lambda\cdot\tau_1}+L_p\cdot i_{C_a}\cdot\lambda^2 \quad (103)$$

$$\frac{1}{C_p}\cdot i_{C_p}=L_2\cdot i_{L_2}\cdot\lambda^2+\frac{V_T}{I_0}\cdot i_{DE}\cdot\lambda-L_p\cdot i_{L_1}\cdot\lambda^2\cdot e^{-\lambda\cdot\tau_1}+L_p\cdot i_{L_2}\cdot\lambda^2\cdot e^{-\lambda\cdot\tau_1}+L_p\cdot i_{C_a}\cdot\lambda^2 \quad (104)$$

Second equation:

$$\frac{1}{C_a}\cdot I_{C_a}=L_2\cdot\frac{d^2I_{L_2}}{dt^2}-L_a\cdot\frac{d^2I_{L_a}}{dt^2}+V_T\cdot\frac{1}{([I_{L_2}-(1-\alpha_f)\cdot i_{DE}]+I_0\cdot(1-\alpha_r))}\cdot[\frac{dI_{L_2}}{dt}-(1-\alpha_f)\cdot\frac{di_{DE}}{dt}] \quad (105)$$

$$\frac{dI_{L_2}}{dt}=i_{L_2}\cdot\lambda\cdot e^{\lambda\cdot t}\ ;\ \frac{di_{DE}}{dt}=i_{DE}\cdot\lambda\cdot e^{\lambda\cdot t} \quad (106)$$

$$\frac{1}{C_a}\cdot(I_{C_a}^{(j)}+i_{C_a}\cdot e^{\lambda\cdot t})=L_2\cdot i_{L_2}\cdot\lambda^2\cdot e^{\lambda\cdot t}-L_a\cdot i_{L_a}\cdot\lambda^2\cdot e^{\lambda\cdot t}$$
$$+V_T\cdot\frac{1}{([I_{L_2}^{(j)}+i_{L_2}\cdot e^{\lambda\cdot t}-(1-\alpha_f)\cdot(i_{DE}^{(j)}+i_{DE}\cdot e^{\lambda\cdot t})]+I_0\cdot(1-\alpha_r))}\cdot[i_{L_2}\cdot\lambda\cdot e^{\lambda\cdot t}-(1-\alpha_f)\cdot i_{DE}\cdot\lambda\cdot e^{\lambda\cdot t}] \quad (107)$$

Since $I_{C_a}^{(j)}=0\ ;\ i_{DE}^{(j)}=I_0\cdot(e^{-\frac{\phi}{V_T}}-1)$

$$(*)\ \frac{1}{C_a}\cdot i_{C_a}\cdot e^{\lambda\cdot t}=L_2\cdot i_{L_2}\cdot\lambda^2\cdot e^{\lambda\cdot t}-L_a\cdot i_{L_a}\cdot\lambda^2\cdot e^{\lambda\cdot t}$$
$$+V_T\cdot\frac{1}{([I_{L_2}^{(j)}+i_{L_2}\cdot e^{\lambda\cdot t}-(1-\alpha_f)\cdot(I_0\cdot(e^{-\frac{\phi}{V_T}}-1)+i_{DE}\cdot e^{\lambda\cdot t})]+I_0\cdot(1-\alpha_r))}\cdot[i_{L_2}-(1-\alpha_f)\cdot i_{DE}]\cdot\lambda\cdot e^{\lambda\cdot t} \quad (108)$$

$I_{L_2}^{(j)}$ (Fixed points coordinate): $I_{L_2}^{(j)}=I_b^{(j)}=I_e^{(j)}-I_c^{(j)}=i_{DE}^{(j)}-\alpha_r\cdot i_{DC}^{(j)}-I_c^{(j)}$; $I_{C_a}(t+\tau_2)=I_c(t)$ (109)

At fixed points: $\lim_{t\to\infty} I_{C_a}(t+\tau_2)|_{t\to\tau_2}=I_{C_a}(t)$ then $I_c^{(j)}=I_{C_a}^{(j)}$ and $I_{L_2}^{(j)}=i_{DE}^{(j)}-\alpha_r\cdot i_{DC}^{(j)}-I_{C_a}^{(j)}$ (110)

$$I_{C_a}^{(j)}=0 \text{ then } I_{L_2}^{(j)}=i_{DE}^{(j)}-\alpha_r\cdot i_{DC}^{(j)}\ .\ i_{DE}^{(j)}=I_0\cdot(e^{-\frac{\phi}{V_T}}-1)\ ;\ i_{DC}^{(j)}=\frac{1}{(1-\alpha_r)}\cdot[I_{L_2}^{(j)}-(1-\alpha_f)\cdot i_{DE}^{(j)}] \quad (111)$$

$$I_{L_2}^{(j)}=I_0\cdot(e^{-\frac{\phi}{V_T}}-1)-\frac{\alpha_r}{(1-\alpha_r)}\cdot[I_{L_2}^{(j)}-(1-\alpha_f)\cdot i_{DE}^{(j)}] \quad (112)$$

$$I_{L_2}^{(j)}=I_0\cdot(e^{-\frac{\phi}{V_T}}-1)-\frac{\alpha_r}{(1-\alpha_r)}\cdot I_{L_2}^{(j)}+\frac{\alpha_r}{(1-\alpha_r)}\cdot(1-\alpha_f)\cdot I_0\cdot(e^{-\frac{\phi}{V_T}}-1) \quad (113)$$

$$I_{L_2}^{(j)}+\frac{\alpha_r}{(1-\alpha_r)}\cdot I_{L_2}^{(j)}=I_0\cdot(e^{-\frac{\phi}{V_T}}-1)+\frac{\alpha_r}{(1-\alpha_r)}\cdot(1-\alpha_f)\cdot I_0\cdot(e^{-\frac{\phi}{V_T}}-1) \quad (114)$$

$$[1+\frac{\alpha_r}{(1-\alpha_r)}]\cdot I_{L_2}^{(j)}=[1+\frac{\alpha_r}{(1-\alpha_r)}\cdot(1-\alpha_f)]\cdot I_0\cdot(e^{-\frac{\phi}{V_T}}-1) \quad (115)$$

$$1+\frac{\alpha_r}{(1-\alpha_r)}=\frac{1}{(1-\alpha_r)}\ ;\ 1+\frac{\alpha_r}{(1-\alpha_r)}\cdot(1-\alpha_f)=(\frac{1-\alpha_r\cdot\alpha_f}{1-\alpha_r}) \quad (116)$$

$$\frac{1}{(1-\alpha_r)}\cdot I_{L_2}^{(j)}=(\frac{1-\alpha_r\cdot\alpha_f}{1-\alpha_r})\cdot I_0\cdot(e^{-\frac{\phi}{V_T}}-1)\Rightarrow I_{L_2}^{(j)}=(1-\alpha_r\cdot\alpha_f)\cdot I_0\cdot(e^{-\frac{\phi}{V_T}}-1) \quad (117)$$

Implementing our last result in (*) and we get the expression:

$$\frac{1}{C_a}\cdot i_{C_a}\cdot e^{\lambda\cdot t}=L_2\cdot i_{L_2}\cdot\lambda^2\cdot e^{\lambda\cdot t}-L_a\cdot i_{L_a}\cdot\lambda^2\cdot e^{\lambda\cdot t}$$
$$+V_T\cdot\frac{1}{\{[(1-\alpha_r\cdot\alpha_f)\cdot I_0\cdot(e^{-\frac{\phi}{V_T}}-1)+i_{L_2}\cdot e^{\lambda\cdot t}}\cdot[i_{L_2}-(1-\alpha_f)\cdot i_{DE}]\cdot\lambda\cdot e^{\lambda\cdot t} \quad (118)$$
$$-(1-\alpha_f)\cdot(I_0\cdot(e^{-\frac{\phi}{V_T}}-1)+i_{DE}\cdot e^{\lambda\cdot t})]+I_0\cdot(1-\alpha_r)\}$$

###

$$[(1-\alpha_r\cdot\alpha_f)\cdot I_0\cdot(e^{-\frac{\phi}{V_T}}-1)+i_{L_2}\cdot e^{\lambda\cdot t}-(1-\alpha_f)\cdot(I_0\cdot(e^{-\frac{\phi}{V_T}}-1)+i_{DE}\cdot e^{\lambda\cdot t})]+I_0\cdot(1-\alpha_r)$$

$$=(1-\alpha_r)\cdot\alpha_f\cdot I_0\cdot(e^{-\frac{\phi}{V_T}}-1)+I_0\cdot(1-\alpha_r)+[i_{L_2}-(1-\alpha_f)\cdot i_{DE}]\cdot e^{\lambda\cdot t}$$

(119)

We define for simplicity global parameter:

$$\Omega=\Omega(\alpha_r,\alpha_f,I_0,e^{-\frac{\phi}{V_T}})=(1-\alpha_r)\cdot\alpha_f\cdot I_0\cdot(e^{-\frac{\phi}{V_T}}-1)+I_0\cdot(1-\alpha_r) \tag{120}$$

$$\begin{aligned}&[(1-\alpha_r\cdot\alpha_f)\cdot I_0\cdot(e^{-\frac{\phi}{V_T}}-1)+i_{L_2}\cdot e^{\lambda\cdot t}-(1-\alpha_f)\cdot(I_0\cdot(e^{-\frac{\phi}{V_T}}-1)+i_{DE}\cdot e^{\lambda\cdot t})]+I_0\cdot(1-\alpha_r)\\&=\Omega+[i_{L_2}-(1-\alpha_f)\cdot i_{DE}]\cdot e^{\lambda\cdot t}\end{aligned} \tag{121}$$

$$\frac{1}{C_a}\cdot i_{C_a}\cdot e^{\lambda\cdot t}=L_2\cdot i_{L_2}\cdot\lambda^2\cdot e^{\lambda\cdot t}-L_a\cdot i_{L_a}\cdot\lambda^2\cdot e^{\lambda\cdot t}+V_T\cdot\frac{1}{\Omega+[i_{L_2}-(1-\alpha_f)\cdot i_{DE}]\cdot e^{\lambda\cdot t}}\cdot[i_{L_2}-(1-\alpha_f)\cdot i_{DE}]\cdot\lambda\cdot e^{\lambda\cdot t} \tag{122}$$

$$\begin{aligned}&\frac{1}{C_a}\cdot i_{C_a}\cdot e^{\lambda\cdot t}=L_2\cdot i_{L_2}\cdot\lambda^2\cdot e^{\lambda\cdot t}-L_a\cdot i_{L_a}\cdot\lambda^2\cdot e^{\lambda\cdot t}\\&+V_T\cdot\frac{1}{\Omega+[i_{L_2}-(1-\alpha_f)\cdot i_{DE}]\cdot e^{\lambda\cdot t}}\cdot[\frac{\Omega-[i_{L_2}-(1-\alpha_f)\cdot i_{DE}]\cdot e^{\lambda\cdot t}}{\Omega-[i_{L_2}-(1-\alpha_f)\cdot i_{DE}]\cdot e^{\lambda\cdot t}}]\cdot[i_{L_2}-(1-\alpha_f)\cdot i_{DE}]\cdot\lambda\cdot e^{\lambda\cdot t}\end{aligned} \tag{123}$$

$$\frac{1}{C_a}\cdot i_{C_a}=L_2\cdot i_{L_2}\cdot\lambda^2-L_a\cdot i_{L_a}\cdot\lambda^2+V_T\cdot\frac{\Omega-[i_{L_2}-(1-\alpha_f)\cdot i_{DE}]\cdot e^{\lambda\cdot t}}{\Omega^2-[i_{L_2}-(1-\alpha_f)\cdot i_{DE}]^2\cdot e^{2\cdot\lambda\cdot t}}\cdot[i_{L_2}-(1-\alpha_f)\cdot i_{DE}]\cdot\lambda \tag{124}$$

$$[i_{L_2}-(1-\alpha_f)\cdot i_{DE}]^2=i_{L_2}^2-2\cdot i_{L_2}\cdot(1-\alpha_f)\cdot i_{DE}+(1-\alpha_f)^2\cdot i_{DE}^2 \tag{125}$$

$$i_{L_2}^2\approx 0\ ;\ i_{L_2}\cdot i_{DE}\approx 0\ ;\ i_{DE}^2\approx 0\ ;\ [i_{L_2}-(1-\alpha_f)\cdot i_{DE}]^2\approx 0 \tag{126}$$

$$\frac{1}{C_a}\cdot i_{C_a}=L_2\cdot i_{L_2}\cdot\lambda^2-L_a\cdot i_{L_a}\cdot\lambda^2+\frac{V_T}{\Omega^2}\cdot(\Omega-[i_{L_2}-(1-\alpha_f)\cdot i_{DE}]\cdot e^{\lambda\cdot t})\cdot[i_{L_2}-(1-\alpha_f)\cdot i_{DE}]\cdot\lambda \tag{127}$$

$$\begin{aligned}&(\Omega-[i_{L_2}-(1-\alpha_f)\cdot i_{DE}]\cdot e^{\lambda\cdot t})\cdot[i_{L_2}-(1-\alpha_f)\cdot i_{DE}]=\Omega\cdot[i_{L_2}-(1-\alpha_f)\cdot i_{DE}]\\&-[i_{L_2}-(1-\alpha_f)\cdot i_{DE}]\cdot[i_{L_2}-(1-\alpha_f)\cdot i_{DE}]\cdot e^{\lambda\cdot t}=[\Omega\cdot i_{L_2}-\Omega\cdot(1-\alpha_f)\cdot i_{DE}]-[i_{L_2}-(1-\alpha_f)\cdot i_{DE}]^2\cdot e^{\lambda\cdot t}\\&=[\Omega\cdot i_{L_2}-\Omega\cdot(1-\alpha_f)\cdot i_{DE}]-[i_{L_2}-(1-\alpha_f)\cdot i_{DE}]^2\cdot e^{\lambda\cdot t}\\&=[\Omega\cdot i_{L_2}-\Omega\cdot(1-\alpha_f)\cdot i_{DE}]-[i_{L_2}^2-2\cdot i_{L_2}\cdot i_{DE}\cdot(1-\alpha_f)+(1-\alpha_f)^2\cdot i_{DE}^2]\cdot e^{\lambda\cdot t}\end{aligned} \tag{128}$$

Assume $i_{L_2}^2\approx 0\ ;\ i_{L_2}\cdot i_{DE}\approx 0\ ;\ i_{DE}^2\approx 0$

$$(\Omega-[i_{L_2}-(1-\alpha_f)\cdot i_{DE}]\cdot e^{\lambda\cdot t})\cdot[i_{L_2}-(1-\alpha_f)\cdot i_{DE}]=\Omega\cdot[i_{L_2}-(1-\alpha_f)\cdot i_{DE}] \tag{129}$$

$$\frac{1}{C_a}\cdot i_{C_a}=L_2\cdot i_{L_2}\cdot\lambda^2-L_a\cdot i_{L_a}\cdot\lambda^2+\frac{V_T}{\Omega^2}\cdot\Omega\cdot[i_{L_2}-(1-\alpha_f)\cdot i_{DE}]\cdot\lambda \tag{130}$$

$$\frac{1}{C_a}\cdot i_{C_a}=L_2\cdot i_{L_2}\cdot\lambda^2-L_a\cdot i_{L_a}\cdot\lambda^2+\frac{V_T}{\Omega}\cdot[i_{L_2}-(1-\alpha_f)\cdot i_{DE}]\cdot\lambda \quad (131)$$

Third equation:

$$\frac{1}{C_b}\cdot[I_{C_a}-I_{L_a}]=L_a\cdot\frac{d^2I_{L_a}}{dt^2}-\frac{dI_{C_b}(t-\tau_3)}{dt}\cdot R_{load} \quad (132)$$

$$\frac{1}{C_b}\cdot[I_{C_a}^{(j)}+i_{C_a}\cdot e^{\lambda\cdot t}-(I_{L_a}^{(j)}+i_{L_a}\cdot e^{\lambda\cdot t})]=L_a\cdot i_{L_a}\cdot\lambda^2\cdot e^{\lambda\cdot t}-i_{C_b}\cdot\lambda\cdot e^{\lambda\cdot(t-\tau_3)}\cdot R_{load} \quad (133)$$

Fixed points: $I_{C_a}^{(j)}=0$; $I_{L_a}^{(j)}=0$

$$\frac{1}{C_b}\cdot[i_{C_a}-i_{L_a}]\cdot e^{\lambda\cdot t}=L_a\cdot i_{L_a}\cdot\lambda^2\cdot e^{\lambda\cdot t}-i_{C_b}\cdot\lambda\cdot e^{\lambda\cdot t}\cdot e^{-\lambda\cdot\tau_3}\cdot R_{load}\ ;\ \frac{1}{C_b}\cdot[i_{C_a}-i_{L_a}]=L_a\cdot i_{L_a}\cdot\lambda^2-i_{C_b}\cdot\lambda\cdot e^{-\lambda\cdot\tau_3}\cdot R_{load} \quad (134)$$

Fourth equation:

$$\frac{1}{C_p}\cdot I_{C_p}=(1+\frac{1}{\phi}\cdot[L_2\cdot\frac{dI_{L_2}}{dt}+V_T\cdot\ln(\frac{i_{DE}}{I_0}+1)])^{\gamma}\cdot\frac{1}{C_0}\cdot I_{C(V)}+\frac{dI_{C(V)}}{dt}\cdot R \quad (135)$$

At fixed points: $\frac{dI_{C(V)}}{dt}=0$; $\frac{dI_{L_2}}{dt}=0$

$\frac{1}{C_p}\cdot I_{C_p}^{(j)}=(1+\frac{1}{\phi}\cdot[V_T\cdot\ln(\frac{i_{DE}^{(j)}}{I_0}+1)])^{\gamma}\cdot\frac{1}{C_0}\cdot I_{C(V)}^{(j)}$. We choose for simplicity $\gamma=1$ then (136)

$$[1+\frac{1}{\phi}\cdot V_T\cdot\ln(\frac{i_{DE}^{(j)}}{I_0}+1)]\cdot\frac{1}{C_0}\cdot I_{C(V)}^{(j)}-\frac{1}{C_p}\cdot I_{C_p}^{(j)}=0 \quad (137)$$

$$\frac{1}{C_p}\cdot I_{C_p}=(1+\frac{1}{\phi}\cdot[L_2\cdot\frac{dI_{L_2}}{dt}+V_T\cdot\ln(\frac{i_{DE}}{I_0}+1)])\cdot\frac{1}{C_0}\cdot I_{C(V)}+\frac{dI_{C(V)}}{dt}\cdot R \quad (138)$$

$$\frac{1}{C_p}\cdot(I_{C_p}^{(j)}+i_{C_p}\cdot e^{\lambda\cdot t})=(1+\frac{1}{\phi}\cdot[L_2\cdot i_{L_2}\cdot\lambda\cdot e^{\lambda\cdot t}+V_T\cdot\ln(\frac{i_{DE}^{(j)}+i_{DE}\cdot e^{\lambda\cdot t}}{I_0}+1)])\cdot\frac{1}{C_0}\cdot(I_{C(V)}^{(j)}+i_{C(V)}\cdot e^{\lambda\cdot t}) \quad (139)$$
$$+i_{C(V)}\cdot\lambda\cdot e^{\lambda\cdot t}\cdot R$$

$$\frac{1}{C_p}\cdot I_{C_p}^{(j)}+\frac{1}{C_p}\cdot i_{C_p}\cdot e^{\lambda\cdot t}=(1+\frac{1}{\phi}\cdot L_2\cdot i_{L_2}\cdot\lambda\cdot e^{\lambda\cdot t}+\frac{1}{\phi}\cdot V_T\cdot\ln(\frac{i_{DE}^{(j)}+i_{DE}\cdot e^{\lambda\cdot t}}{I_0}+1))\cdot\frac{1}{C_0}\cdot(I_{C(V)}^{(j)}+i_{C(V)}\cdot e^{\lambda\cdot t})$$
$$+i_{C(V)}\cdot\lambda\cdot e^{\lambda\cdot t}\cdot R$$
(140)

We use the summation rule which is especially useful in probability theory. In practice A and B have to be switched on the right hand side of the equations if B > A then ($\ln(A+B)=\ln(A)+\ln(1+\frac{B}{A})$.

$$\ln(\frac{i_{DE}^{(j)}+i_{DE}\cdot e^{\lambda\cdot t}}{I_0}+1)=\ln([1+\frac{i_{DE}^{(j)}}{I_0}]+\frac{i_{DE}\cdot e^{\lambda\cdot t}}{I_0})\ ;A=1+\frac{i_{DE}^{(j)}}{I_0}\ ;B=\frac{i_{DE}\cdot e^{\lambda\cdot t}}{I_0} \tag{141}$$

$$\ln(\frac{i_{DE}^{(j)}+i_{DE}\cdot e^{\lambda\cdot t}}{I_0}+1)=\ln(1+\frac{i_{DE}^{(j)}}{I_0})+\ln(1+\frac{\frac{i_{DE}\cdot e^{\lambda\cdot t}}{I_0}}{1+\frac{i_{DE}^{(j)}}{I_0}})=\ln(1+\frac{i_{DE}^{(j)}}{I_0})+\ln(1+\frac{i_{DE}\cdot e^{\lambda\cdot t}}{I_0+i_{DE}^{(j)}}) \tag{142}$$

$$\frac{1}{C_p}\cdot I_{C_p}^{(j)}+\frac{1}{C_p}\cdot i_{C_p}\cdot e^{\lambda\cdot t}=\{1+\frac{1}{\phi}\cdot L_2\cdot i_{L_2}\cdot\lambda\cdot e^{\lambda\cdot t}+\frac{1}{\phi}\cdot V_T\cdot[\ln(1+\frac{i_{DE}^{(j)}}{I_0})+\ln(1+\frac{i_{DE}\cdot e^{\lambda\cdot t}}{I_0+i_{DE}^{(j)}})]\}\cdot\frac{1}{C_0}\cdot(I_{C(V)}^{(j)}+i_{C(V)}\cdot e^{\lambda\cdot t}) \tag{143}$$
$$+i_{C(V)}\cdot\lambda\cdot e^{\lambda\cdot t}\cdot R$$

$$\frac{1}{C_p}\cdot I_{C_p}^{(j)}+\frac{1}{C_p}\cdot i_{C_p}\cdot e^{\lambda\cdot t}=[1+\frac{1}{\phi}\cdot L_2\cdot i_{L_2}\cdot\lambda\cdot e^{\lambda\cdot t}+\frac{1}{\phi}\cdot V_T\cdot\ln(1+\frac{i_{DE}^{(j)}}{I_0})+\frac{1}{\phi}\cdot V_T\cdot\ln(1+\frac{i_{DE}\cdot e^{\lambda\cdot t}}{I_0+i_{DE}^{(j)}})]\cdot\frac{1}{C_0}\cdot I_{C(V)}^{(j)}$$
$$+[1+\frac{1}{\phi}\cdot L_2\cdot i_{L_2}\cdot\lambda\cdot e^{\lambda\cdot t}+\frac{1}{\phi}\cdot V_T\cdot\ln(1+\frac{i_{DE}^{(j)}}{I_0})+\frac{1}{\phi}\cdot V_T\cdot\ln(1+\frac{i_{DE}\cdot e^{\lambda\cdot t}}{I_0+i_{DE}^{(j)}})]\cdot\frac{1}{C_0}\cdot i_{C(V)}\cdot e^{\lambda\cdot t} \tag{144}$$
$$+i_{C(V)}\cdot\lambda\cdot e^{\lambda\cdot t}\cdot R$$

$$\frac{1}{C_p}\cdot I_{C_p}^{(j)}+\frac{1}{C_p}\cdot i_{C_p}\cdot e^{\lambda\cdot t}=\frac{1}{C_0}\cdot I_{C(V)}^{(j)}+\frac{1}{\phi}\cdot L_2\cdot i_{L_2}\cdot\frac{1}{C_0}\cdot I_{C(V)}^{(j)}\cdot\lambda\cdot e^{\lambda\cdot t}+\frac{1}{\phi}\cdot V_T\cdot\frac{1}{C_0}\cdot I_{C(V)}^{(j)}\cdot\ln(1+\frac{i_{DE}^{(j)}}{I_0})+\frac{1}{\phi}\cdot V_T\cdot\frac{1}{C_0}\cdot I_{C(V)}^{(j)}\cdot\ln(1+\frac{i_{DE}\cdot e^{\lambda\cdot t}}{I_0+i_{DE}^{(j)}})$$
$$+\frac{1}{C_0}\cdot i_{C(V)}\cdot e^{\lambda\cdot t}+\frac{1}{\phi}\cdot L_2\cdot i_{L_2}\cdot\frac{1}{C_0}\cdot i_{C(V)}\cdot e^{\lambda\cdot t}\cdot\lambda\cdot e^{\lambda\cdot t}+\frac{1}{\phi}\cdot V_T\cdot\frac{1}{C_0}\cdot i_{C(V)}\cdot e^{\lambda\cdot t}\cdot\ln(1+\frac{i_{DE}^{(j)}}{I_0})+\frac{1}{\phi}\cdot V_T\cdot\frac{1}{C_0}\cdot i_{C(V)}\cdot e^{\lambda\cdot t}\cdot\ln(1+\frac{i_{DE}\cdot e^{\lambda\cdot t}}{I_0+i_{DE}^{(j)}}) \tag{145}$$
$$+i_{C(V)}\cdot\lambda\cdot e^{\lambda\cdot t}\cdot R$$

$$-\frac{1}{C_p}\cdot I_{C_p}^{(j)}-\frac{1}{C_p}\cdot i_{C_p}\cdot e^{\lambda\cdot t}+\frac{1}{C_0}\cdot I_{C(V)}^{(j)}+\frac{1}{\phi}\cdot L_2\cdot i_{L_2}\cdot\frac{1}{C_0}\cdot I_{C(V)}^{(j)}\cdot\lambda\cdot e^{\lambda\cdot t}+\frac{1}{\phi}\cdot V_T\cdot\frac{1}{C_0}\cdot I_{C(V)}^{(j)}\cdot\ln(1+\frac{i_{DE}^{(j)}}{I_0})+\frac{1}{\phi}\cdot V_T\cdot\frac{1}{C_0}\cdot I_{C(V)}^{(j)}\cdot\ln(1+\frac{i_{DE}\cdot e^{\lambda\cdot t}}{I_0+i_{DE}^{(j)}})$$
$$+\frac{1}{C_0}\cdot i_{C(V)}\cdot e^{\lambda\cdot t}+\frac{1}{\phi}\cdot L_2\cdot i_{L_2}\cdot\frac{1}{C_0}\cdot i_{C(V)}\cdot e^{\lambda\cdot t}\cdot\lambda\cdot e^{\lambda\cdot t}+\frac{1}{\phi}\cdot V_T\cdot\frac{1}{C_0}\cdot i_{C(V)}\cdot e^{\lambda\cdot t}\cdot\ln(1+\frac{i_{DE}^{(j)}}{I_0})+\frac{1}{\phi}\cdot V_T\cdot\frac{1}{C_0}\cdot i_{C(V)}\cdot e^{\lambda\cdot t}\cdot\ln(1+\frac{i_{DE}\cdot e^{\lambda\cdot t}}{I_0+i_{DE}^{(j)}}) \tag{146}$$
$$+i_{C(V)}\cdot\lambda\cdot e^{\lambda\cdot t}\cdot R=0$$

$$-\frac{1}{C_p}\cdot I_{C_p}^{(j)}+\frac{1}{C_0}\cdot I_{C(V)}^{(j)}+\frac{1}{\phi}\cdot V_T\cdot\frac{1}{C_0}\cdot I_{C(V)}^{(j)}\cdot\ln(1+\frac{i_{DE}^{(j)}}{I_0})-\frac{1}{C_p}\cdot i_{C_p}\cdot e^{\lambda\cdot t}+\frac{1}{\phi}\cdot L_2\cdot i_{L_2}\cdot\frac{1}{C_0}\cdot I_{C(V)}^{(j)}\cdot\lambda\cdot e^{\lambda\cdot t}$$
$$+\frac{1}{\phi}\cdot V_T\cdot\frac{1}{C_0}\cdot I_{C(V)}^{(j)}\cdot\ln(1+\frac{i_{DE}\cdot e^{\lambda\cdot t}}{I_0+i_{DE}^{(j)}})+\frac{1}{C_0}\cdot i_{C(V)}\cdot e^{\lambda\cdot t}+\frac{1}{\phi}\cdot L_2\cdot i_{L_2}\cdot\frac{1}{C_0}\cdot i_{C(V)}\cdot e^{\lambda\cdot t}\cdot\lambda\cdot e^{\lambda\cdot t}+\frac{1}{\phi}\cdot V_T\cdot\frac{1}{C_0}\cdot i_{C(V)}\cdot e^{\lambda\cdot t}\cdot\ln(1+\frac{i_{DE}^{(j)}}{I_0}) \tag{147}$$
$$+\frac{1}{\phi}\cdot V_T\cdot\frac{1}{C_0}\cdot i_{C(V)}\cdot e^{\lambda\cdot t}\cdot\ln(1+\frac{i_{DE}\cdot e^{\lambda\cdot t}}{I_0+i_{DE}^{(j)}})+i_{C(V)}\cdot\lambda\cdot e^{\lambda\cdot t}\cdot R=0$$

$$-\frac{1}{C_p}\cdot I_{C_p}^{(j)}+\frac{1}{C_0}\cdot I_{C(V)}^{(j)}\cdot[1+\frac{1}{\phi}\cdot V_T\cdot\ln(1+\frac{i_{DE}^{(j)}}{I_0})]-\frac{1}{C_p}\cdot i_{C_p}\cdot e^{\lambda\cdot t}+\frac{1}{\phi}\cdot L_2\cdot i_{L_2}\cdot\frac{1}{C_0}\cdot I_{C(V)}^{(j)}\cdot\lambda\cdot e^{\lambda\cdot t}$$
$$+\frac{1}{\phi}\cdot V_T\cdot\frac{1}{C_0}\cdot I_{C(V)}^{(j)}\cdot\ln(1+\frac{i_{DE}\cdot e^{\lambda\cdot t}}{I_0+i_{DE}^{(j)}})+\frac{1}{C_0}\cdot i_{C(V)}\cdot e^{\lambda\cdot t}+\frac{1}{\phi}\cdot L_2\cdot i_{L_2}\cdot\frac{1}{C_0}\cdot i_{C(V)}\cdot e^{\lambda\cdot t}\cdot\lambda\cdot e^{\lambda\cdot t}+\frac{1}{\phi}\cdot V_T\cdot\frac{1}{C_0}\cdot i_{C(V)}\cdot e^{\lambda\cdot t}\cdot\ln(1+\frac{i_{DE}^{(j)}}{I_0}) \quad (148)$$
$$+\frac{1}{\phi}\cdot V_T\cdot\frac{1}{C_0}\cdot i_{C(V)}\cdot e^{\lambda\cdot t}\cdot\ln(1+\frac{i_{DE}\cdot e^{\lambda\cdot t}}{I_0+i_{DE}^{(j)}})+i_{C(V)}\cdot\lambda\cdot e^{\lambda\cdot t}\cdot R=0$$

At fixed points $-\frac{1}{C_p}\cdot I_{C_p}^{(j)}+\frac{1}{C_0}\cdot I_{C(V)}^{(j)}\cdot[1+\frac{1}{\phi}\cdot V_T\cdot\ln(1+\frac{i_{DE}^{(j)}}{I_0})]=0$ then (149)

$$-\frac{1}{C_p}\cdot i_{C_p}\cdot e^{\lambda\cdot t}+\frac{1}{\phi}\cdot L_2\cdot i_{L_2}\cdot\frac{1}{C_0}\cdot I_{C(V)}^{(j)}\cdot\lambda\cdot e^{\lambda\cdot t}+\frac{1}{\phi}\cdot V_T\cdot\frac{1}{C_0}\cdot I_{C(V)}^{(j)}\cdot\ln(1+\frac{i_{DE}\cdot e^{\lambda\cdot t}}{I_0+i_{DE}^{(j)}})+\frac{1}{C_0}\cdot i_{C(V)}\cdot e^{\lambda\cdot t}$$
$$+\frac{1}{\phi}\cdot L_2\cdot i_{L_2}\cdot\frac{1}{C_0}\cdot i_{C(V)}\cdot e^{\lambda\cdot t}\cdot\lambda\cdot e^{\lambda\cdot t}+\frac{1}{\phi}\cdot V_T\cdot\frac{1}{C_0}\cdot i_{C(V)}\cdot e^{\lambda\cdot t}\cdot\ln(1+\frac{i_{DE}^{(j)}}{I_0})+\frac{1}{\phi}\cdot V_T\cdot\frac{1}{C_0}\cdot i_{C(V)}\cdot e^{\lambda\cdot t}\cdot\ln(1+\frac{i_{DE}\cdot e^{\lambda\cdot t}}{I_0+i_{DE}^{(j)}}) \quad (150)$$
$$+i_{C(V)}\cdot\lambda\cdot e^{\lambda\cdot t}\cdot R=0$$

$$-\frac{1}{C_p}\cdot i_{C_p}\cdot e^{\lambda\cdot t}+\frac{1}{\phi}\cdot L_2\cdot i_{L_2}\cdot\frac{1}{C_0}\cdot I_{C(V)}^{(j)}\cdot\lambda\cdot e^{\lambda\cdot t}+\frac{1}{\phi}\cdot V_T\cdot\frac{1}{C_0}\cdot I_{C(V)}^{(j)}\cdot\ln(1+\frac{i_{DE}\cdot e^{\lambda\cdot t}}{I_0+i_{DE}^{(j)}})+\frac{1}{C_0}\cdot i_{C(V)}\cdot e^{\lambda\cdot t}$$
$$+\frac{1}{\phi}\cdot V_T\cdot\frac{1}{C_0}\cdot i_{C(V)}\cdot e^{\lambda\cdot t}\cdot\ln(1+\frac{i_{DE}^{(j)}}{I_0})+\frac{1}{\phi}\cdot V_T\cdot\frac{1}{C_0}\cdot i_{C(V)}\cdot e^{\lambda\cdot t}\cdot\ln(1+\frac{i_{DE}\cdot e^{\lambda\cdot t}}{I_0+i_{DE}^{(j)}}) \quad (151)$$
$$+i_{C(V)}\cdot\lambda\cdot e^{\lambda\cdot t}\cdot R+\frac{1}{\phi}\cdot L_2\cdot i_{L_2}\cdot i_{C(V)}\cdot\frac{1}{C_0}\cdot e^{\lambda\cdot t}\cdot\lambda\cdot e^{\lambda\cdot t}=0$$

Assume $i_{L_2}\cdot i_{C(V)}\approx 0$

(**)
$$-\frac{1}{C_p}\cdot i_{C_p}\cdot e^{\lambda\cdot t}+\frac{1}{\phi}\cdot L_2\cdot i_{L_2}\cdot\frac{1}{C_0}\cdot I_{C(V)}^{(j)}\cdot\lambda\cdot e^{\lambda\cdot t}+\frac{1}{\phi}\cdot V_T\cdot\frac{1}{C_0}\cdot I_{C(V)}^{(j)}\cdot\ln(1+\frac{i_{DE}\cdot e^{\lambda\cdot t}}{I_0+i_{DE}^{(j)}})+\frac{1}{C_0}\cdot i_{C(V)}\cdot e^{\lambda\cdot t} \quad (152)$$
$$+\frac{1}{\phi}\cdot V_T\cdot\frac{1}{C_0}\cdot i_{C(V)}\cdot e^{\lambda\cdot t}\cdot\ln(1+\frac{i_{DE}^{(j)}}{I_0})+\frac{1}{\phi}\cdot V_T\cdot\frac{1}{C_0}\cdot i_{C(V)}\cdot e^{\lambda\cdot t}\cdot\ln(1+\frac{i_{DE}\cdot e^{\lambda\cdot t}}{I_0+i_{DE}^{(j)}})+i_{C(V)}\cdot\lambda\cdot e^{\lambda\cdot t}\cdot R=0$$

We define $f(i_{DE},i_{DE}^{(j)})=\frac{i_{DE}\cdot e^{\lambda\cdot t}}{I_0+i_{DE}^{(j)}}$; $\ln(1+f(i_{DE},i_{DE}^{(j)}))=\ln(1+\frac{i_{DE}\cdot e^{\lambda\cdot t}}{I_0+i_{DE}^{(j)}})$ (153)

By using Taylor series: $\ln(1+f(i_{DE},i_{DE}^{(j)}))=\sum_{n\geq 0}\frac{(-1)^n\cdot[f(i_{DE},i_{DE}^{(j)})]^{n+1}}{n+1}=f(i_{DE},i_{DE}^{(j)})-\frac{1}{2}\cdot f^2(i_{DE},i_{DE}^{(j)})+\ldots$ (154)

$$\ln(1+f(i_{DE},i_{DE}^{(j)}))=\frac{i_{DE}\cdot e^{\lambda\cdot t}}{I_0+i_{DE}^{(j)}}-\frac{1}{2}\cdot\frac{i_{DE}^2\cdot e^{2\cdot\lambda\cdot t}}{(I_0+i_{DE}^{(j)})^2}+\ldots \quad (155)$$

Since $i_{DE}^2\approx 0$ then $\ln(1+f(i_{DE},i_{DE}^{(j)}))=\ln(1+\frac{i_{DE}\cdot e^{\lambda\cdot t}}{I_0+i_{DE}^{(j)}})\approx\frac{i_{DE}\cdot e^{\lambda\cdot t}}{I_0+i_{DE}^{(j)}}$ (156)

$$\ln(1+f(i_{DE},i_{DE}^{(j)}))=\ln(1+\frac{i_{DE}\cdot e^{\lambda\cdot t}}{I_0+i_{DE}^{(j)}})\approx\frac{i_{DE}\cdot e^{\lambda\cdot t}}{I_0+i_{DE}^{(j)}}\underset{I_0\gg i_{DE}^{(j)}}{=}\frac{1}{I_0}\cdot i_{DE}\cdot e^{\lambda\cdot t} \tag{157}$$

Implementing $\ln(1+\frac{i_{DE}\cdot e^{\lambda\cdot t}}{I_0+i_{DE}^{(j)}})\approx\frac{i_{DE}\cdot e^{\lambda\cdot t}}{I_0+i_{DE}^{(j)}}\underset{I_0\gg i_{DE}^{(j)}}{=}\frac{1}{I_0}\cdot i_{DE}\cdot e^{\lambda\cdot t}$ in (**) (158)

$$\begin{aligned}&-\frac{1}{C_p}\cdot i_{C_p}\cdot e^{\lambda\cdot t}+\frac{1}{\phi}\cdot L_2\cdot i_{L_2}\cdot\frac{1}{C_0}\cdot I_{C(V)}^{(j)}\cdot\lambda\cdot e^{\lambda\cdot t}+\frac{1}{\phi}\cdot V_T\cdot\frac{1}{C_0}\cdot I_{C(V)}^{(j)}\cdot\frac{1}{I_0}\cdot i_{DE}\cdot e^{\lambda\cdot t}+\frac{1}{C_0}\cdot i_{C(V)}\cdot e^{\lambda\cdot t}\\&+\frac{1}{\phi}\cdot V_T\cdot\frac{1}{C_0}\cdot i_{C(V)}\cdot e^{\lambda\cdot t}\cdot\ln(1+\frac{i_{DE}^{(j)}}{I_0})+\frac{1}{\phi}\cdot V_T\cdot\frac{1}{C_0}\cdot i_{C(V)}\cdot e^{\lambda\cdot t}\cdot\frac{1}{I_0}\cdot i_{DE}\cdot e^{\lambda\cdot t}+i_{C(V)}\cdot\lambda\cdot e^{\lambda\cdot t}\cdot R=0\end{aligned} \tag{159}$$

Divide the two sides of the above equation by $e^{\lambda\cdot t}$ and assuming

$$\begin{aligned}&-\frac{1}{C_p}\cdot i_{C_p}+\frac{1}{\phi}\cdot L_2\cdot i_{L_2}\cdot\frac{1}{C_0}\cdot I_{C(V)}^{(j)}\cdot\lambda+\frac{1}{\phi}\cdot V_T\cdot\frac{1}{C_0}\cdot I_{C(V)}^{(j)}\cdot\frac{1}{I_0}\cdot i_{DE}+\frac{1}{C_0}\cdot i_{C(V)}\\&+\frac{1}{\phi}\cdot V_T\cdot\frac{1}{C_0}\cdot i_{C(V)}\cdot\ln(1+\frac{i_{DE}^{(j)}}{I_0})+\frac{1}{\phi}\cdot V_T\cdot\frac{1}{C_0}\cdot i_{C(V)}\cdot i_{DE}\cdot\frac{1}{I_0}\cdot e^{\lambda\cdot t}+i_{C(V)}\cdot\lambda\cdot R=0\end{aligned} \tag{160}$$

$$i_{C(V)}\cdot i_{DE}\approx 0\ ;\ i_{DE}^{(j)}=I_0\cdot(e^{-\frac{\phi}{V_T}}-1) \tag{161}$$

$$\begin{aligned}&-\frac{1}{C_p}\cdot i_{C_p}+\frac{1}{\phi}\cdot L_2\cdot i_{L_2}\cdot\frac{1}{C_0}\cdot I_{C(V)}^{(j)}\cdot\lambda+\frac{1}{\phi}\cdot V_T\cdot\frac{1}{C_0}\cdot I_{C(V)}^{(j)}\cdot\frac{1}{I_0}\cdot i_{DE}+\frac{1}{C_0}\cdot i_{C(V)}\\&+\frac{1}{\phi}\cdot V_T\cdot\frac{1}{C_0}\cdot i_{C(V)}\cdot\ln(1+\frac{i_{DE}^{(j)}}{I_0})+i_{C(V)}\cdot\lambda\cdot R=0\end{aligned} \tag{162}$$

$$-\frac{1}{C_p}\cdot i_{C_p}+\frac{1}{\phi}\cdot L_2\cdot i_{L_2}\cdot\frac{1}{C_0}\cdot I_{C(V)}^{(j)}\cdot\lambda+\frac{1}{\phi}\cdot V_T\cdot\frac{1}{C_0}\cdot I_{C(V)}^{(j)}\cdot\frac{1}{I_0}\cdot i_{DE}+[\frac{1}{C_0}+\frac{V_T}{\phi\cdot C_0}\cdot\ln(1+\frac{I_0\cdot(e^{-\frac{\phi}{V_T}}-1)}{I_0})+\lambda\cdot R]\cdot i_{C(V)}=0 \tag{163}$$

$$-\frac{1}{C_p}\cdot i_{C_p}+\frac{1}{\phi}\cdot L_2\cdot i_{L_2}\cdot\frac{1}{C_0}\cdot I_{C(V)}^{(j)}\cdot\lambda+\frac{1}{\phi}\cdot V_T\cdot\frac{1}{C_0}\cdot I_{C(V)}^{(j)}\cdot\frac{1}{I_0}\cdot i_{DE}+[\frac{1}{C_0}+\frac{V_T}{\phi\cdot C_0}\cdot\ln(e^{-\frac{\phi}{V_T}})+\lambda\cdot R]\cdot i_{C(V)}=0 \tag{164}$$

$$-\frac{1}{C_p}\cdot i_{C_p}+\frac{1}{\phi}\cdot L_2\cdot i_{L_2}\cdot\frac{1}{C_0}\cdot I_{C(V)}^{(j)}\cdot\lambda+\frac{1}{\phi}\cdot V_T\cdot\frac{1}{C_0}\cdot I_{C(V)}^{(j)}\cdot\frac{1}{I_0}\cdot i_{DE}+\lambda\cdot R\cdot i_{C(V)}=0 \tag{165}$$

We can summery our equations with arbitrarily small increments of exponential form (1):

(A) $$\frac{1}{C_p}\cdot i_{C_p}=L_2\cdot i_{L_2}\cdot\lambda^2+\frac{V_T}{I_0}\cdot i_{DE}\cdot\lambda-L_p\cdot i_{L_1}\cdot\lambda^2\cdot e^{-\lambda\cdot\tau_1}+L_p\cdot i_{L_2}\cdot\lambda^2\cdot e^{-\lambda\cdot\tau_1}+L_p\cdot i_{C_a}\cdot\lambda^2 \tag{166}$$

(B) $$\frac{1}{C_a}\cdot i_{C_a}=L_2\cdot i_{L_2}\cdot\lambda^2-L_a\cdot i_{L_a}\cdot\lambda^2+\frac{V_T}{\Omega}\cdot[i_{L_2}-(1-\alpha_f)\cdot i_{DE}]\cdot\lambda \tag{167}$$

(C) $$\frac{1}{C_b}\cdot[i_{C_a}-i_{L_a}]=L_a\cdot i_{L_a}\cdot\lambda^2-i_{C_b}\cdot\lambda\cdot e^{-\lambda\cdot\tau_3}\cdot R_{load} \tag{168}$$

(D) $$-\frac{1}{C_p}\cdot i_{C_p}+\frac{1}{\phi}\cdot L_2\cdot i_{L_2}\cdot\frac{1}{C_0}\cdot I_{C(V)}^{(j)}\cdot\lambda+\frac{1}{\phi}\cdot V_T\cdot\frac{1}{C_0}\cdot I_{C(V)}^{(j)}\cdot\frac{1}{I_0}\cdot i_{DE}+\lambda\cdot R\cdot i_{C(V)}=0 \tag{169}$$

Taking equation (D): $-\frac{1}{C_p}\cdot i_{C_p}+\frac{1}{\phi}\cdot L_2\cdot i_{L_2}\cdot\frac{1}{C_0}\cdot I_{C(V)}^{(j)}\cdot\lambda+\frac{1}{\phi}\cdot V_T\cdot\frac{1}{C_0}\cdot I_{C(V)}^{(j)}\cdot\frac{1}{I_0}\cdot i_{DE}+\lambda\cdot R\cdot i_{C(V)}=0$ (170)

$$\frac{1}{\phi}\cdot V_T\cdot\frac{1}{C_0}\cdot I_{C(V)}^{(j)}\cdot\frac{1}{I_0}\cdot i_{DE}=\frac{1}{C_p}\cdot i_{C_p}-\frac{1}{\phi}\cdot L_2\cdot i_{L_2}\cdot\frac{1}{C_0}\cdot I_{C(V)}^{(j)}\cdot\lambda-\lambda\cdot R\cdot i_{C(V)} \quad (171)$$

$$i_{DE}=\frac{\frac{1}{C_p}\cdot i_{C_p}-\frac{1}{\phi}\cdot L_2\cdot i_{L_2}\cdot\frac{1}{C_0}\cdot I_{C(V)}^{(j)}\cdot\lambda-\lambda\cdot R\cdot i_{C(V)}}{\frac{1}{\phi}\cdot V_T\cdot\frac{1}{C_0}\cdot I_{C(V)}^{(j)}\cdot\frac{1}{I_0}} \quad (172)$$

$$i_{DE}=\frac{\frac{1}{C_p}\cdot i_{C_p}-i_{L_2}\cdot\frac{L_2\cdot I_{C(V)}^{(j)}}{C_0\cdot\phi}\cdot\lambda-\lambda\cdot R\cdot i_{C(V)}}{\frac{V_T\cdot I_{C(V)}^{(j)}}{\phi\cdot C_0\cdot I_0}}\ ;\ i_{DE}=\frac{\phi\cdot C_0\cdot I_0}{V_T\cdot I_{C(V)}^{(j)}}\cdot\frac{1}{C_p}\cdot i_{C_p}-\frac{I_0\cdot L_2}{V_T}\cdot i_{L_2}\cdot\lambda-\lambda\cdot i_{C(V)}\cdot\frac{\phi\cdot C_0\cdot I_0\cdot R}{V_T\cdot I_{C(V)}^{(j)}} \quad (173)$$

We define for simplicity global parameters: $\Xi_1=\frac{\phi\cdot C_0\cdot I_0}{V_T\cdot I_{C(V)}^{(j)}}\cdot\frac{1}{C_p}\ ;\ \Xi_2=\frac{I_0\cdot L_2}{V_T}\ ;\ \Xi_3=\frac{\phi\cdot C_0\cdot I_0\cdot R}{V_T\cdot I_{C(V)}^{(j)}}$ (174)

$$i_{DE}=\Xi_1\cdot i_{C_p}-\Xi_2\cdot i_{L_2}\cdot\lambda-\lambda\cdot i_{C(V)}\cdot\Xi_3 \quad (175)$$

Implement the last result in (B):

$$\frac{1}{C_a}\cdot i_{C_a}=L_2\cdot i_{L_2}\cdot\lambda^2-L_a\cdot i_{L_a}\cdot\lambda^2+\frac{V_T}{\Omega}\cdot[i_{L_2}-(1-\alpha_f)\cdot(\Xi_1\cdot i_{C_p}-\Xi_2\cdot i_{L_2}\cdot\lambda-\lambda\cdot i_{C(V)}\cdot\Xi_3)]\cdot\lambda \quad (180)$$

$$\frac{1}{C_a}\cdot i_{C_a}=L_2\cdot i_{L_2}\cdot\lambda^2-L_a\cdot i_{L_a}\cdot\lambda^2+i_{L_2}\cdot\frac{V_T}{\Omega}\cdot\lambda-\frac{V_T}{\Omega}\cdot(1-\alpha_f)\cdot\Xi_1\cdot i_{C_p}\cdot\lambda+\frac{V_T}{\Omega}\cdot(1-\alpha_f)\cdot\Xi_2\cdot i_{L_2}\cdot\lambda^2$$
$$+\frac{V_T}{\Omega}\cdot(1-\alpha_f)\cdot\lambda^2\cdot i_{C(V)}\cdot\Xi_3 \quad (181)$$

$$\frac{1}{C_a}\cdot i_{C_a}=[(L_2+\frac{V_T}{\Omega}\cdot(1-\alpha_f)\cdot\Xi_2)\cdot\lambda^2+\frac{V_T}{\Omega}\cdot\lambda]\cdot i_{L_2}-L_a\cdot i_{L_a}\cdot\lambda^2-\frac{V_T}{\Omega}\cdot(1-\alpha_f)\cdot\Xi_1\cdot i_{C_p}\cdot\lambda$$
$$+\frac{V_T}{\Omega}\cdot(1-\alpha_f)\cdot\lambda^2\cdot i_{C(V)}\cdot\Xi_3 \quad (182)$$

Implement the last result in (A):

$$\frac{1}{C_p}\cdot i_{C_p}=L_2\cdot i_{L_2}\cdot\lambda^2+\frac{V_T}{I_0}\cdot i_{DE}\cdot\lambda-L_p\cdot i_{L_1}\cdot\lambda^2\cdot e^{-\lambda\cdot\tau_1}+L_p\cdot i_{L_2}\cdot\lambda^2\cdot e^{-\lambda\cdot\tau_1}+L_p\cdot i_{C_a}\cdot\lambda^2 \quad (183)$$

$$\frac{1}{C_p}\cdot i_{C_p}=L_2\cdot i_{L_2}\cdot\lambda^2+\frac{V_T}{I_0}\cdot(\Xi_1\cdot i_{C_p}-\Xi_2\cdot i_{L_2}\cdot\lambda-\lambda\cdot i_{C(V)}\cdot\Xi_3)\cdot\lambda-L_p\cdot i_{L_1}\cdot\lambda^2\cdot e^{-\lambda\cdot\tau_1}+L_p\cdot i_{L_2}\cdot\lambda^2\cdot e^{-\lambda\cdot\tau_1}+L_p\cdot i_{C_a}\cdot\lambda^2 \quad (184)$$

$$\frac{1}{C_p}\cdot i_{C_p} = L_2\cdot i_{L_2}\cdot\lambda^2 + \frac{V_T}{I_0}\cdot\Xi_1\cdot i_{C_p}\cdot\lambda - \frac{V_T}{I_0}\cdot\Xi_2\cdot i_{L_2}\cdot\lambda^2 - \frac{V_T}{I_0}\cdot\lambda^2\cdot i_{C(V)}\cdot\Xi_3 - L_p\cdot i_{L_1}\cdot\lambda^2\cdot e^{-\lambda\cdot\tau_1} + L_p\cdot i_{L_2}\cdot\lambda^2\cdot e^{-\lambda\cdot\tau_1} + L_p\cdot i_{C_a}\cdot\lambda^2 \quad (185)$$

$$\frac{1}{C_p}\cdot i_{C_p} = [L_2\cdot\lambda^2 - \frac{V_T}{I_0}\cdot\Xi_2\cdot\lambda^2 + L_p\cdot\lambda^2\cdot e^{-\lambda\cdot\tau_1}]\cdot i_{L_2} + \frac{V_T}{I_0}\cdot\Xi_1\cdot i_{C_p}\cdot\lambda - \frac{V_T}{I_0}\cdot\lambda^2\cdot i_{C(V)}\cdot\Xi_3 - L_p\cdot i_{L_1}\cdot\lambda^2\cdot e^{-\lambda\cdot\tau_1} + L_p\cdot i_{C_a}\cdot\lambda^2 \quad (186)$$

We can summery our equations with arbitrarily small increments of exponential form (2):

(E) $$\frac{1}{C_p}\cdot i_{C_p} = [L_2\cdot\lambda^2 - \frac{V_T}{I_0}\cdot\Xi_2\cdot\lambda^2 + L_p\cdot\lambda^2\cdot e^{-\lambda\cdot\tau_1}]\cdot i_{L_2} + \frac{V_T}{I_0}\cdot\Xi_1\cdot i_{C_p}\cdot\lambda - \frac{V_T}{I_0}\cdot\lambda^2\cdot i_{C(V)}\cdot\Xi_3 - L_p\cdot i_{L_1}\cdot\lambda^2\cdot e^{-\lambda\cdot\tau_1} + L_p\cdot i_{C_a}\cdot\lambda^2 \quad (187)$$

(F) $$\frac{1}{C_a}\cdot i_{C_a} = [(L_2 + \frac{V_T}{\Omega}\cdot(1-\alpha_f)\cdot\Xi_2)\cdot\lambda^2 + \frac{V_T}{\Omega}\cdot\lambda]\cdot i_{L_2} - L_a\cdot i_{L_a}\cdot\lambda^2 - \frac{V_T}{\Omega}\cdot(1-\alpha_f)\cdot\Xi_1\cdot i_{C_p}\cdot\lambda + \frac{V_T}{\Omega}\cdot(1-\alpha_f)\cdot\lambda^2\cdot i_{C(V)}\cdot\Xi_3 \quad (188)$$

(G) $$\frac{1}{C_b}\cdot[i_{C_a} - i_{L_a}] = L_a\cdot i_{L_a}\cdot\lambda^2 - i_{C_b}\cdot\lambda\cdot e^{-\lambda\cdot\tau_3}\cdot R_{load} \quad (189)$$

Taking equation (F):

$$\frac{V_T}{\Omega}\cdot(1-\alpha_f)\cdot\lambda^2\cdot i_{C(V)}\cdot\Xi_3 = \frac{1}{C_a}\cdot i_{C_a} - [(L_2 + \frac{V_T}{\Omega}\cdot(1-\alpha_f)\cdot\Xi_2)\cdot\lambda^2 + \frac{V_T}{\Omega}\cdot\lambda]\cdot i_{L_2} + L_a\cdot i_{L_a}\cdot\lambda^2 + \frac{V_T}{\Omega}\cdot(1-\alpha_f)\cdot\Xi_1\cdot i_{C_p}\cdot\lambda \quad (190)$$

$$V_T\cdot\lambda^2\cdot i_{C(V)}\cdot\Xi_3\cdot\frac{1}{\Omega}\cdot(1-\alpha_f) = \frac{1}{C_a}\cdot i_{C_a} - [(L_2 + \frac{V_T}{\Omega}\cdot(1-\alpha_f)\cdot\Xi_2)\cdot\lambda^2 + \frac{V_T}{\Omega}\cdot\lambda]\cdot i_{L_2} + L_a\cdot i_{L_a}\cdot\lambda^2 + \frac{V_T}{\Omega}\cdot(1-\alpha_f)\cdot\Xi_1\cdot i_{C_p}\cdot\lambda \quad (191)$$

$$V_T\cdot\lambda^2\cdot i_{C(V)}\cdot\Xi_3 = \frac{1}{\frac{1}{\Omega}\cdot(1-\alpha_f)}\cdot\frac{1}{C_a}\cdot i_{C_a} - \frac{1}{\frac{1}{\Omega}\cdot(1-\alpha_f)}\cdot[(L_2 + \frac{V_T}{\Omega}\cdot(1-\alpha_f)\cdot\Xi_2)\cdot\lambda^2 + \frac{V_T}{\Omega}\cdot\lambda]\cdot i_{L_2} + \frac{1}{\frac{1}{\Omega}\cdot(1-\alpha_f)}\cdot L_a\cdot i_{L_a}\cdot\lambda^2 + \frac{1}{\frac{1}{\Omega}\cdot(1-\alpha_f)}\cdot\frac{V_T}{\Omega}\cdot(1-\alpha_f)\cdot\Xi_1\cdot i_{C_p}\cdot\lambda \quad (192)$$

$$V_T\cdot\lambda^2\cdot i_{C(V)}\cdot\Xi_3=\frac{\Omega}{(1-\alpha_f)\cdot C_a}\cdot i_{C_a}-\frac{1}{\frac{1}{\Omega}\cdot(1-\alpha_f)}\cdot[(L_2+\frac{V_T}{\Omega}\cdot(1-\alpha_f)\cdot\Xi_2)\cdot\lambda^2+\frac{V_T}{\Omega}\cdot\lambda]\cdot i_{L_2}$$
$$+\frac{\Omega\cdot L_a}{(1-\alpha_f)}\cdot i_{L_a}\cdot\lambda^2+V_T\cdot\Xi_1\cdot i_{C_p}\cdot\lambda \quad (193)$$

$$V_T\cdot\lambda^2\cdot i_{C(V)}\cdot\Xi_3=\frac{\Omega}{(1-\alpha_f)\cdot C_a}\cdot i_{C_a}-[(\frac{\Omega\cdot L_2}{(1-\alpha_f)}+V_T\cdot\Xi_2)\cdot\lambda^2+\frac{V_T}{(1-\alpha_f)}\cdot\lambda]\cdot i_{L_2}$$
$$+\frac{\Omega\cdot L_a}{(1-\alpha_f)}\cdot i_{L_a}\cdot\lambda^2+V_T\cdot\Xi_1\cdot i_{C_p}\cdot\lambda \quad (194)$$

We define for simplicity global parameters: $\Xi_4=\frac{\Omega}{(1-\alpha_f)\cdot C_a}$; $\Xi_5=\frac{\Omega\cdot L_2}{(1-\alpha_f)}+V_T\cdot\Xi_2$ (195)

$$\Xi_6=\frac{V_T}{(1-\alpha_f)}\ ;\ \Xi_7=\frac{\Omega\cdot L_a}{(1-\alpha_f)}\ ;\ \Xi_8=V_T\cdot\Xi_1 \quad (196)$$

$$V_T\cdot\lambda^2\cdot i_{C(V)}\cdot\Xi_3=\Xi_4\cdot i_{C_a}-[\Xi_5\cdot\lambda^2+\Xi_6\cdot\lambda]\cdot i_{L_2}+\Xi_7\cdot i_{L_a}\cdot\lambda^2+\Xi_8\cdot i_{C_p}\cdot\lambda \quad (197)$$

Implement the last result in (E):

$$\frac{1}{C_p}\cdot i_{C_p}=[L_2\cdot\lambda^2-\frac{V_T}{I_0}\cdot\Xi_2\cdot\lambda^2+L_p\cdot\lambda^2\cdot e^{-\lambda\cdot\tau_1}]\cdot i_{L_2}+\frac{V_T}{I_0}\cdot\Xi_1\cdot i_{C_p}\cdot\lambda-\frac{1}{I_0}\cdot V_T\cdot\lambda^2\cdot i_{C(V)}\cdot\Xi_3$$
$$-L_p\cdot i_{L_1}\cdot\lambda^2\cdot e^{-\lambda\cdot\tau_1}+L_p\cdot i_{C_a}\cdot\lambda^2 \quad (198)$$

$$\frac{1}{C_p}\cdot i_{C_p}=[L_2\cdot\lambda^2-\frac{V_T}{I_0}\cdot\Xi_2\cdot\lambda^2+L_p\cdot\lambda^2\cdot e^{-\lambda\cdot\tau_1}]\cdot i_{L_2}+\frac{V_T}{I_0}\cdot\Xi_1\cdot i_{C_p}\cdot\lambda$$
$$-\frac{1}{I_0}\cdot(\Xi_4\cdot i_{C_a}-[\Xi_5\cdot\lambda^2+\Xi_6\cdot\lambda]\cdot i_{L_2}+\Xi_7\cdot i_{L_a}\cdot\lambda^2+\Xi_8\cdot i_{C_p}\cdot\lambda)-L_p\cdot i_{L_1}\cdot\lambda^2\cdot e^{-\lambda\cdot\tau_1}+L_p\cdot i_{C_a}\cdot\lambda^2 \quad (199)$$

$$\frac{1}{C_p}\cdot i_{C_p}=[L_2\cdot\lambda^2-\frac{V_T}{I_0}\cdot\Xi_2\cdot\lambda^2+L_p\cdot\lambda^2\cdot e^{-\lambda\cdot\tau_1}]\cdot i_{L_2}+\frac{V_T}{I_0}\cdot\Xi_1\cdot i_{C_p}\cdot\lambda$$
$$-(\frac{1}{I_0}\cdot\Xi_4\cdot i_{C_a}-\frac{1}{I_0}\cdot[\Xi_5\cdot\lambda^2+\Xi_6\cdot\lambda]\cdot i_{L_2}+\frac{1}{I_0}\cdot\Xi_7\cdot i_{L_a}\cdot\lambda^2+\frac{1}{I_0}\cdot\Xi_8\cdot i_{C_p}\cdot\lambda)-L_p\cdot i_{L_1}\cdot\lambda^2\cdot e^{-\lambda\cdot\tau_1}+L_p\cdot i_{C_a}\cdot\lambda^2 \quad (200)$$

$$\frac{1}{C_p}\cdot i_{C_p}=[L_2\cdot\lambda^2-\frac{V_T}{I_0}\cdot\Xi_2\cdot\lambda^2+L_p\cdot\lambda^2\cdot e^{-\lambda\cdot\tau_1}]\cdot i_{L_2}+\frac{V_T}{I_0}\cdot\Xi_1\cdot i_{C_p}\cdot\lambda$$
$$-\frac{1}{I_0}\cdot\Xi_4\cdot i_{C_a}+\frac{1}{I_0}\cdot[\Xi_5\cdot\lambda^2+\Xi_6\cdot\lambda]\cdot i_{L_2}-\frac{1}{I_0}\cdot\Xi_7\cdot i_{L_a}\cdot\lambda^2-\frac{1}{I_0}\cdot\Xi_8\cdot i_{C_p}\cdot\lambda-L_p\cdot i_{L_1}\cdot\lambda^2\cdot e^{-\lambda\cdot\tau_1}+L_p\cdot i_{C_a}\cdot\lambda^2 \quad (201)$$

$$i_{C_p}\cdot(\frac{1}{C_p}+[\Xi_8-V_T\cdot\Xi_1]\cdot\frac{1}{I_0}\cdot\lambda)=[L_2\cdot\lambda^2-\frac{V_T}{I_0}\cdot\Xi_2\cdot\lambda^2+L_p\cdot\lambda^2\cdot e^{-\lambda\cdot\tau_1}]\cdot i_{L_2}+\frac{1}{I_0}\cdot[\Xi_5\cdot\lambda^2+\Xi_6\cdot\lambda]\cdot i_{L_2}$$
$$+(L_p\cdot\lambda^2-\frac{1}{I_0}\cdot\Xi_4)\cdot i_{C_a}-\frac{1}{I_0}\cdot\Xi_7\cdot i_{L_a}\cdot\lambda^2-L_p\cdot i_{L_1}\cdot\lambda^2\cdot e^{-\lambda\cdot\tau_1} \quad (202)$$

$$\Xi_8-V_T\cdot\Xi_1=0 \text{ Since } \Xi_8=V_T\cdot\Xi_1 \quad (203)$$

$$i_{C_p}\cdot\frac{1}{C_p}=[L_2\cdot\lambda^2-\frac{V_T}{I_0}\cdot\Xi_2\cdot\lambda^2+L_p\cdot\lambda^2\cdot e^{-\lambda\cdot\tau_1}]\cdot i_{L_2}+\frac{1}{I_0}\cdot[\Xi_5\cdot\lambda^2+\Xi_6\cdot\lambda]\cdot i_{L_2}$$
$$+(L_p\cdot\lambda^2-\frac{1}{I_0}\cdot\Xi_4)\cdot i_{C_a}-\frac{1}{I_0}\cdot\Xi_7\cdot i_{L_a}\cdot\lambda^2-L_p\cdot i_{L_1}\cdot\lambda^2\cdot e^{-\lambda\cdot\tau_1} \quad (204)$$

We can summery our equations with arbitrarily small increments of exponential form (3):

(H)
$$i_{C_p}\cdot\frac{1}{C_p}=[L_2\cdot\lambda^2-\frac{V_T}{I_0}\cdot\Xi_2\cdot\lambda^2+L_p\cdot\lambda^2\cdot e^{-\lambda\cdot\tau_1}]\cdot i_{L_2}+\frac{1}{I_0}\cdot[\Xi_5\cdot\lambda^2+\Xi_6\cdot\lambda]\cdot i_{L_2}$$
$$+(L_p\cdot\lambda^2-\frac{1}{I_0}\cdot\Xi_4)\cdot i_{C_a}-\frac{1}{I_0}\cdot\Xi_7\cdot i_{L_a}\cdot\lambda^2-L_p\cdot i_{L_1}\cdot\lambda^2\cdot e^{-\lambda\cdot\tau_1} \quad (205)$$

(I)
$$\frac{1}{C_b}\cdot[i_{C_a}-i_{L_a}]=L_a\cdot i_{L_a}\cdot\lambda^2-i_{C_b}\cdot\lambda\cdot e^{-\lambda\cdot\tau_3}\cdot R_{load} \quad (206)$$

Taking equation (I): $$\frac{1}{C_b}\cdot[i_{C_a}-i_{L_a}]=L_a\cdot i_{L_a}\cdot\lambda^2-i_{C_b}\cdot\lambda\cdot e^{-\lambda\cdot\tau_3}\cdot R_{load} \quad (207)$$

$$L_a\cdot i_{L_a}\cdot\lambda^2=\frac{1}{C_b}\cdot[i_{C_a}-i_{L_a}]+i_{C_b}\cdot\lambda\cdot e^{-\lambda\cdot\tau_3}\cdot R_{load}\Rightarrow i_{L_a}\cdot\lambda^2=\frac{1}{C_b\cdot L_a}\cdot[i_{C_a}-i_{L_a}]+i_{C_b}\cdot\lambda\cdot e^{-\lambda\cdot\tau_3}\cdot\frac{R_{load}}{L_a} \quad (208)$$

Implement it in (H):

$$i_{C_p}\cdot\frac{1}{C_p}=[L_2\cdot\lambda^2-\frac{V_T}{I_0}\cdot\Xi_2\cdot\lambda^2+L_p\cdot\lambda^2\cdot e^{-\lambda\cdot\tau_1}]\cdot i_{L_2}+\frac{1}{I_0}\cdot[\Xi_5\cdot\lambda^2+\Xi_6\cdot\lambda]\cdot i_{L_2}$$
$$+(L_p\cdot\lambda^2-\frac{1}{I_0}\cdot\Xi_4)\cdot i_{C_a}-\frac{1}{I_0}\cdot\Xi_7\cdot(\frac{1}{C_b\cdot L_a}\cdot[i_{C_a}-i_{L_a}]+i_{C_b}\cdot\lambda\cdot e^{-\lambda\cdot\tau_3}\cdot\frac{R_{load}}{L_a})-L_p\cdot i_{L_1}\cdot\lambda^2\cdot e^{-\lambda\cdot\tau_1} \quad (209)$$

$$i_{C_p}\cdot\frac{1}{C_p}=[L_2\cdot\lambda^2-\frac{V_T}{I_0}\cdot\Xi_2\cdot\lambda^2+L_p\cdot\lambda^2\cdot e^{-\lambda\cdot\tau_1}]\cdot i_{L_2}+\frac{1}{I_0}\cdot[\Xi_5\cdot\lambda^2+\Xi_6\cdot\lambda]\cdot i_{L_2}$$
$$+(L_p\cdot\lambda^2-\frac{1}{I_0}\cdot\Xi_4)\cdot i_{C_a}-\frac{1}{I_0}\cdot\Xi_7\cdot\frac{1}{C_b\cdot L_a}\cdot[i_{C_a}-i_{L_a}]-\frac{1}{I_0}\cdot\Xi_7\cdot i_{C_b}\cdot\lambda\cdot e^{-\lambda\cdot\tau_3}\cdot\frac{R_{load}}{L_a}-L_p\cdot i_{L_1}\cdot\lambda^2\cdot e^{-\lambda\cdot\tau_1} \quad (210)$$

$$i_{C_p}\cdot\frac{1}{C_p}=[L_2\cdot\lambda^2-\frac{V_T}{I_0}\cdot\Xi_2\cdot\lambda^2]\cdot i_{L_2}+L_p\cdot\lambda^2\cdot e^{-\lambda\cdot\tau_1}\cdot i_{L_2}+\frac{1}{I_0}\cdot[\Xi_5\cdot\lambda^2+\Xi_6\cdot\lambda]\cdot i_{L_2}$$
$$+(L_p\cdot\lambda^2-\frac{1}{I_0}\cdot\Xi_4)\cdot i_{C_a}-\frac{1}{I_0}\cdot\Xi_7\cdot\frac{1}{C_b\cdot L_a}\cdot[i_{C_a}-i_{L_a}]-\frac{1}{I_0}\cdot\Xi_7\cdot i_{C_b}\cdot\lambda\cdot e^{-\lambda\cdot\tau_3}\cdot\frac{R_{load}}{L_a}-L_p\cdot i_{L_1}\cdot\lambda^2\cdot e^{-\lambda\cdot\tau_1} \quad (211)$$

$$i_{C_p}\cdot\frac{1}{C_p}=[L_2\cdot\lambda^2-\frac{V_T}{I_0}\cdot\Xi_2\cdot\lambda^2]\cdot i_{L_2}+\frac{1}{I_0}\cdot[\Xi_5\cdot\lambda^2+\Xi_6\cdot\lambda]\cdot i_{L_2}$$
$$+(L_p\cdot\lambda^2-\frac{1}{I_0}\cdot\Xi_4)\cdot i_{C_a}-\frac{1}{I_0}\cdot\Xi_7\cdot\frac{1}{C_b\cdot L_a}\cdot[i_{C_a}-i_{L_a}]-\frac{1}{I_0}\cdot\Xi_7\cdot i_{C_b}\cdot\lambda\cdot e^{-\lambda\cdot\tau_3}\cdot\frac{R_{load}}{L_a} \quad (212)$$
$$+(i_{L_2}-i_{L_1})\cdot L_p\cdot\lambda^2\cdot e^{-\lambda\cdot\tau_1}$$

Assumption: $i_{L_2}=i_{L_1}\Rightarrow i_{L_2}-i_{L_1}\approx 0$

$$i_{C_p}\cdot\frac{1}{C_p}=[L_2\cdot\lambda^2-\frac{V_T}{I_0}\cdot\Xi_2\cdot\lambda^2]\cdot i_{L_2}+\frac{1}{I_0}\cdot[\Xi_5\cdot\lambda^2+\Xi_6\cdot\lambda]\cdot i_{L_2}$$
$$+(L_p\cdot\lambda^2-\frac{1}{I_0}\cdot\Xi_4)\cdot i_{C_a}-\frac{1}{I_0}\cdot\Xi_7\cdot\frac{1}{C_b\cdot L_a}\cdot[i_{C_a}-i_{L_a}]-\frac{1}{I_0}\cdot\Xi_7\cdot i_{C_b}\cdot\lambda\cdot e^{-\lambda\cdot\tau_3}\cdot\frac{R_{load}}{L_a} \quad (213)$$

$$i_{C_p}\cdot\frac{1}{C_p}=[L_2\cdot\lambda^2-\frac{V_T}{I_0}\cdot\Xi_2\cdot\lambda^2]\cdot i_{L_2}+\frac{1}{I_0}\cdot[\Xi_5\cdot\lambda^2+\Xi_6\cdot\lambda]\cdot i_{L_2}$$
$$+(L_p\cdot\lambda^2-\frac{1}{I_0}\cdot\Xi_4)\cdot i_{C_a}-\frac{1}{I_0}\cdot\Xi_7\cdot\frac{1}{C_b\cdot L_a}\cdot i_{C_a}+\frac{1}{I_0}\cdot\Xi_7\cdot\frac{1}{C_b\cdot L_a}\cdot i_{L_a}-\frac{1}{I_0}\cdot\Xi_7\cdot i_{C_b}\cdot\lambda\cdot e^{-\lambda\cdot\tau_3}\cdot\frac{R_{load}}{L_a} \quad (214)$$

$$i_{C_p}\cdot\frac{1}{C_p}=[L_2\cdot\lambda^2-\frac{V_T}{I_0}\cdot\Xi_2\cdot\lambda^2]\cdot i_{L_2}+\frac{1}{I_0}\cdot[\Xi_5\cdot\lambda^2+\Xi_6\cdot\lambda]\cdot i_{L_2}$$
$$+L_p\cdot\lambda^2\cdot i_{C_a}-\frac{1}{I_0}\cdot(\Xi_4+\Xi_7\cdot\frac{1}{C_b\cdot L_a})\cdot i_{C_a}+\frac{1}{I_0}\cdot\Xi_7\cdot\frac{1}{C_b\cdot L_a}\cdot i_{L_a}-\frac{1}{I_0}\cdot\Xi_7\cdot i_{C_b}\cdot\lambda\cdot e^{-\lambda\cdot\tau_3}\cdot\frac{R_{load}}{L_a} \quad (215)$$

We divide the two sides of the above equation by i_{L_2}.

$$\frac{i_{C_p}}{i_{L_2}}\cdot\frac{1}{C_p}=[L_2\cdot\lambda^2-\frac{V_T}{I_0}\cdot\Xi_2\cdot\lambda^2]+\frac{1}{I_0}\cdot[\Xi_5\cdot\lambda^2+\Xi_6\cdot\lambda]$$
$$+L_p\cdot\lambda^2\cdot\frac{i_{C_a}}{i_{L_2}}-\frac{1}{I_0}\cdot(\Xi_4+\Xi_7\cdot\frac{1}{C_b\cdot L_a})\cdot\frac{i_{C_a}}{i_{L_2}}+\frac{1}{I_0}\cdot\Xi_7\cdot\frac{1}{C_b\cdot L_a}\cdot\frac{i_{L_a}}{i_{L_2}}-\frac{1}{I_0}\cdot\Xi_7\cdot\frac{i_{C_b}}{i_{L_2}}\cdot\lambda\cdot e^{-\lambda\cdot\tau_3}\cdot\frac{R_{load}}{L_a} \quad (216)$$

Assumption: $\frac{i_{C_p}}{i_{L_2}}\approx 1\ ;\ \frac{i_{C_a}}{i_{L_2}}\approx 1\ ;\ \frac{i_{L_a}}{i_{L_2}}\approx 1\ ;\ \frac{i_{C_b}}{i_{L_2}}\approx 1$ (217)

$$\frac{1}{C_p}=[L_2\cdot\lambda^2-\frac{V_T}{I_0}\cdot\Xi_2\cdot\lambda^2]+\frac{1}{I_0}\cdot[\Xi_5\cdot\lambda^2+\Xi_6\cdot\lambda]+L_p\cdot\lambda^2-\frac{1}{I_0}\cdot(\Xi_4+\Xi_7\cdot\frac{1}{C_b\cdot L_a})$$
$$+\frac{1}{I_0}\cdot\Xi_7\cdot\frac{1}{C_b\cdot L_a}-\frac{1}{I_0}\cdot\Xi_7\cdot\lambda\cdot e^{-\lambda\cdot\tau_3} \quad (218)$$

$$\frac{1}{C_p}=L_2\cdot\lambda^2-\frac{V_T}{I_0}\cdot\Xi_2\cdot\lambda^2+\frac{1}{I_0}\cdot\Xi_5\cdot\lambda^2+\frac{1}{I_0}\cdot\Xi_6\cdot\lambda+L_p\cdot\lambda^2-\frac{1}{I_0}\cdot(\Xi_4+\Xi_7\cdot\frac{1}{C_b\cdot L_a})$$
$$+\frac{1}{I_0}\cdot\Xi_7\cdot\frac{1}{C_b\cdot L_a}-\frac{1}{I_0}\cdot\Xi_7\cdot\lambda\cdot e^{-\lambda\cdot\tau_3} \quad (219)$$

$$\frac{1}{C_p}=(L_2-\frac{V_T}{I_0}\cdot\Xi_2+\frac{1}{I_0}\cdot\Xi_5+L_p)\cdot\lambda^2+\frac{1}{I_0}\cdot\Xi_6\cdot\lambda-\frac{1}{I_0}\cdot(\Xi_4+\Xi_7\cdot\frac{1}{C_b\cdot L_a})$$
$$+\frac{1}{I_0}\cdot\Xi_7\cdot\frac{1}{C_b\cdot L_a}-\frac{1}{I_0}\cdot\Xi_7\cdot\lambda\cdot e^{-\lambda\cdot\tau_3} \quad (220)$$

$$\frac{1}{C_p}-(L_2-\frac{V_T}{I_0}\cdot\Xi_2+\frac{1}{I_0}\cdot\Xi_5+L_p)\cdot\lambda^2-\frac{1}{I_0}\cdot\Xi_6\cdot\lambda+\frac{1}{I_0}\cdot(\Xi_4+\Xi_7\cdot\frac{1}{C_b\cdot L_a})$$
$$-\frac{1}{I_0}\cdot\Xi_7\cdot\frac{1}{C_b\cdot L_a}+\frac{1}{I_0}\cdot\Xi_7\cdot\lambda\cdot e^{-\lambda\cdot\tau_3}=0 \quad (221)$$

$$-(L_2-\frac{V_T}{I_0}\cdot\Xi_2+\frac{1}{I_0}\cdot\Xi_5+L_p)\cdot\lambda^2-\frac{1}{I_0}\cdot\Xi_6\cdot\lambda+\frac{1}{I_0}\cdot\Xi_4+\frac{1}{I_0}\cdot\Xi_7\cdot\frac{1}{C_b\cdot L_a}+\frac{1}{C_p}$$
$$-\frac{1}{I_0}\cdot\Xi_7\cdot\frac{1}{C_b\cdot L_a}+\frac{1}{I_0}\cdot\Xi_7\cdot\lambda\cdot e^{-\lambda\cdot\tau_3}=0 \quad (222)$$

$$-(L_2-\frac{V_T}{I_0}\cdot\Xi_2+\frac{1}{I_0}\cdot\Xi_5+L_p)\cdot\lambda^2-\frac{1}{I_0}\cdot\Xi_6\cdot\lambda+[\frac{1}{I_0}\cdot\Xi_4+\frac{1}{C_p}]+\frac{1}{I_0}\cdot\Xi_7\cdot\lambda\cdot e^{-\lambda\cdot\tau_3}=0 \quad (223)$$

Remark: All the assumptions which been taken need to be check numerically before implementation.

4 Free Running VCO Based on an Unstable Transistor Stability Switching

$$\tau_1=\tau\ ;\ \tau_1=\tau_2\ ;\ \tau_3=\tau$$

We get the characteristic equation ($\tau_3=\tau$):

$$-(L_2-\frac{V_T}{I_0}\cdot\Xi_2+\frac{1}{I_0}\cdot\Xi_5+L_p)\cdot\lambda^2-\frac{1}{I_0}\cdot\Xi_6\cdot\lambda+[\frac{1}{I_0}\cdot\Xi_4+\frac{1}{C_p}]+\frac{1}{I_0}\cdot\Xi_7\cdot\lambda\cdot e^{-\lambda\cdot\tau}=0 \quad (224)$$

$$-(L_2-\frac{V_T}{I_0}\cdot\frac{I_0\cdot L_2}{V_T}+\frac{1}{I_0}\cdot[\frac{\Omega\cdot L_2}{(1-\alpha_f)}+V_T\cdot\frac{I_0\cdot L_2}{V_T}]+L_p)\cdot\lambda^2-\frac{1}{I_0}\cdot\Xi_6\cdot\lambda+[\frac{1}{I_0}\cdot\Xi_4+\frac{1}{C_p}]+\frac{1}{I_0}\cdot\Xi_7\cdot\lambda\cdot e^{-\lambda\cdot\tau}=0 \quad (225)$$

$$-(\frac{1}{I_0}\cdot[\frac{\Omega}{(1-\alpha_f)}+V_T\cdot\frac{I_0}{V_T}]\cdot L_2+L_p)\cdot\lambda^2-\frac{1}{I_0}\cdot\Xi_6\cdot\lambda+[\frac{1}{I_0}\cdot\Xi_4+\frac{1}{C_p}]+\frac{1}{I_0}\cdot\Xi_7\cdot\lambda\cdot e^{-\lambda\cdot\tau}=0 \quad (226)$$

$$D(\lambda,\tau)=-(\frac{1}{I_0}\cdot[\frac{\Omega}{(1-\alpha_f)}+V_T\cdot\frac{I_0}{V_T}]\cdot L_2+L_p)\cdot\lambda^2-\frac{1}{I_0}\cdot\Xi_6\cdot\lambda+[\frac{1}{I_0}\cdot\Xi_4+\frac{1}{C_p}]+\frac{1}{I_0}\cdot\Xi_7\cdot\lambda\cdot e^{-\lambda\cdot\tau} \quad (227)$$

We study the occurrence of any possible stability switching, resulting from the increase of the value of the time delay τ for the general characteristic equation $D(\lambda,\tau)$ [5][6].

$$D(\lambda,\tau)=P_n(\lambda,\tau)+Q_m(\lambda,\tau)\cdot e^{-\lambda\cdot\tau}\ ;\ n,m\in\square_0\ ;\ n>m\ ;\ n=2\ ;\ m=1\ ;\ P_n(\lambda,\tau)=P_n(\lambda)\ ;\ Q_m(\lambda,\tau)=Q_m(\lambda) \quad (228)$$

$$P_{n=2}(\lambda)=-(\frac{1}{I_0}\cdot[\frac{\Omega}{(1-\alpha_f)}+V_T\cdot\frac{I_0}{V_T}]\cdot L_2+L_p)\cdot\lambda^2-\frac{1}{I_0}\cdot\Xi_6\cdot\lambda+[\frac{1}{I_0}\cdot\Xi_4+\frac{1}{C_p}] \quad (229)$$

$$P_{n=2}(\lambda)=-(\frac{1}{I_0}\cdot[\frac{\Omega}{(1-\alpha_f)}+V_T\cdot\frac{I_0}{V_T}]\cdot L_2+L_p)\cdot\lambda^2-\frac{1}{I_0}\cdot\frac{V_T}{(1-\alpha_f)}\cdot\lambda+[\frac{1}{I_0}\cdot\frac{\Omega}{(1-\alpha_f)\cdot C_a}+\frac{1}{C_p}] \quad (230)$$

$$Q_{m=1}(\lambda)=\frac{1}{I_0}\cdot\Xi_7\cdot\lambda\ ;\ P_{n=2}(\lambda,\tau)=\sum_{k=0}^{2}p_k(\tau)\cdot\lambda^k=p_0(\tau)+p_1(\tau)\cdot\lambda+p_2(\tau)\cdot\lambda^2 \quad (231)$$

$$p_0(\tau)=\frac{1}{I_0}\cdot\Xi_4+\frac{1}{C_p}\ ;\ p_1(\tau)=-\frac{1}{I_0}\cdot\Xi_6\ ;\ p_2(\tau)=-(\frac{1}{I_0}\cdot[\frac{\Omega}{(1-\alpha_f)}+V_T\cdot\frac{I_0}{V_T}]\cdot L_2+L_p) \quad (232)$$

$$p_0(\tau)=\frac{1}{I_0}\cdot\frac{\Omega}{(1-\alpha_f)\cdot C_a}+\frac{1}{C_p}\ ;\ p_1(\tau)=-\frac{1}{I_0}\cdot\frac{V_T}{(1-\alpha_f)} \quad (233)$$

$$Q_{m=1}(\lambda,\tau)=\sum_{k=0}^{1}q_k(\tau)\cdot\lambda^k=q_0(\tau)+q_1(\tau)\cdot\lambda\ ;\ q_0(\tau)=0\ ;\ q_1(\tau)=\frac{1}{I_0}\cdot\Xi_7=\frac{1}{I_0}\cdot\frac{\Omega\cdot L_a}{(1-\alpha_f)} \quad (234)$$

The homogeneous system for $I_{C_p},I_{L_2},i_{DE},I_{L_1},I_{C_a},I_{L_a},I_{C_b},I_{C(V)}$ (which can be reduce) leads to characteristic equation (after some assumptions) for the eigenvalue λ having the form $\mathrm{P}(\lambda,\tau)+\mathrm{Q}(\lambda,\tau)\cdot e^{-\lambda\cdot\tau}=0$,

$P(\lambda)=\sum_{j=0}^{2}a_j\cdot\lambda^j\ ;\ Q(\lambda)=\sum_{j=0}^{1}c_j\cdot\lambda^j$. The coefficients $\{a_j(q_i,q_k,\tau),c_j(q_i,q_k,\tau)\}\in\square$ depend on q_i,q_k and delay τ. Parameters q_i,q_k are any Free running VCO is based on an unstable transistor circuit's global parameters, other parameters kept as constant.

$$a_0(\tau)=\frac{1}{I_0}\cdot\frac{\Omega}{(1-\alpha_f)\cdot C_a}+\frac{1}{C_p}\ ;\ a_1(\tau)=-\frac{1}{I_0}\cdot\frac{V_T}{(1-\alpha_f)}\ ;\ a_2(\tau)=-(\frac{1}{I_0}\cdot[\frac{\Omega}{(1-\alpha_f)}+V_T\cdot\frac{I_0}{V_T}]\cdot L_2+L_p) \quad (235)$$

$$c_0(\tau)=0\ ;\ c_1(\tau)=\frac{1}{I_0}\cdot\Xi_7=\frac{1}{I_0}\cdot\frac{\Omega\cdot L_a}{(1-\alpha_f)} \quad (236)$$

Unless strictly necessary, the designation of the varies arguments (q_i, q_k) will be omitted from P, Q, a_j, c_j. The coefficients a_j, c_j are continuous, and differentiable functions of their arguments, and direct substitution shows that $a_0 + c_0 \neq 0$ ($\frac{1}{I_0} \cdot \frac{\Omega}{(1-\alpha_f) \cdot C_a} + \frac{1}{C_p} \neq 0$) for $q_i, q_k \in \mathbb{R}_+$; that is, $\lambda = 0$ is not of $\mathrm{P}(\lambda) + \mathrm{Q}(\lambda) \cdot e^{-\lambda \cdot \tau} = 0$. Furthermore $\mathrm{P}(\lambda), \mathrm{Q}(\lambda)$ are analytic functions of λ, for which the following requirements of the analysis (Kuang J and Cong Y 2005 ; Kuang Y 1993) can also be verified in the present case:

(a) If $\lambda = i \cdot \omega$; $\omega \in \mathbb{R}$ then $P(i \cdot \omega) + Q(i \cdot \omega) \neq 0$.

(b) If $|\frac{Q(\lambda)}{P(\lambda)}|$ is bounded for $|\lambda| \to \infty$; $\mathrm{Re}\lambda \geq 0$. No roots bifurcation from ∞.

(c) $F(\omega) = |P(i \cdot \omega)|^2 - |Q(i \cdot \omega)|^2$ has a finite number of zeros, Indeed, this is a polynomial in ω.

(d) Each positive root $\omega(q_i, q_k)$ of $F(\omega) = 0$ is continuous and differentiable with respect to q_i, q_k.

We assume $P_n(\lambda, \tau)$ and $Q_m(\lambda, \tau)$ cannot have common imaginary roots. That is for any real number ω:

$$P_n(\lambda = i \cdot \omega, \tau) + Q_m(\lambda = i \cdot \omega, \tau) \neq 0.$$

$$P_n(\lambda = i \cdot \omega, \tau) = (\frac{1}{I_0} \cdot [\frac{\Omega}{(1-\alpha_f)} + V_T \cdot \frac{I_0}{V_T}] \cdot L_2 + L_p) \cdot \omega^2 + [\frac{1}{I_0} \cdot \Xi_4 + \frac{1}{C_p}] - \frac{1}{I_0} \cdot \Xi_6 \cdot i \cdot \omega \tag{237}$$

$$Q_m(\lambda = i \cdot \omega, \tau) = \frac{1}{I_0} \cdot \Xi_7 \cdot i \cdot \omega \; ; \; |Q(i \cdot \omega, \tau)|^2 = (\frac{1}{I_0} \cdot \Xi_7 \cdot \omega)^2 \tag{238}$$

$$|P(i \cdot \omega, \tau)|^2 = ((\frac{1}{I_0} \cdot [\frac{\Omega}{(1-\alpha_f)} + V_T \cdot \frac{I_0}{V_T}] \cdot L_2 + L_p) \cdot \omega^2 + [\frac{1}{I_0} \cdot \Xi_4 + \frac{1}{C_p}])^2 + (\frac{1}{I_0} \cdot \Xi_6 \cdot \omega)^2 \tag{239}$$

$$F(\omega, \tau) = |P(i \cdot \omega, \tau)|^2 - |Q(i \cdot \omega, \tau)|^2 = ((\frac{1}{I_0} \cdot [\frac{\Omega}{(1-\alpha_f)} + V_T \cdot \frac{I_0}{V_T}] \cdot L_2 + L_p) \cdot \omega^2 + [\frac{1}{I_0} \cdot \Xi_4 + \frac{1}{C_p}])^2$$
$$+ (\frac{1}{I_0} \cdot \Xi_6 \cdot \omega)^2 - (\frac{1}{I_0} \cdot \Xi_7 \cdot \omega)^2 \tag{240}$$

$$F(\omega, \tau) = |P(i \cdot \omega, \tau)|^2 - |Q(i \cdot \omega, \tau)|^2 = (\frac{1}{I_0} \cdot [\frac{\Omega}{(1-\alpha_f)} + V_T \cdot \frac{I_0}{V_T}] \cdot L_2 + L_p)^4 \cdot \omega^4$$
$$+ [2 \cdot (\frac{1}{I_0} \cdot [\frac{\Omega}{(1-\alpha_f)} + V_T \cdot \frac{I_0}{V_T}] \cdot L_2 + L_p) \cdot (\frac{1}{I_0} \cdot \Xi_4 + \frac{1}{C_p}) + (\frac{1}{I_0} \cdot \Xi_6)^2 - (\frac{1}{I_0} \cdot \Xi_7)^2] \cdot \omega^2 + (\frac{1}{I_0} \cdot \Xi_4 + \frac{1}{C_p})^2 \tag{241}$$

We define the following parameters for simplicity: Π_0, Π_2, Π_4

$$\Pi_0 = (\frac{1}{I_0} \cdot \Xi_4 + \frac{1}{C_p})^2 \; ; \; \Pi_2 = 2 \cdot (\frac{1}{I_0} \cdot [\frac{\Omega}{(1-\alpha_f)} + V_T \cdot \frac{I_0}{V_T}] \cdot L_2 + L_p) \cdot (\frac{1}{I_0} \cdot \Xi_4 + \frac{1}{C_p}) + (\frac{1}{I_0} \cdot \Xi_6)^2 - (\frac{1}{I_0} \cdot \Xi_7)^2 \tag{242}$$

$$\Pi_4 = (\frac{1}{I_0} \cdot [\frac{\Omega}{(1-\alpha_f)} + V_T \cdot \frac{I_0}{V_T}] \cdot L_2 + L_p)^4 \tag{243}$$

Hence $F(\omega,\tau)=0$ implies $\sum_{k=0}^{2}\Pi_{2\cdot k}\cdot\omega^{2\cdot k}=0$ and its roots are given by solving the above polynomial.

$$P_R(i\cdot\omega,\tau)=(\frac{1}{I_0}\cdot[\frac{\Omega}{(1-\alpha_f)}+V_T\cdot\frac{I_0}{V_T}]\cdot L_2+L_p)\cdot\omega^2+[\frac{1}{I_0}\cdot\Xi_4+\frac{1}{C_p}]\ ;\ P_I(i\cdot\omega,\tau)=-\frac{1}{I_0}\cdot\Xi_6\cdot\omega \tag{244}$$

$$Q_R(i\cdot\omega,\tau)=0\ ;\ Q_I(i\cdot\omega,\tau)=\frac{1}{I_0}\cdot\Xi_7\cdot\omega \tag{245}$$

$$\sin\theta(\tau)=\frac{-P_R(i\cdot\omega,\tau)\cdot Q_I(i\cdot\omega,\tau)+P_I(i\cdot\omega,\tau)\cdot Q_R(i\cdot\omega,\tau)}{|Q(i\cdot\omega,\tau)|^2} \tag{246}$$

$$\cos\theta(\tau)=-\frac{P_R(i\cdot\omega,\tau)\cdot Q_R(i\cdot\omega,\tau)+P_I(i\cdot\omega,\tau)\cdot Q_I(i\cdot\omega,\tau)}{|Q(i\cdot\omega,\tau)|^2} \tag{247}$$

We use different parameters terminology from our last characteristics parameters definition:

$$k\to j\ ;\ p_k(\tau)\to a_j\ ;\ q_k(\tau)\to c_j\ ;\ n=2\ ;\ m=1\ ;\ n>m\ ;\ P_n(\lambda,\tau)\to P(\lambda)\ ;\ Q_m(\lambda,\tau)\to Q(\lambda) \tag{248}$$

$$P(\lambda)=\sum_{j=0}^{2}a_j\cdot\lambda^j\ ;\ Q(\lambda)=\sum_{j=0}^{1}c_j\cdot\lambda^j\ ;\ P(\lambda)=a_0+a_1\cdot\lambda+a_2\cdot\lambda^2\ ;\ Q(\lambda)=c_0+c_1\cdot\lambda \tag{249}$$

$n,m\in\mathbb{N}_0$; $n>m$ and $a_j,c_j:\mathbb{R}_{+0}\to\mathbb{R}$ are continuous and differentiable function of τ such that $a_0+c_0\neq 0$. In the following "—"denotes complex and conjugate. $P(\lambda),Q(\lambda)$ are analytic functions in λ and differentiable in τ . The coefficients $a_j(C_p,L_1,L_p,L_2,C_a,C_b,L_a,R_{load},\ldots)\in\mathbb{R}$ and $c_j(C_p,L_1,L_p,L_2,C_a,C_b,L_a,R_{load},\ldots)\in\mathbb{R}$ depend on Free running VCO is based on an unstable transistor circuit's $C_p,L_1,L_p,L_2,C_a,C_b,L_a,R_{load},\ldots$ values. Unless strictly necessary, the designation of the varied arguments: ($C_p,L_1,L_p,L_2,C_a,C_b,L_a,R_{load},\tau,\ldots$) will subsequently be omitted from P,Q,a_j,c_j. The coefficients a_j,c_j are continuous and differentiable functions of their arguments, and direct substitution shows that $a_0+c_0\neq 0$.

$$a_0=\frac{1}{I_0}\cdot\frac{\Omega}{(1-\alpha_f)\cdot C_a}+\frac{1}{C_p}\ ;\ c_0=0\ ;\ \frac{1}{I_0}\cdot\frac{\Omega}{(1-\alpha_f)\cdot C_a}+\frac{1}{C_p}\neq 0 \tag{250}$$

$\forall\ C_p,L_1,L_p,L_2,C_a,C_b,L_a,R_{load},\tau,\ldots\in\mathbb{R}_+$, i.e. $\lambda=0$ is not a root of the characteristic equation. Furthermore $P(\lambda)$; $Q(\lambda)$ are analytic functions of λ for which the following requirements of the analysis (see Kuang, 1993, section 3.4) can be varied in the present case [5][6].

(a) If $\lambda=i\cdot\omega$; $\omega\in\mathbb{R}$ then $P(i\cdot\omega)+Q(i\cdot\omega)\neq 0$, i.e. P and Q have no common imaginary roots. This condition was verified numerically in the entire ($C_p,L_1,L_p,L_2,C_a,C_b,L_a,R_{load},\tau,\ldots$) domain of interest.

(b) $|\frac{P(\lambda)}{Q(\lambda)}|$ is bounded for $|\lambda| \to \infty$; $\mathrm{Re}\,\lambda \geq 0$. No roots bifurcation from ∞ . Indeed, in the limit:

$$|\frac{P(\lambda)}{Q(\lambda)}| = |\frac{-(\frac{1}{I_0}\cdot[\frac{\Omega}{(1-\alpha_f)}+V_T\cdot\frac{I_0}{V_T}]\cdot L_2+L_p)\cdot\lambda^2-\frac{1}{I_0}\cdot\frac{V_T}{(1-\alpha_f)}\cdot\lambda}{+[\frac{1}{I_0}\cdot\frac{\Omega}{(1-\alpha_f)\cdot C_a}+\frac{1}{C_p}]}|$$
$$\frac{1}{I_0}\cdot\Xi_7\cdot\lambda \qquad (251)$$

(c) The following expressions exist: $F(\omega) = |P(i\cdot\omega)|^2 - |Q(i\cdot\omega)|^2$; $F(\omega) = \sum_{k=0}^{2}\Pi_{2\cdot k}\cdot\omega^{2\cdot k}$ (252)

Has at most a finite number of zeros. Indeed, this is a polynomial in ω (degree in ω^4).

(d) Each positive root $\omega(C_p, L_1, L_p, L_2, C_a, C_b, L_a, R_{load}, \tau, ...)$ of $F(\omega) = 0$ is continuous and differentiable with respect to $C_p, L_1, L_p, L_2, C_a, C_b, L_a, R_{load}, \tau, ...$. The condition can only be assessed numerically.

In addition, since the coefficients in P and Q are real, we have $\overline{P(-i\cdot\omega)} = P(i\cdot\omega)$; $\overline{Q(-i\cdot\omega)} = Q(i\cdot\omega)$ thus, $\omega > 0$ maybe on eigenvalue of characteristic equations. The analysis consists in identifying the roots of the characteristic equation situated on the imaginary axis of the complex λ - plane, whereby increasing the parameters:

$C_p, L_1, L_p, L_2, C_a, C_b, L_a, R_{load}, \tau, ...$ $\mathrm{Re}\,\lambda$ may, at the crossing, change its sign from (-) to (+), i.e. from a stable focus $E^*(I^*_{C_p}, I^*_{C_a}, I^*_{L_a}, I^*_{C_b}, i^*_{DE}, I^*_{C(V)}, I^*_{L_p}, i^*_{DC}, I^*_{L_1}, I^*_{L_2})$ to an unstable one, or vice versa. This feature may be further assessed by examining the sign of the partial derivatives with respect to $C_p, L_1, L_p, L_2, C_a, C_b, L_a, R_{load}, \tau, ...$ and system parameters.

$$\Lambda^{-1}(C_p) = (\frac{\partial\,\mathrm{Re}\,\lambda}{\partial C_p})_{\lambda=i\cdot\omega} ; L_1, L_p, L_2, C_a, C_b, L_a, R_{load}, \tau, ... = const \qquad (253)$$

$$\Lambda^{-1}(L_2) = (\frac{\partial\,\mathrm{Re}\,\lambda}{\partial L_2})_{\lambda=i\cdot\omega} ; C_p, L_1, L_p, C_a, C_b, L_a, R_{load}, \tau, ... = const \qquad (254)$$

$$\Lambda^{-1}(L_1) = (\frac{\partial\,\mathrm{Re}\,\lambda}{\partial L_1})_{\lambda=i\cdot\omega} ; C_p, L_p, L_2, C_a, C_b, L_a, R_{load}, \tau, ... = const \qquad (255)$$

$$\Lambda^{-1}(C_a) = (\frac{\partial\,\mathrm{Re}\,\lambda}{\partial C_a})_{\lambda=i\cdot\omega} ; C_p, L_1, L_p, L_2, C_b, L_a, R_{load}, \tau, ... = const \qquad (256)$$

$$\Lambda^{-1}(\tau) = (\frac{\partial\,\mathrm{Re}\,\lambda}{\partial \tau})_{\lambda=i\cdot\omega} ; L_1, L_p, L_2, C_a, C_b, L_a, R_{load}, ... = const \qquad (257)$$

$$P(\lambda) = P_R(\lambda) + i\cdot P_I(\lambda) ; Q(\lambda) = Q_R(\lambda) + i\cdot Q_I(\lambda) \qquad (258)$$

When writing and inserting $\lambda = i \cdot \omega$ into system's characteristic equation ω must satisfy the following equations.

$$\sin(\omega \cdot \tau) = g(\omega) = \frac{-P_R(i \cdot \omega, \tau) \cdot Q_I(i \cdot \omega, \tau) + P_I(i \cdot \omega, \tau) \cdot Q_R(i \cdot \omega, \tau)}{|Q(i \cdot \omega, \tau)|^2} \tag{259}$$

$$\cos(\omega \cdot \tau) = h(\omega) = -\frac{P_R(i \cdot \omega, \tau) \cdot Q_R(i \cdot \omega, \tau) + P_I(i \cdot \omega, \tau) \cdot Q_I(i \cdot \omega, \tau)}{|Q(i \cdot \omega, \tau)|^2} \tag{260}$$

Where $|Q(i \cdot \omega, \tau)|^2 \neq 0$ in view of requirement (a) above, and $(g, h) \in \square$. Furthermore, it follows above $\sin(\omega \cdot \tau)$ and $\cos(\omega \cdot \tau)$ equations, that by squaring and adding the sides, ω must be a positive root of $F(\omega) = |P(i \cdot \omega)|^2 - |Q(i \cdot \omega)|^2 = 0$. Note: $F(\omega)$ is independent on τ . It is important to notice that if $\tau \notin I$ (assume that $I \subseteq \square_{+0}$ is the set where $\omega(\tau)$ is a positive root of $F(\omega)$ and for: $\tau \notin I$; $\omega(\tau)$ is not defined. Then for all τ in I , $\omega(\tau)$ is satisfied that $F(\omega) = 0$. Then there are no positive $\omega(\tau)$ solutions for $F(\omega, \tau) = 0$, and we cannot have stability switches. For $\tau \in I$ where $\omega(\tau)$ is a positive solution of $F(\omega, \tau) = 0$, we can define the angle $\theta(\tau) \in [0, 2 \cdot \pi]$ as the solution of $\sin\theta(\tau) = \ldots.$; $\cos\theta(\tau) = \ldots$

$$\sin\theta(\tau) = \frac{-P_R(i \cdot \omega) \cdot Q_I(i \cdot \omega) + P_I(i \cdot \omega) \cdot Q_R(i \cdot \omega)}{|Q(i \cdot \omega)|^2} \tag{261}$$

$$\cos\theta(\tau) = -\frac{P_R(i \cdot \omega) \cdot Q_R(i \cdot \omega) + P_I(i \cdot \omega) \cdot Q_I(i \cdot \omega)}{|Q(i \cdot \omega)|^2} \tag{262}$$

And the relation between the argument $\theta(\tau)$ and $\tau \cdot \omega(\tau)$ for $\tau \in I$ must be as describe below.

$$I \to \square \ ; S_n(\tau) = \tau - \tau_n(\tau) \ ; \ \tau \in I \ ; n \in \square_0 \tag{263}$$

That is continuous and differentiable in τ . In the following, the subscripts $\lambda, \omega, L_1, L_p, L_2, C_a, C_b, L_a, R_{load}, C_p, \ldots$ indicate the corresponding partial derivatives. Let us first concentrate on $\Lambda(x)$, remember in $\lambda(L_1, L_p, L_2, C_a, C_b, L_a, R_{load}, C_p, \ldots)$ and $\omega(L_1, L_p, L_2, C_a, C_b, L_a, R_{load}, C_p, \ldots)$, and keeping all parameters except (x) and τ . The derivation closely follows that in [BK]. Differentiating system characteristic equation $\mathrm{P}(\lambda) + \mathrm{Q}(\lambda) \cdot e^{-\lambda \cdot \tau} = 0$ with respect to specific parameter (x), and inverting the derivative, for convenience, one calculates: $x = L_1, L_p, L_2, C_a, C_b, L_a, R_{load}, C_p, \ldots$

$$\left(\frac{\partial \lambda}{\partial x}\right)^{-1} = \frac{-P_\lambda(\lambda, x) \cdot Q(\lambda, x) + Q_\lambda(\lambda, x) \cdot P(\lambda, x) - \tau \cdot P(\lambda, x) \cdot Q(\lambda, x)}{P_x(\lambda, x) \cdot Q(\lambda, x) - Q_X(\lambda, x) \cdot P(\lambda, x)} \tag{264}$$

Where $P_\lambda = \frac{\partial P}{\partial \lambda}$; $Q_\lambda = \frac{\partial Q}{\partial \lambda}$; $P_x = \frac{\partial P}{\partial x}$; $Q_x = \frac{\partial Q}{\partial x}$, substituting $\lambda = i \cdot \omega$ and bearing $\overline{P(-i \cdot \omega)} = P(i \cdot \omega)$ and $\overline{Q(-i \cdot \omega)} = Q(i \cdot \omega)$ then $i \cdot P_\lambda(i \cdot \omega) = P_\omega(i \cdot \omega)$; $i \cdot Q_\lambda(i \cdot \omega) = Q_\omega(i \cdot \omega)$ and that on the surface

$|P(i\cdot\omega)|^2=|Q(i\cdot\omega)|^2$, one obtains:

$$(\frac{\partial\lambda}{\partial x})^{-1}|_{\lambda=i\cdot\omega}=(\frac{i\cdot P_\omega(i\cdot\omega,x)\cdot\overline{P(i\cdot\omega,x)}+i\cdot Q_\lambda(i\cdot\omega,x)\cdot\overline{Q(i\cdot\omega,x)}-\tau\cdot|P(i\cdot\omega,x)|^2}{P_x(i\cdot\omega,x)\cdot\overline{P(i\cdot\omega,x)}-Q_x(i\cdot\omega,x)\cdot\overline{Q(i\cdot\omega,x)}}) \quad (265)$$

Upon separating into real and imaginary parts, with $P=P_R+i\cdot P_I$; $Q=Q_R+i\cdot Q_I$; $P_\omega=P_{R\omega}+i\cdot P_{I\omega}$

$$Q_\omega=Q_{R\omega}+i\cdot Q_{I\omega}\ ;\ P_x=P_{Rx}+i\cdot P_{Ix}\ ;\ Q_x=Q_{Rx}+i\cdot Q_{Ix}\ ;\ P^2=P_R^2+P_I^2 \quad (266)$$

When (x) can be any Free running VCO is based on an unstable transistor circuit parameter $L_1,L_p,L_2,C_a,C_b,L_a,\ldots$ and time delay τ etc. Where for convenience, we have dropped the arguments $(i\cdot\omega,x)$ and where

$$F_\omega=2\cdot[(P_{R\omega}\cdot P_R+P_{I\omega}\cdot P_I)-(Q_{R\omega}\cdot Q_R+Q_{I\omega}\cdot Q_I)]\ ;\ F_x=2\cdot[(P_{Rx}\cdot P_R+P_{Ix}\cdot P_I)-(Q_{Rx}\cdot Q_R+Q_{Ix}\cdot Q_I)] \quad (267)$$

$\omega_x=-\frac{F_x}{F_\omega}$. We define U and V:

$$U=(P_R\cdot P_{I\omega}-P_I\cdot P_{R\omega})-(Q_R\cdot Q_{I\omega}-Q_I\cdot Q_{R\omega})\ ;\ V=(P_R\cdot P_{Ix}-P_I\cdot P_{Rx})-(Q_R\cdot Q_{Ix}-Q_I\cdot Q_{Rx}) \quad (268)$$

We choose our specific parameter as time delay $x=\tau$.

$$P_R=(\frac{1}{I_0}\cdot[\frac{\Omega}{(1-\alpha_f)}+V_T\cdot\frac{I_0}{V_T}]\cdot L_2+L_p)\cdot\omega^2+[\frac{1}{I_0}\cdot\Xi_4+\frac{1}{C_p}]\ ;\ P_I=-\frac{1}{I_0}\cdot\Xi_6\cdot\omega \quad (269)$$

$$Q_R=0\ ;\ Q_I=\frac{1}{I_0}\cdot\Xi_7\cdot\omega\ ;\ P_{R\omega}=2\cdot(\frac{1}{I_0}\cdot[\frac{\Omega}{(1-\alpha_f)}+V_T\cdot\frac{I_0}{V_T}]\cdot L_2+L_p)\cdot\omega\ ;\ P_{I\omega}=-\frac{1}{I_0}\cdot\Xi_6 \quad (270)$$

$$Q_{R\omega}=0\ ;\ Q_{I\omega}=\frac{1}{I_0}\cdot\Xi_7\ ;\ P_{R\tau}=0\ ;\ P_{I\tau}=0\ ;\ Q_{R\tau}=0\ ;\ Q_{I\tau}=0\ ;\ \omega_\tau=-\frac{F_\tau}{F_\omega} \quad (271)$$

$$P_{R\omega}\cdot P_R=2\cdot(\frac{1}{I_0}\cdot[\frac{\Omega}{(1-\alpha_f)}+V_T\cdot\frac{I_0}{V_T}]\cdot L_2+L_p)^2\cdot\omega^3\ ;\ Q_{R\omega}\cdot Q_R=0\ ;\ F_\tau=0 \quad (272)$$

$$P_I\cdot P_{R\omega}=-\frac{1}{I_0}\cdot\Xi_6\cdot2\cdot(\frac{1}{I_0}\cdot[\frac{\Omega}{(1-\alpha_f)}+V_T\cdot\frac{I_0}{V_T}]\cdot L_2+L_p)\cdot\omega^2\ ;\ Q_R\cdot Q_{I\omega}=0\ ;\ V=0 \quad (273)$$

$F(\omega,\tau)=0$. Differentiating with respect to τ and we get

$$F_\omega\cdot\frac{\partial\omega}{\partial\tau}+F_\tau=0\ ;\ \tau\in I\Rightarrow\frac{\partial\omega}{\partial\tau}=-\frac{F_\tau}{F_\omega}\ ;\ \Lambda^{-1}(\tau)=\mathrm{Re}\{\frac{-2\cdot[U+\tau\cdot|P|^2]+i\cdot F_\omega}{F_\tau+2\cdot i\cdot[V+\omega\cdot|P|^2]}\} \quad (274)$$

$$sign\{\Lambda^{-1}(\tau)\}=sign\{(\frac{\partial\,\mathrm{Re}\,\lambda}{\partial\tau})_{\lambda=i\cdot\omega}\}\ ;\ sign\{\Lambda^{-1}(\tau)\}=sign\{F_\omega\}\cdot sign\{\frac{V+\frac{\partial\omega}{\partial\tau}\cdot U}{|P|^2}+\omega+\frac{\partial\omega}{\partial\tau}\cdot\tau\} \quad (275)$$

We shall presently examine the possibility of stability transitions (bifurcation) Free running VCO is based on an unstable transistor circuit, about the equilibrium point $E^*(I^*_{C_p}, I^*_{C_a}, I^*_{L_a}, I^*_{C_b}, i^*_{DE}, I^*_{C(V)}, I^*_{L_p}, i^*_{DC}, I^*_{L_1}, I^*_{L_2})$ as a result of a variation of delay parameter τ . The analysis consists in identifying the roots of our system characteristic equation situated on the imaginary axis of the complex λ - plane, where by increasing the delay parameter τ , $\mathrm{Re}\,\lambda$ may at the crossing, changes its sign from – to +, i.e. from a stable focus E^* to an unstable one, or vice versa. This feature may be further assessed by examining the sign of the partial derivatives with respect to τ .

$$\Lambda^{-1}(\tau)=(\frac{\partial \mathrm{Re}\,\lambda}{\partial \tau})_{\lambda=i\cdot\omega}\ ;\ L_1,L_p,L_2,C_a,C_b,L_a,R_{load},...=const\ ;\ \omega\in\square_{+}$$

$$P_R\cdot P_{I\omega}=-\{(\frac{1}{I_0}\cdot[\frac{\Omega}{(1-\alpha_f)}+V_T\cdot\frac{I_0}{V_T}]\cdot L_2+L_p)\cdot\omega^2+[\frac{1}{I_0}\cdot\Xi_4+\frac{1}{C_p}]\}\cdot\frac{1}{I_0}\cdot\Xi_6\ ;\ Q_R\cdot Q_{I\omega}=0\ ;\ Q_I\cdot Q_{R\omega}=0 \tag{276}$$

$$\begin{aligned}U&=(P_R\cdot P_{I\omega}-P_I\cdot P_{R\omega})-(Q_R\cdot Q_{I\omega}-Q_I\cdot Q_{R\omega})=-\{(\frac{1}{I_0}\cdot[\frac{\Omega}{(1-\alpha_f)}+V_T\cdot\frac{I_0}{V_T}]\cdot L_2+L_p)\cdot\omega^2\\&+[\frac{1}{I_0}\cdot\Xi_4+\frac{1}{C_p}]\}\cdot\frac{1}{I_0}\cdot\Xi_6+\frac{1}{I_0}\cdot\Xi_6\cdot 2\cdot(\frac{1}{I_0}\cdot[\frac{\Omega}{(1-\alpha_f)}+V_T\cdot\frac{I_0}{V_T}]\cdot L_2+L_p)\cdot\omega^2\end{aligned} \tag{277}$$

Then we get the expression for $F(\omega,\tau)$ circuit parameter values. We find those ω,τ values which fulfill $F(\omega,\tau)=0$. We ignore negative, complex, and imaginary values of ω for specific $\tau\in[0.001...10]$ second. We plot the stability switch diagram based on different delay values of our free running VCO is based on an unstable transistor circuit.

$$sign\{\Lambda^{-1}(\tau)\}=sign\{F_\omega(\omega(\tau),\tau)\}\cdot sign\{\tau\cdot\omega_\tau(\omega(\tau))+\omega(\tau)+\frac{U(\omega(\tau))\cdot\omega_\tau(\omega(\tau))+V(\omega(\tau))}{|P(\omega(\tau))|^2}\} \tag{278}$$

Remark: We know $F(\omega,\tau)=0$ implies its roots $\omega_i(\tau)$ and finding those delays values τ which ω_i is feasible. There are τ values which give complex ω_i or imaginary number, then unable to analyze stability [5][6]. F - Function is independent on τ the parameter $F(\omega,\tau)=0$. The results: We find those ω,τ values which fulfill $F(\omega,\tau)=0$. We ignore negative, complex, and imaginary values of ω . Next is to find those ω,τ values which fulfill $\sin\theta(\tau)=....$; $\cos\theta(\tau)=....$.

$$\sin(\omega\cdot\tau)=\frac{-P_R\cdot Q_I+P_I\cdot Q_R}{|Q|^2}\ ;\ \cos(\omega\cdot\tau)=-\frac{P_R\cdot Q_R+P_I\cdot Q_I}{|Q|^2}\ ;\ |Q|^2=Q_R^2+Q_I^2 \tag{279}$$

Finally, we plot the stability switch diagram.

$$g(\tau)=\Lambda^{-1}(\tau)=(\frac{\partial \mathrm{Re}\,\lambda}{\partial \tau})_{\lambda=i\cdot\omega}=\frac{2\cdot\{F_\omega\cdot(V+\omega\cdot P^2)-F_\tau\cdot(U+\tau\cdot P^2)\}}{F_\tau^2+4\cdot(V+\omega\cdot P^2)^2} \tag{280}$$

$$sign[g(\tau)]=sign[\Lambda^{-1}(\tau)]=sign[(\frac{\partial \mathrm{Re}\,\lambda}{\partial \tau})_{\lambda=i\cdot\omega}]=sign[\frac{2\cdot\{F_\omega\cdot(V+\omega\cdot P^2)-F_\tau\cdot(U+\tau\cdot P^2)\}}{F_\tau^2+4\cdot(V+\omega\cdot P^2)^2}] \tag{281}$$

$$F_\tau^2+4\cdot(V+\omega\cdot P^2)^2>0\ ;\ sign[\Lambda^{-1}(\tau)]=sign\{F_\omega\cdot(V+\omega\cdot P^2)-F_\tau\cdot(U+\tau\cdot P^2)\} \tag{282}$$

$$sign[\Lambda^{-1}(\tau)]=sign\{[F_\omega]\cdot[(V+\omega\cdot P^2)-\frac{F_\tau}{F_\omega}\cdot(U+\tau\cdot P^2)]\}\ ;\ \omega_\tau=-\frac{F_\tau}{F_\omega}\ ;\ \omega_\tau=(\frac{\partial\omega}{\partial\tau})^{-1}=-\frac{\partial F/\partial\omega}{\partial F/\partial\tau} \tag{283}$$

$$sign[\Lambda^{-1}(\tau)]=sign\{[F_\omega]\cdot[V+\omega_\tau\cdot U+\omega\cdot P^2+\omega_\tau\cdot\tau\cdot P^2]\} \tag{284}$$

$$sign[\Lambda^{-1}(\tau)]=sign\{[F_\omega]\cdot[P^2]\cdot[\frac{V+\omega_\tau\cdot U}{P^2}+\omega+\omega_\tau\cdot\tau]\} \tag{285}$$

$$sign[P^2]>0\Rightarrow sign[\Lambda^{-1}(\tau)]=sign\{[F_\omega]\cdot[\frac{V+\omega_\tau\cdot U}{P^2}+\omega+\omega_\tau\cdot\tau]\} \tag{286}$$

$$sign[\Lambda^{-1}(\tau)]=sign[F_\omega]\cdot sign[\frac{V+\omega_\tau\cdot U}{P^2}+\omega+\omega_\tau\cdot\tau] \tag{287}$$

$$P_{I\omega}\cdot P_I=(\frac{1}{I_0}\cdot\Xi_6)^2\cdot\omega\ ;\ Q_{I\omega}\cdot Q_I=(\frac{1}{I_0}\cdot\Xi_7)^2\cdot\omega$$

$$F_\omega=2\cdot[(P_{R\omega}\cdot P_R+P_{I\omega}\cdot P_I)-(Q_{R\omega}\cdot Q_R+Q_{I\omega}\cdot Q_I)]$$
$$=2\cdot[(2\cdot(\frac{1}{I_0}\cdot[\frac{\Omega}{(1-\alpha_f)}+V_T\cdot\frac{I_0}{V_T}]\cdot L_2+L_p)^2\cdot\omega^3+(\frac{1}{I_0}\cdot\Xi_6)^2\cdot\omega)-(\frac{1}{I_0}\cdot\Xi_7)^2\cdot\omega] \tag{288}$$

We check the sign $\Lambda^{-1}(\tau)$ according the following rule (Table 1):

Table 1. Free running VCO is based on an unstable transistor circuit sign of $sign[\Lambda^{-1}(\tau)]$

$sign[F_\omega]$	$sign[\frac{V+\omega_\tau\cdot U}{P^2}+\omega+\omega_\tau\cdot\tau]$	$sign[\Lambda^{-1}(\tau)]$
+/-	+/-	+
+/-	-/+	-

If $sign[\Lambda^{-1}(\tau)]>0$ then the crossing proceeds from (-) to (+), respectively (stable to unstable). If $sign[\Lambda^{-1}(\tau)]<0$ then the crossing proceeds from (+) to (-) respectively (unstable to stable).

5 Free Running VCO based on an Unstable Transistor Applicable Integrated Circuits

In many RF and microwave systems, a frequency synthesizer is required. Free running VCO (based on unstable transistor) is an integral part of these systems. The frequency synthesizer creates the local oscillator signal that drives mixers, modulators, demodulators, and many other RF and microwave components. The key element of creating a synthesizer is using a phase-locked loop (PLL) frequency synthesizer. A simple PLL divided down the voltage controlled oscillator (Free running VCO) output

frequency, compared this to a reference signal, and then tweaked the free running VCO voltage to weak its output frequency. The PLL and VCO have been two separate chips – a discrete solution. The free running VCO creates the actual output signal; the PLL monitors the output signals and tunes the free running VCO to lock it relative to a known reference signal. There are a number of strengths to the discrete solution: Each discrete chip can be designed to give its best performance, the typical distance between the PLL and the free running VCO reduces cross-coupling effects and minimizes unwanted spurious signals on the output. In case that one chip in the loop is damaged, fewer components need to be replaced. Discrete solutions which included VCOs, PLLs, DLLs, etc., dominated the synthesizer industrial applications. One major issue is that the discrete solution requires a lot of board space to hold the two chips and all their supporting components. Another major issue with the discrete solution is that traditional VCOs have a narrow output frequency range while the free running VCO is a very low cost and good solution to generate a WBFM signal. A typical VCO bandwidth is 50MHz to 500MHz; it's possible to go up around 2GHz but this requires an Op-amp based active filter. The major engineering challenge is to implement a system with a wider frequency range. To create a wider frequency range synthesizer, multiple PLLs, VCOs, supporting components, filtering, switches, and power supplies are needed. It increases the board space and cost of a design. Additional there is a huge amount of overhead work in qualifying, creating software for, and inventory controlling each device. The integrated solution meant the VCO architecture could change to create a wideband synthesizer from one component. The integrated PLL/VCO solution uses a different type of VCO architecture that builds on the traditional architecture. The integrated PLL/VCO effectively combines several traditional VCOs side-by-side to create a VCO with a remarkably wide bandwidth. The fact that the PLL and VCO are integrated onto one chip makes the multiband architecture possible. Every time the user wants to lock to a new frequency, the device initiates a VCO calibration process where the chip quickly sorts through the VCO bands and chooses the optimum one for the required output frequency. Once the VCO band has been selected, the PLL then locks the loop and keeps the output at the desired frequency. Important group of PLL/VCO chips has over 4GHz of bandwidth. We compare it to the discrete 100MHz to 300MHz bandwidth – and this frequency range is possible from a tiny chip relative to the previously required banks of PLLs, VCOs, filters, and switches. While this technology was a huge step forward in frequency range, board space, cost, and overhead, there were still drawbacks that stopped the integrated solution completely taking over from the discrete solution. In many applications, the most important performance specification (after frequency range) is phase noise. There is an additional drive for phase noise performance from the electric test and measurement industry. Whatever phase noise performance is used by the communications industry, the electric test and measurement instruments need better phase noise performance and they can measure the communication protocols. Many solutions were able to move from discrete to integrated – saving money in the process – the phase noise performance of the first generation PLL/VCOs simply was not good enough to replace many of the low phase noise requirement applications. As well as the phase noise performance, the frequency range was low compared to many of the applications that require a discrete PLL and VCO. The frequency range issue can be mitigated by frequency doubles and other multipliers, but there are high power consumption and add additional cost and board space to the solution. The new integrated PLL/VCOs have the following requirements: output frequencies greater than 4.4GHz, phase noise performance comparable with discrete solutions, an integrated PLL and VCO in a single and small package, and lower cost than discrete solutions. The second generation of integrated PLL/VCOs products

is greater than 10GHz output frequency range, phase noise comparable to a discrete VCO, 5mm x 5mm packages, and at lower prices than a similar discrete PLL and VCO solution (which would have a much narrow frequency range). There is a phase noise performance which benefits of a discrete solution, plus all the other benefits of an integrated solution. The is a combination of the first generation of PLL/VCOs, PLL blocks and maximum phase frequency detector (PFD) frequencies around 32MHz and fractional-N divider resolutions of around 12 bits. This combination meant typical channel resolution is in the tens of kHz. The second generation of PLLs/VCO has maximum PFD frequencies greater than 100MHz and fractional— divider resolutions of 25 bits or even up to 49 bits. This had two main benefits – the higher PFD frequency allowed for lower PLL phase noise; and 25 bit or even more resolution allows exact frequency generation and Sub-Hz channel spacing. A very important aspect of the integrated PLL/VCO is spurious performance. One of the benefits of the discrete solution listed above is that the physical isolation between the two chips reduces cross coupling between the PLL and VCO and therefore reduces the power of unwanted spurious signals. When the PLL and VCO are integrated, it is inevitable that the spurious performance will degrade. We must keep this degradation very low and have surprisingly good spurious performance for a PLL/VCO. Other PLL/VCO parts need extra application work to improve the spurious levels for some high performance applications. The close proximity of the PLL and VCO circuits can result in unwanted coupling. To mitigate this, it is possible to use two chip solutions to physically separate the PLL and VCO circuits. This gives the discrete advantages of low spurious signals and the integrated advantages of a wide output frequency range. The following figure describes how to lock the microwave wideband synthesizer with integrated VCO and with an external Fractional-N PLL (typically 8GHz, 19 bit) to improve spurious performance. The R counter output Fractional-N PLL is calibrating /GND when synthesizer is holding lock (Fig. 3).

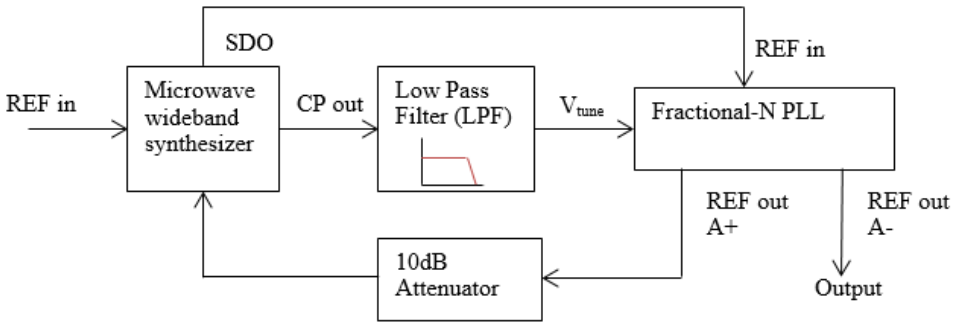

Fig. 3 Synthesizer with integrated VCO and an external Fractional-N PLL

PLL (phase lock loop) system is a control system that generates output signal which his phase is related to input signal phase. The PLL system includes the following main functional circuit, Variable frequency oscillator (Free running VCO), phase detector, and feedback loop. The frequency variable oscillator (Free running VCO) creates a periodic wave and the phase detector compares the signal phase to input periodic signal phase. It sets the oscillator frequency for keeping phase adaptation (Fig. 4).

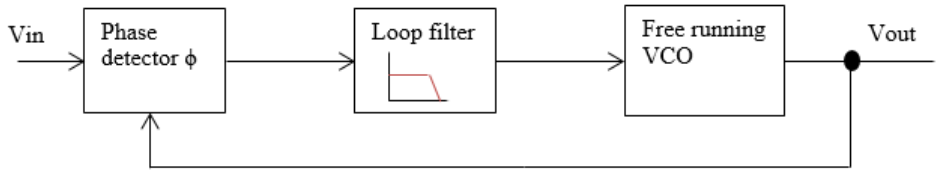

Fig. 4 Analog phase Locked loop based on free running VCO

We lock in input and output signals phase, and then the input signal frequency and the output signal frequency are equal. The PLL unit tracks the input signal frequency or generates output signal which his frequency is multiplication of input signal frequency. We use PLL units for some typical applications: computer clock synchronization, demodulation, frequency synthesizer (Fig. 5). One important application is the process of comparing the input phase to the output phase of clock distribution.

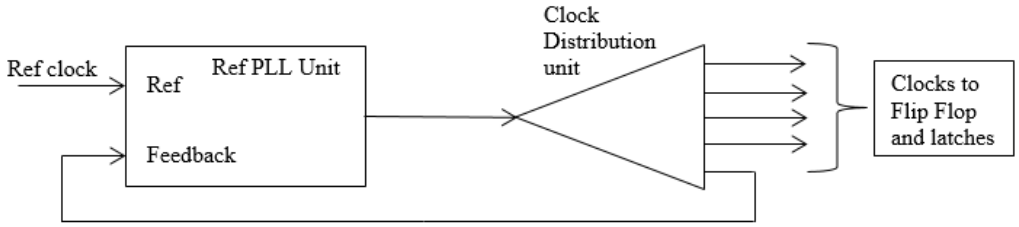

Fig. 5 Clock distribution system with PLL

Additional applications are in demodulator unit which is tracking the modulation phase or modulation frequency. PLL unit can tracks on the carrier signal or changeable synchronization signal with frequency or time. When the PLL works as demodulator (detector), it is filter which is coherent detector. When PLL works as a carrier tracking system then it functions as narrow band filter which remove the noise from the signal. In one integrated package it includes a double balanced phase detector and highly linear VCO (Free running VCO). We set the frequency by external capacitor or resistor. The following block diagram describes the PLL signals and internal elements (Fig. 6).

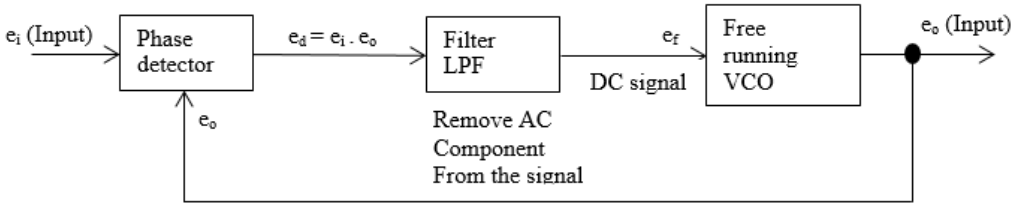

Fig. 6 PLL block diagram with signals

e_i - input signal, e_o - output signal, e_d - output signal from phase detector, e_f - DC signal from LPF. PLL fundamental operational equations: $e_i = \sqrt{2} \cdot E_i \cdot \sin[\omega_0 \cdot t + \theta_1(t)]$; $e_o = \sqrt{2} \cdot E_o \cdot \cos[\omega_0 \cdot t + \theta_2(t)]$. The output from phase detector is $e_d = e_i \cdot e_o$.

$$e_d = e_i \cdot e_o = 2 \cdot E_i \cdot E_o \cdot \sin[\omega_0 \cdot t + \theta_1(t)] \cdot \cos[\omega_0 \cdot t + \theta_2(t)]$$

$$e_d = e_i \cdot e_o = E_i \cdot E_o \cdot \sin[\theta_1(t) - \theta_2(t)] + E_i \cdot E_o \cdot \sin[2 \cdot \omega_0 \cdot t + \sum_{k=1}^{2} \theta_k(t)]$$

PLL's Low Pass Filter (LPF) unit filters the AC component of multiplication output. The filter's output DC component is a function of the phase between the VCO output and the input signal. The output of VCO unit is related to his input by the following differential equation:

$$\frac{d\theta_2(t)}{dt} = k_0 \cdot e_f \ ; \ \frac{d\theta_2(t)}{dt} = \omega \cdot \theta \Rightarrow \theta_2(t) = \int e_f(t) \cdot dt$$

The free running VCO activated as a feedback integration network. Assumption: The PLL loop is not lock and the frequency of input signal (e_i) and the free running VCO (e_o) are very close. Output signal from the phase detector (e_d) is different and the frequency is equal to the gradient frequency of e_o and e_i . We feed the signal to VCO unit and the VCO's frequency is changed with time. If the frequency of VCO equal to the input signal frequency then we are in lock state. Signal e_f will keep the VCO output frequency to be equal to PLL input frequency and we are in lock state. The following flowchart describes the PLL frequency locking due to input signal frequency variation (Fig. 7).

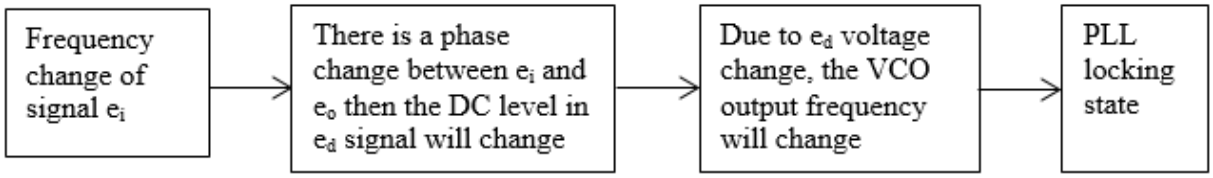

Fig. 7 PLL frequency locking mechanism

We can detect the phase error due to frequency variation by knowing the "DC" loop gain of the system. We consider that PLL's phase detector unit with transfer function $E_d = k_D \cdot (\theta_1 - \theta_2)$, the free running VCO transfer function is $\frac{d\theta_2(t)}{dt} = k_0 \cdot e_f$. The phase of free running VCO output is proportional to the integration of control voltage. The PLL free running frequency is established by PLL internal circuit and external capacitor and resistor. The following diagram describes the application of free running VCO as a FM demodulator system (Fig. 8).

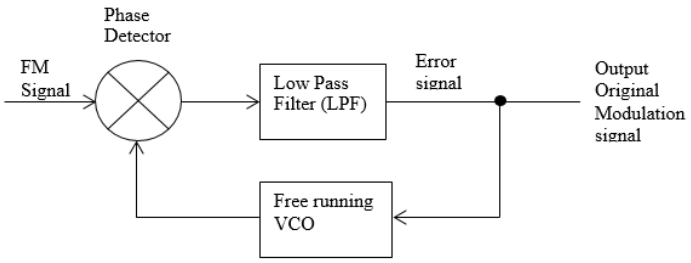

Fig. 8 Free running VCO as a FM demodulator system

Once locked, PLL tracks the frequency changes of the input signal. Thus, a PLL goes through three stages: (1) free running (2) Capture and (3) locked and tracking. Lock range and capture range in PLL: The lock range (tracking range) is defined as the range of frequencies over which the PLL system follows the changes in the input frequency (f_{IN}). Capture range is the frequency range in which the PLL acquires phase lock (Fig. 9).

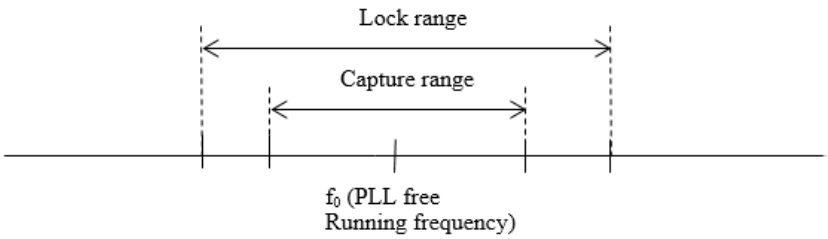

Fig. 9 PLL lock range and capture range

Other applications to use free running VCO are CMOS/Bi-CMOS/Indium integrated circuit and DLL (Delay locked loop). A delay locked loop (DLL) is a digital circuit similar to a phase lock loop (PLL), with the main difference being the absence of an internal VCO, replaced by a delay line. A DLL can be used to change the phase of a lock signal, usually to enhance the clock rise-to-data output valid timing characteristics of integrated circuits. DLLs can also be used for clock recovery (CDR). A DLL can be seen as a negative-delay gate placed in the clock path of a digital circuit. The main component of a DLL is a delay chain composed of many delay gates connected output to input. The input of the chain is connected to the clock that is to be negatively delayed. A multiplexer is connected to each stage of the delay chain; the selector of this multiplexer is automatically updated by a control circuit to produce the negative delay effect. The output of the DLL is the resulting, negatively delayed clock signal. Indium phosphide Heterojunction Bipolar Transistors are used in RF and mixed signal circuits operating at frequencies from below 10GHz up to 0.2THz. At these high frequencies, digital circuit blocks are simulated carefully with techniques traditional to analog and millimeter wave circuit design. Transmission line techniques are used to interconnect sub-circuits and additionally static frequency dividers circuits with HBT technology, applications in frequency agile digital radar and wireless communications systems. HBTs are excellent for implementing VCOs (free running VCO) due to their low $\frac{1}{f}$ noise. A W-band VCO can be integrated with a high speed divider. The differential outputs of the VCO are DC coupled to the input buffer of the divider with microstrip

transmission lines. SiGe HBT mm-wave VCOs have the advantage of large transistor voltage swings and low phase noise. Their power dissipation is excessive. CMOS VCOs at lower frequencies are popular due to their low power dissipation brought about by the significantly lower power supply voltage. A mm-wave CMOS VCOs suffer from inadequate output power levels, reduced tuning range and a very poor phase noise. There are applications which include SiGe BiCMOS PLL with integrated VCO RFICs. It enables miniature LO solutions. It includes an advanced fractional-N synthesizer and an ultra-low noise VCO while requiring a minimal number of external components. The PLL/Synthesizer can incorporates a cycle slip prevention (CSP) mode, which holds the PFD gain at maximum until the frequency difference is near zero reducing the time to arrive at the new frequency. PLL with integrated VCOs uniquely combine the attributes of low phase noise, wide frequency coverage, advanced features and ultra-small size, making them ideal for numerous small form factor applications.

6 Conclusion

We demonstrate the use of Varactor diode in a free running VCO based on an unstable transistor circuit system. The VCO is a key element to generate WBFM signals, such as chirp signals. Varactor diode is a simple tunable elements and it has inherently nonlinear behavior which disqualifies it for use in modern communication standards. The capacitance of a single Varactor diode can usually be expressed as $C(V)=\frac{K}{(\phi+V)^n}$ where ϕ is the built-in potential of the diode, V is the applied voltage, n is the power law exponent of the diode capacitance, and K is the capacitance constant. The power law exponent can exhibit wide variation in different situations. It is value of $n\approx 0.3$ for the implanted junction to $n\approx 0.5$ for a uniformly doped junction to $n\approx 1.5$ for a hyper-abrupt junction. The capacitance of Varactor diode may be varies by varying the reverse voltage applied to it thus, the Varactor also known as VVC (Voltage Variable Capacitor) diode. Their mode of operation depends on the capacitance that exists at the PN junction when it is reverse biased. As the Varactor diode reverse potential increases the width of the depletion region increases which in turn reduces the transition capacitance. When the Varactor diode reverse bias voltage decrease, the depletion layer narrows down. This decreases the dielectric thickness, which increases the capacitance. The variation of capacitance is maximum when the reverse voltage is equal to zero. It reduces in a nonlinear manner, as the value of reverse voltage is increased. In this diode the variation of capacitance are controlled by the method of doping in the depletion layer or the size and geometry of diode construction. The outcome of this article is an analysis of the stability, Free running VCO based on an unstable transistor circuit. Apply variable bias voltage to Varactor diode causes to capacitance change and the oscillating frequency is changed accordingly. The equivalent circuit includes three delay lines, the first delay line (τ_1) represents the electromagnetic interference in the Varactor diode. The second and third delay lines (τ_2,τ_3) represent the circuit microstrip lines parasitic effects before and after the matching circuit. We neglect the voltages on the three delay lines. We represent our system by DDEs which depend on variable parameters and delay parameters (τ_1,τ_2,τ_3). We inspect the stability of any one of the equilibrium points of the Free running VCO which based on an unstable transistor circuit. The system of homogeneous equations leads to polynomial characteristic equation in the eigenvalues (under some assumptions). The stability switching is inspected for different values of τ parameter by using Beretta and Kuang stability criteria. There are many applications to use free running

VCO, are CMOS/Bi-CMOS/Indium integrated circuit, PLLs, and DLL (Delay locked loop), our mathematical analysis help as to understand the operation of those application with integrated free running VCO.

REFERENCES

[1] Muhammad Taher Abuelma'Atti, Parametric amplification/mixing using Varactor diode, Active and Passive Elec. Comp, Vol.19, pp. 177–187, 1966.

[2] O. Aluf, Microwave RF antennas and circuits, Nonlinearity applications in Engineering, Springer (2016).

[3] Sean V. Hum, Michael Okoniewski, and Robert J. Davies, Realizing an electronically tunable reflectarray using Varactor Diode-Tuned elements, IEEE Microwave and Wireless components letters, Vol. 15, No. 6, 2005.

[4] K. Buisman, L. C. N. de Vreede, L. E. Larson, …, "Distortion-Free" Varactor diode topologies for RF additivity, Microwave Symposium Digest, 2005 IEEE MTT-S International.

[5] E. Beretta, Y. Kuang, Geometric stability switch criteria in delay differential systems with delay dependent parameters, SIAM J. Math. Anal. Vol. 33, No. 5, pp. 1144-1165, 2002.

[6] Kuang, Y., 1993. Delay Differential Equations with Applications in Population Dynamics. Academic Press, Boston.

[7] Jiaoxun Kuang & Yuhao cong., 2007. Stability of Numerical methods for Delay Differential Equations. Elsevier Science.

[8] Balakumar Balachandran & Tamás Kalmár-Nagy & David E. Gilsinn., Delay Differential Equations: Recent Advances and New Directions (Hardcover). Springer; 1 edition (March 5, 2009).

[9] Jack K. Hale. *Dynamics and Bifurcations*. Texts in Applied Mathematics, Vol. 3, Springer-Verlag; 1996.

[10] Steven H. Strogatz, *Nonlinear Dynamics and Chaos*, CRC Press; 1 edition (December 29, 2000)

[11] John Guckenheimer, Nonlinear Oscillations, Dynamical Systems, and Bifurcations of Vector Fields, Applied Mathematical Sciences Vol 42, Springer; 1st ed. 1983. Corr. 6th printing 2002 edition (February 8, 2002)

[12] Stephen Wiggins, Introduction to Applied Nonlinear Dynamical Systems and Chaos, Text in Applied Mathematics (Hardcover), Springer; 2nd edition (October 1, 2003)

[13] Guillermo Gonzalez, Microwave transistor amplifiers: Analysis and design (2nd Edition), Pearson, 1996.

[14] Ali Behagi and Maou Ghanevati, Fundamentals of RF and Microwave circuit design: Practical analysis and design tools, RFPTA, 2017.

[15] David M. Pozar, Mocrowave engineering, Wiley; 4 th edition 1901.

[16] Arrl Inc, Antenna physics; An introduction, Amer radio relay League, 2016.

[17] ARRL Inc, The ARRL Handbook for radio communications 2018 Hardcover, Amer radio relay League; 95th, 2017.

[18] ARRL Inc, ARRL's wire antenna classics, ARRL the national association for Amateur radio, 2006.

[19] L. Chiu, T. Y. Yum, Q. Xue, and C. H. Chan, A wideband compact parallel-strip 180^0 wilkinson power divider for push-pull circuitries, IEEE microwave and wireless components letters, Vol. 16, No. 1, 2006.

[20] Jianpeng Wang, Jia Ni, Yong-Xin Guo, and Dagang Fang, Miniaturized microstrip Wilkinson power divider with Harmonic suppression, IEEE microwave and wireless components letters, Vol. 19, No. 7, 2009.

